OPTICAL FIBER COMMUNICATION SYSTEM FOR THE GMRT

A Thesis

Submitted for the Degree of

Master of Science

in the Faculty of Engineering

By

D. S. SIVARAJ

Department of Electrical Communication Engineering

INDIAN INSTITUTE OF SCIENCE

BANGALORE – 560 012 (INDIA)

MARCH 1994

Acknowledgements

I wish to express my sincere gratitude to Prof.G.Swarup for his invaluable guidance and kind cooperation. I would like to particulary thank him for sparing his precious time on several occassions, despite his hectic schedules.

I am grateful to Prof.A.Selvarajan for his valuable guidance and kind cooperation. I am extremely thankful to him for helping me with the course work and enabling me to submit the work despite the delays in thesis compilation.

I wish to acknowledge the early work done by Dr Vivek Srinivas during the feasibility study of the Project. I would also like to acknowledge the support given by Dr D.L.Narayana and Dr Sophie Borderieux during the important phase of design and development of the Project.

I am grateful to Prof.S.Ananthakrishnan for his valuable support and encouragement during the entire work of the project.

Thanks are due to Mr T.L.Venkatasubramani, Mr Goutam Chattopadhyay Mr Sanjay Bhatnagar, Mr Rakesh Malik, Mr Ajit Kumar and other colleagues at NCRA for their encouragement and enlightening discussions.

I like to acknowledge the support extended by Mr M.R.Sankararaman, S.Suresh Kumar and S.Ramesh during the later part of the project.

Thanks are due to Mr M.K.Bhaskaran, Mr S.K.Venkatraman and Mr N.V.Nagarathnam for all the field work at Project site.

Abstract

The Giant Meterwave Radio Telescope (GMRT) is a synthesis radio telescope consisting of steerable parabolic dishes spread over a circular area of 14 km radius . It is expected to detect very faint celestial radio objects with fulx densities of the order of 100 μJansky .Due to the stringent RFI and EMI requirements and the long distances involved, optical fibers are required for communication purposes.

In this work, a detailed analysis of the communication system is carried out. For reasons mentioned in the text, analog communication system is used instead of a digital system. The analog parameters such as linearity, dynamic range, signal to noise ratio and phase stable local oscillator distribution are studied. Theoretical analysis of the various noise sources present in a fiber optic communication system viz., laser noise, shot noise and thermal noise is presented and the measurements of signal to noise ratio are carried out. Various types of laser diodes and photodiodes are considered and the experimental data are presented. The types of lasers include :Low power ridge waveguide lasers, high power ridge waveguide lasers and MTBH low power lasers. The photodiodes include: PINFET receivers, InGaAs PIN photodiodes, and Ge APD devices.

The linearity of the system is analyzed theoretically and the predicted performance is verified experimentally. 1 dB compression point of deterministic and statistical signals is measured and compared against theory. 3rd order IMD products and and harmonic distortion products are also measured to gauge the linearity of the communication system. The effect of optical reflections on linearity and signal to noise ratio is measured and the data is presented.

The dynamic range of the system is described in detail and the requirements for the telescope are analysed.

The effect of temperature on the phase stability of local oscillator distribution is also studied and the relevant data are presented .

The worst case signal to noise ratio is measured to be 25 dB for the longest link (20 km, 32 MHz noise bandwidth). Linearity measurements indicate -65 dBc of third order IMD products at an optical modulation depth of 0.3. The 1 dB compression point of bandlimited random signal is +10 dBm while the third order intercept point is found to be +18 dBm.

The communication system of the GMRT has been realised using high power ridge waveguide lasers, InGaAsP PIN photodiodes, low reflection optical connectors, and single mode fiber operating at 1.3 μm. The system performance is within the radio astronomy requirements in terms of SNR and linearity.

Further study is required to analyse the effect of laser noise and optical reflections on phase stable local oscillator reference.

Optical Fiber Communication System for the GMRT

Contents

Chapter 1

Optical Fibers in Radio Astronomy - an Overview

1.0 Introduction

The invention of photophone by Alexander Graham Bell laid the foundation for modern optical communications, but progress remained very slow until the advent of lasers in the 1960s. With the invention of optical waveguides in the 70s, there has been rapid growth in this area and optical fibers have matured in technology and are fast replacing the existing communication systems such as coaxial cables, metallic waveguides, radio and microwave links and even satellite communications. Optical fibers have become extremely popular due to the following advantages:

- High bandwidth
- Low loss
- No Radio Frequency Interference & Electromagnetic Interference
- Flexibility
- Small size & light weight

and many other advantages depending upon the specific application.

Optical fibers have been used in a wide variety of applications ranging from transoceanic communications systems to high quality laser beam delivery in surgery. Recently optical fibers have been used for optical and radio astronomy applications. In optical astronomy, optical telescopes use the fibers for delivering the optical beam at the focus to a physically accessible location where data recording is carried out. In Radio astronomy, the use of optical fibers is a little more involved.

Radio telescopes usually consist of antenna dishes with large collecting area spread over long distances to achieve high resolution by means of interferometry [1]. By using a number of antennas suitably, a large aperture is synthesized. Information received at each of the antennas is conveyed to a central location for further signal processing, by means of a communication channel. In synthesis radio telescopes, such as the one at Cambridge, UK, coaxial cables were used, as the distances were limited to a few kms. In Ooty synthesis radio telescope, radio links were used with a distance of about 4 kms. The Very Large Array at Socorro, New Mexico, USA, uses low loss TE_{01} waveguides operating at microwave frequencies for the communication over distances ranging up to 21 km. The Australia Telescope at Melbourne, Australia is the first instrument to use optical fibers for communication purposes for the antenna array [2]. The distances covered are of the order of 6 kms. Radio signals received at each of the antennas are digitized and the optical fibers are then used to convey the digital signals.

The GMRT consists of 30 antennas spread over 20 km dia. circular area. The signals picked up at each antenna are down converted to an IF and the analog signal is transported on the optical fibers. GMRT is the first of its kind to use optical fibers for interferometry applications using analog communication system. The analog communication system simplifies the electronics required at remote antenna stations. This enhances reliability and ease of maintenance of the instrument. In addition, the bandwidth required is much less than a digital system, enabling the use of low cost systems. Moreover, digitizing the signals at remote locations produces radiation at RF frequencies which may interfere with the observations.

1.1 Synthesis Radio Telescopes and the GMRT

Telescopes were first used at optical frequencies starting from the days of Galileo. Now, with the help of advanced technology, the present telescopes cover a wide range of the electromagnetic spectrum. However, it was observed that a large fraction of the radiation received from celestial objects is concentrated at radio frequencies [3]. As a result, radio telescopes are increasingly being used for frontline research in astronomy, all over the world. But, unlike optical telescopes, radio telescopes suffer from low resolution limitation, due to large wavelength at radio frequencies.(resolution $\cong \lambda/D$, λ:observation wavelength, D:aperture [4]). In order to overcome this limitation, the aperture D, has to be increased. Due to practical limitations, D cannot be more than a few 100 meters. To obtain a resolution comparable to (or better than) the optical telescopes, one synthesizes a large aperture using a number of antennas spread over a large area. This type of telescopes are known as synthesis radio telescopes. The synthesized aperture is approximately equal to the maximum distance between the antennas.

Operating Principle

The synthesis of a large aperture is based on the well known principle of interferometry and Fourier transforms [5]. Essentially, the array antennas sample the astronomical image in the spatial frequency domain and the Fourier transform of this data gives the required image.

In the block diagram of an interferometer, shown in Fig.1.1, each antenna points towards the source in the direction shown by the unit vector $\underline{s_0}$. It receives radiation from all parts of the source in the direction $\underline{s}$. The separation 'b' between the antenna elements is called the baseline . Assuming that the source is far away compared to the separation between the antennas, the wavefront reaches one of the antennas after a time lag of τ where $\tau = b.s/c$, which is equal to a phase of $2\pi\nu b.s/c$, where ν is the radio frequency. The output of the two antennas is fed to a correlator which is a voltage multiplier followed by an integrator .
If we represent the output of the antennas as complex numbers $v_1 e^{-j2\pi\nu t}$ and $v_2 e^{-j2\pi\nu(t-\tau)}$, then the correlator output would be

$$r = v_1 v_2 e^{-j2\pi\nu\tau}$$

If the source is represented by the vectors Δs measured with respect to s_0 then $s = s_0 + \Delta s$. As the earth rotates, the vector s_0 changes in the sky . The resulting oscillations in r are called fringes . This is the unwanted part and is purely due to the earths' rotation . The source structure information is in the $b.\Delta s$ term .

The output of the correlator, is therefore calibrated w.r.t the direction s_0 in the sky called the phase center . Then r can be written as

$$r = v_1 v_2 e^{-j2\pi b.s\nu/c}$$

or

$$r = v_1 v_2 e^{-j2\pi b.(s_0+\Delta s)\nu/c}$$

If we define 'V' such that

$$V = v_1 v_2 e^{-j2\pi b.\Delta s\nu/c}$$

then, we can express V in terms of r .

$$V = r\, e^{j2\pi b.s_0 v/c}$$

V is called the visibility function and is the spatial coherence function r with phases measured w.r.t the phase center in the direction of s_0 to eliminate the oscillations due to earth's rotation. It can be shown that this visibility function is the spatial Fourier transform of the brightness distribution of the celestial object being observed. The value of V obtained from an interferometer corresponds to a particular frequency component . As the earth rotates, s_0 changes direction which yields other frequency components . In order to determine all the frequency components, the projected baselines will have to cover the entire spectrum . As this is not practically feasible, an array of interferometers are used to sample the Fourier spectrum and with the help of earths' rotation, additional frequency components are obtained [6]. Signal processing techniques are used to extract the image of the sky from the incomplete spectrum [7]. This is known as Earth rotation synthesis.

Receiver System

The performance of a synthesis radio telescope is measured by its resolution and sensitivity. Resolution depends upon the frequency of observation and the longest baseline of the array. Some of the synthesis instruments existing today are listed below for comparison [1]:

Table 1.1

Sl.No.	Name of Telescope	Max. baseline	No.of antennas	Resolution, arc.sec λ= 6cm
1	Cambridge 5 km telescope	5 km	8	2.5
2	Westerbork synthesis telescope	1.6 km	12	8
3.	The Very Large Array	26 km	27	0.5
4.	MERLIN (Multi element radio linked interferometer network)	130 km	6	0.1

Ground based optical telescopes of 6 m dia.. can achieve a resolution of 1 arc second [8] (although theoretical limit is about 0.025 arc sec., it cannot be attained due to turbulence in the troposphere).

Sensitivity of the telescope essentially defines the weakest radio object, which the telescope can observe unambiguously. It is determined by the sky background noise at the frequency of operation, the noise factor of the front end amplifiers and other electronic systems, and the antenna noise produced as a result of surface irregularities and ground reflections [8].

System temperature is a convenient parameter used to quantify sensitivity [3]. It is defined as that temperature of a matched resistor which would produce an equivalent amount of noise power present in the system. Quantitatively,

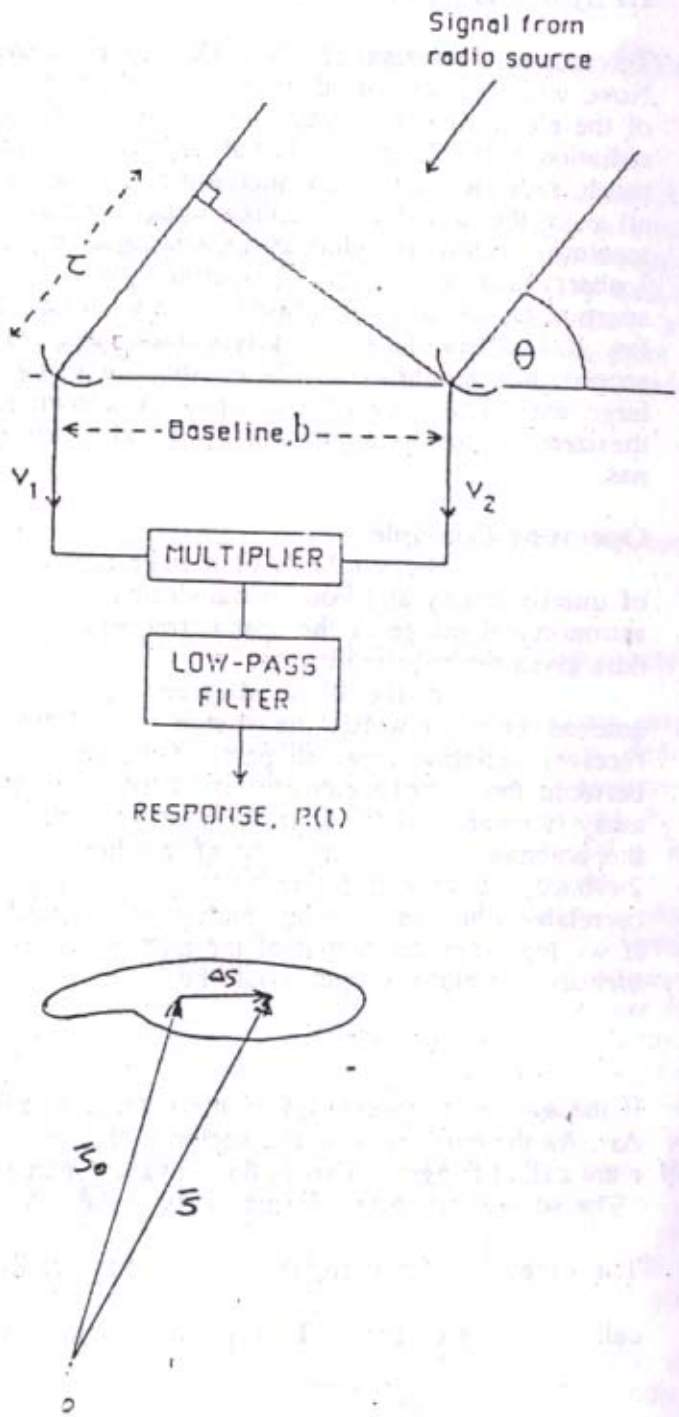

Fig.1.1 The tracking Interferometer

$$N_{system} = kT_{sys}\Delta f$$

where
N_{system} is the total noise power of the system
k : Boltzmann's constant
and
Δf is the noise bandwidth

Fig.1.2 shows a simplified schematic diagram of the receiving system of a synthesis radio telescope (only one antenna is shown for clarity; in practice several antennas are linked to the observing room having identical receiver systems). The overall sensitivity of the antenna is given by [8],

$$T_{sys} = T_A + (L_1 - 1).T + T_{R1} + T_{R2}\frac{L_1}{G_1} + T_{R3}\frac{L_1}{G_1.G_2} + \cdots$$

where T_A indicates the noise temperature of the antenna (due to surface irregularities, atmospheric turbulence etc., ground reflections etc.) L_1 is the power loss factor (≥ 1) of the transmission line connecting the antenna to the first stage of the receiver, and T is the temperature of the line; T_{Ri} is the noise temperature of the ith receiver stage and G_i is its power gain.
At very high frequencies of observation (> 10 GHz), the first stage is usually a mixer of gain less than unity. In such cases, cryogenic cooling is employed to reduce the noise temperature. Usually the gain of the first stage is significant in T_{sys} considerations, as can be seen from the above equation. If G_1 and G_2 are moderately high, (> 10 dB) the succeeding stages contribute less and less to T_{sys}. The low noise amplifier and the succeeding stages up to the mixer stage, are known as front end system [9].

Local oscillator signal is required at each antenna location for downconverting the RF signals. Further, the corresponding LO frequencies at different antenna locations must be in phase synchronism to preserve the coherence of the astronomy signals, for interferometry purposes. The phases of the oscillators at each of the antennas need not be identical, but the difference in phase must be stable enough to permit calibration. Phase synchronization is achieved by transmitting one or more reference signals from a Master reference located at the observing room to each of the antennas. Phase locked loops are used at the antenna locations to lock on to the reference signals and the required LO frequency is generated by frequency synthesizers.

After the downconversion to IF, the signals pass through various IF amplifiers, filters, bandwidth selectors, IF attenuators and possibly AGC before being transmitted to the correlator. Transmission between antennas and the Observation room (or central location) is done by various means. If the distances are short, coaxial cables are generally used. For distances longer than a few kilometers, generally waveguides, optical fibers, radio and microwave links are used. Coaxial cables, waveguides and optical fibers can be buried at depths of 1 - 2 meters to reduce temperature variations.

Signals reach the Central location through the communication channel and go through further processing before feeding the correlator. Usually the signals are converted to a final IF, where time delays are compensated. Phase errors due to temperature effects and delay setting errors are minimized by setting the lowest possible frequency as the final IF. Accordingly, the final IF amplifiers often have a baseband response. Sharp cut off at the zero frequency of the baseband is achieved by means of a single sideband mixer which converts the final IF to baseband [10].

The correlator is the heart of the interferometer systems. It can be realized using analog or digital techniques. It consists of a delay system to compensate for the geometric and cable delays followed by a multiplier and an integrator. The analog

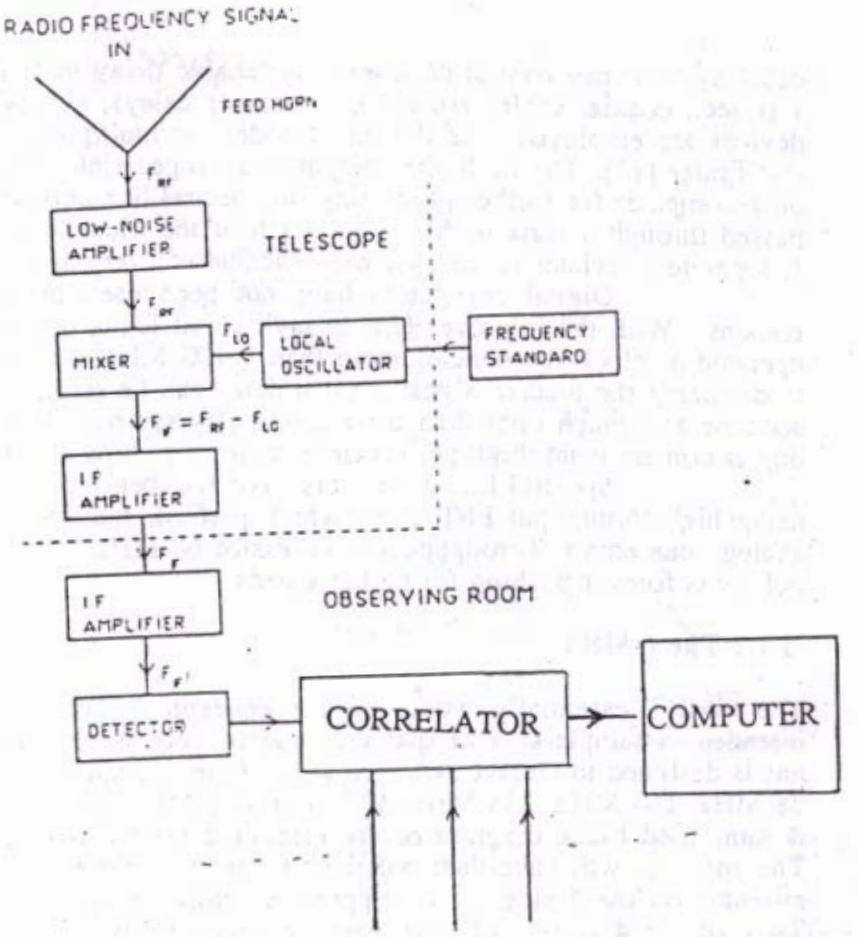

Fig.1.2 Superheterodyne Receiver used in Radio Astronomy

delay system may consist of several switchable delay units in series. For delays up to 1 μ sec., coaxial cables are used; for longer delays, generally, surface acoustic wave devices are employed. The design of wideband multipliers has been studied by Allen and Frater [11]. The multiplier output is averaged (integrated), digitized and recorded on a computer for further processing. In spectral line correlator, the baseband signal is passed through a bank of filters and each of the filter outputs is processed separately. A separate correlator is used for each channel of every antenna pair.

Digital correlators have not been used in the past due to their slow response. With the improvements in high speed logic, digital circuits capable of being operated at clock frequencies more than a 100 MHz have been realized. This has led to digitizing the final IF signal, so that delay can be set digitally. Digital delay is more accurate and much finer than the analog delay system. Correlation is performed in the digital domain using high performance multiplier chips and associated circuitry.

Spectral line correlators have also been realized in the digital domain by using high throughput FFT chips which perform the operation of filter banks of the analog counterpart. Throughputs in excess of 60 MHz have been realized and the technology is forever pushing for higher speeds.

1.1.2 The GMRT

The GMRT essentially works on the concept, outlined above. The shape of Y is intended to sample several spatial frequency components (Fig.1.3). Each of the antennas is designed to receive radiation at 6 different frequencies :
38 MHz, 153 MHz, 233 MHz, 327 MHz, 610 MHz and 1420 MHz .
A simplified block diagram of the electronic system of GMRT is shown in Fig.1.4. The antennas will have dual polarised feeds at all the 6 frequencies. The feeds will be mounted on the 4 sides of a computer controlled rotating turret near the prime focus. Two of the 4 sides will have dual frequency feeds. The front end consisting of RF, LO and IF electronics is designed for low system temperature and good phase stability. The linearly polarised signals are first converted to right hand and left hand circularly polarised signals by low noise quadrature hybrids and then amplified in low noise RF amplifiers. After phase switching, signals are brought through low loss cables to the base of the antenna. The RF signals are converted to a 32 MHz wide intermediate frequency (IF) centered at 70 MHz using suitable LO signals . Since the receiver is required to preserve the phase of the incoming signal the LO signals used for down-conversion at each of the antennas should be synchronized. This is achieved by synchronizing all the local oscillators to a frequency standard located at CEB. Moreover, since the observations are spread over 12 hours of time periods, the phase of the local oscillators should not drift with respect to one another . Main contributions to the drift are the electronics at each end of the signals , noise in the system and path length variations in the signal path . Round trip phase method is a scheme which circumvents this problem . Chapter 4 describes this in greater detail .(The back end of the receiver will consist of a large state of the art FX type Correlator system which uses about 1650 special purpose high speed FFT and multiplier chips . A 256 spectral channel correlator has been designed for the 30 antennas of GMRT, which gives (30 x 31/2) x 256 x 2 = 238080 correlated outputs, each of which is a complex number to be averaged over integration times selectable from 0.04 to 10 seconds . The maximum bandwidth of the system is 32 MHz . The correlator will allow measurement of all polarisation parameters with 128 spectral channels for Δf= 16 MHz only.)
The output from the correlator acquired by the online computer will lead to a database of about 4 Gbytes for a full synthesis observation . The online computer will also control the synchronized rotation of the antennas, feeds etc. and monitor the entire system besides performing preliminary analysis of the received data .

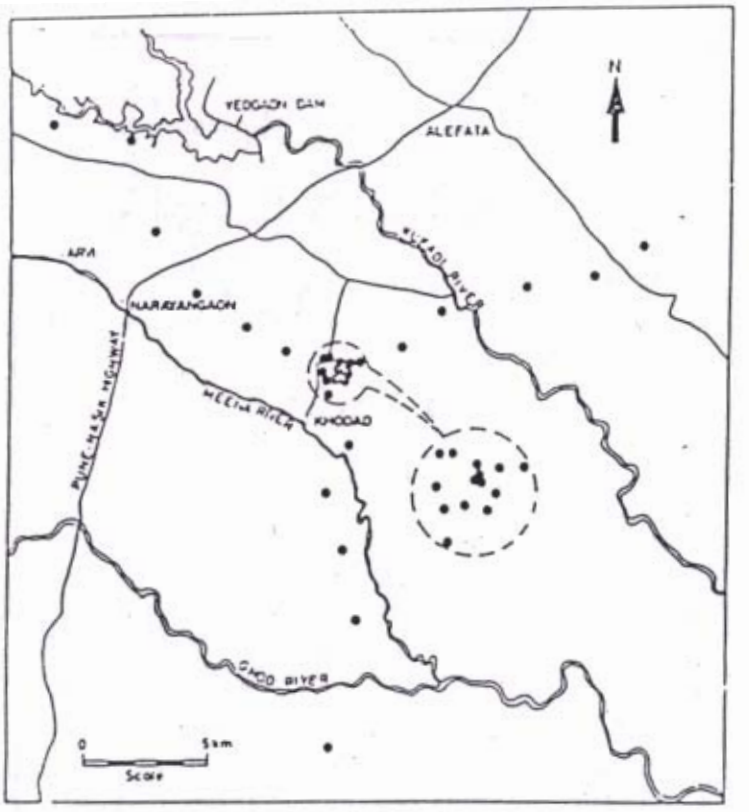

Half of the 30 dishes of GMRT are being located in a compact array in a region of about 1 km x 1 km. The remaining dishes are along the 3 arms of an approximate 'Y' configuration giving maximum baseline of about 25 kms.

Fig.1.3 GMRT Array Configuration

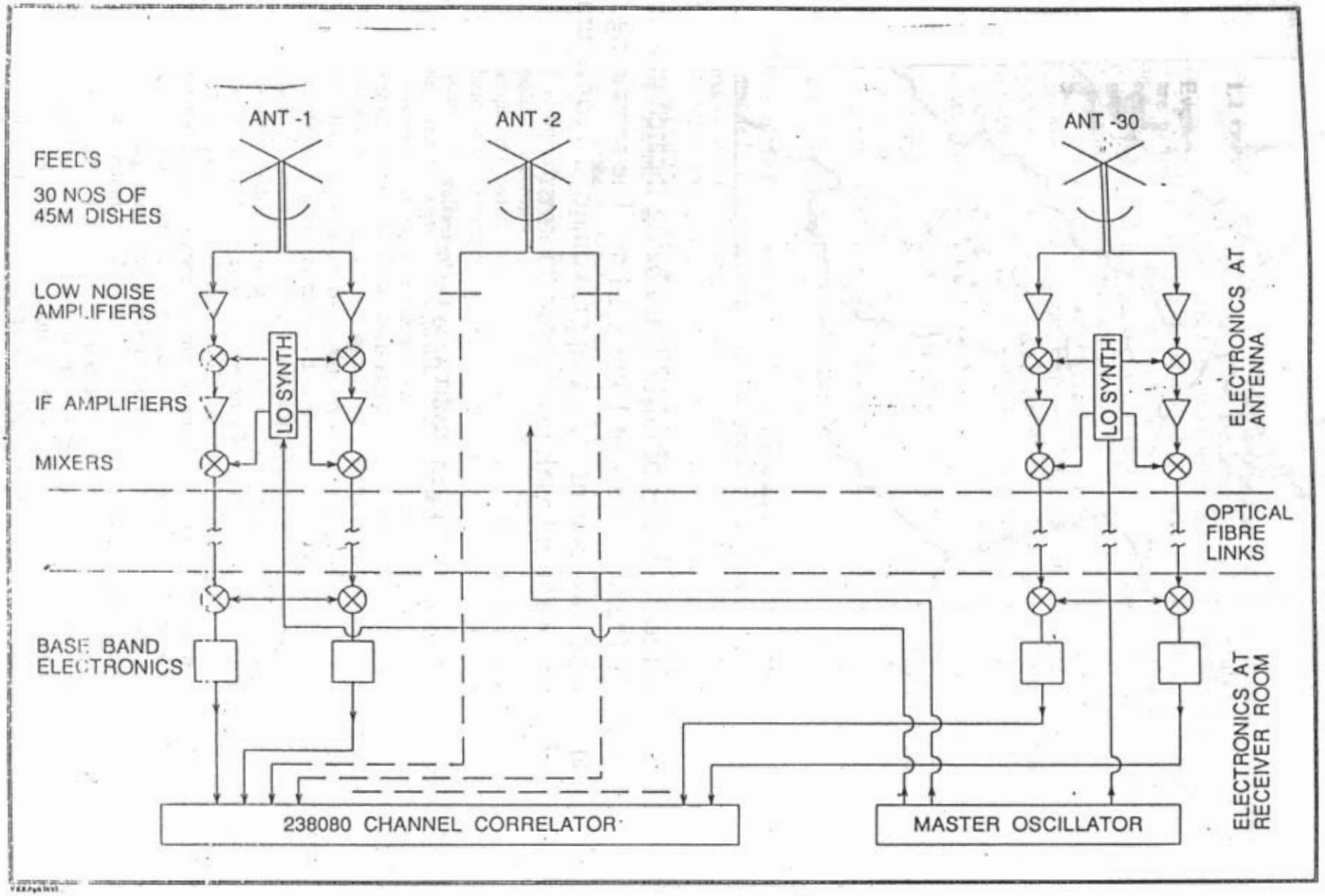

Fig.1.4 Block diagram of GMRT Receiver system

1.2 Optical Fiber Communication

Eventhough the principles of optical fiber communication and the system requirements are well known, a brief description is given here for the sake of completeness. The optical fiber is a transmission medium that has become extremely popular in less than two decades after its invention. Its primary advantages of low loss, wide bandwidth, small size, strength, flexibility, low cost, and immunity to electromagnetic noise meet the challenging requirements of today's communication systems, unparalleled by any other medium.

Optical fibers were originally conceived as weakly guiding waveguides of coherent electromagnetic radiation at optical frequencies. The losses were reported at 1 dB/m [13]. Technology improved rapidly, in the fabrication of low loss fibers, optical sources and detectors for the generation of coherent radiation and detection; in less than 20 years, optical fibers have nearly achieved the theoretical limit of 0.14 dB/km @ 1550 nm wavelength. Single mode fibers with very low dispersion over a wide spectral range are being fabricated routinely at low cost. Repeater distances of over 200 km are realized in commercial applications [14]. Data rates of 2.4 Gbits/sec are used in telecom applications worldwide, and 10Gb/s have been reported.[15]. With the advent of optical amplifiers and solitons (based on nonlinear effects in optical fibers), the data rates are pushing towards much higher speeds than ever anticipated, with transmission distances exceeding 10000 km [15]. With the improvement in fiber bandwidth, optical sources and detectors also kept pace with the advancements. GaAs technology is increasingly being used to realize high speed sources and detectors capable of generating/responding to picosecond optical pulses. Coherent communication and Photonics are currently in intensive R&D phase and the breakthroughs will have far reaching effects in communications and signal processing.

1.2.1 Properties of optical fibers.

Optical fibers are cylindrical dielectric waveguides capable of guiding light, based on the principle of total internal reflection [16]. The material consists of silica and some dopants such as GeO_2. The optical fiber consists of an inner dielectric material called a *core* which is surrounded by another dielectric material called a *cladding* with smaller refractive index. The core and the cladding form the structure of a waveguide. Usually this waveguide is protected by another layer of plastic/polymer called a *jacket*. This jacket is mainly required for prevention of cross talk and mechanical and chemical abrasion. Fig.1.5 gives the cross sectional view of an optical fiber.

Fiber types:

Optical fibers are classified according to the refractive index profile of the core and cladding and the number of modes they can support. A mode is a transverse pattern of energy propagating at a specific velocity. As shown in Fig.1.6, there are two main types of profiles viz. Step index and Graded index. In step index fibers, the refractive index of the core is homogeneous and there is an abrupt transition in the profile at the core-cladding interface. In graded index fibers, the core refractive index varies gradually from the center of the fiber and there is a smooth transition in the profile at the cladding interface.

Depending on the no.of modes a fiber can support as a waveguide, further classification of fibers is made [17]. This consists of Single mode fibers which allow only one mode to propagate, Multimode fibers in which several modes exist and Dual mode fibers.

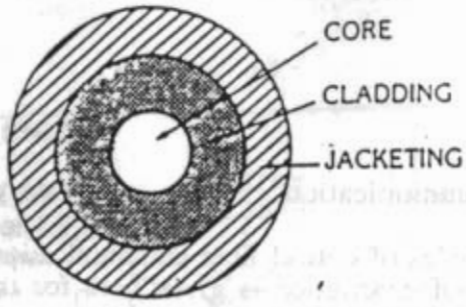

Fig.1.5 Cross-sectional view of an optical fiber

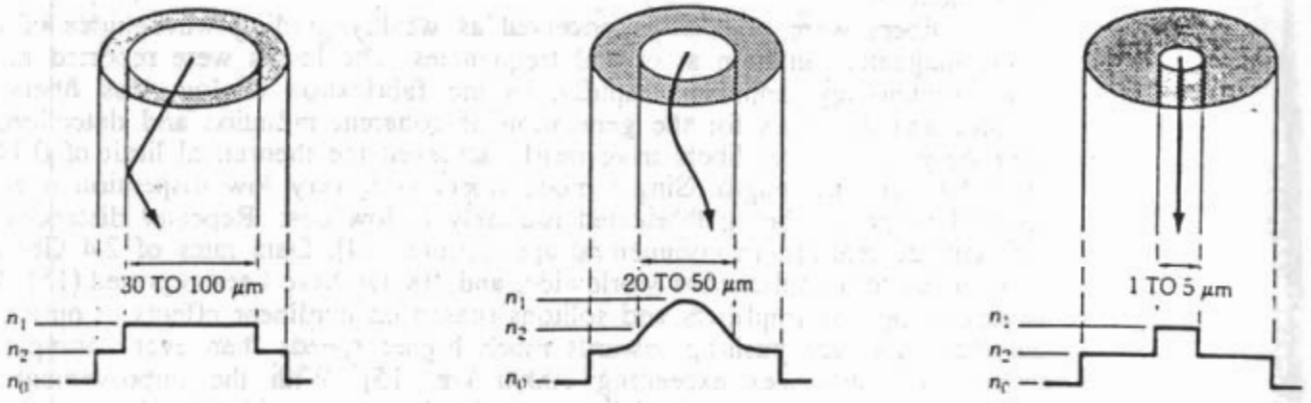

(a) Step-index multimode. *(b) Graded-index multimode.* *(c) Step-index single-mode.*

Fig.1.6 Refractive-index profiles and classifications of fibers

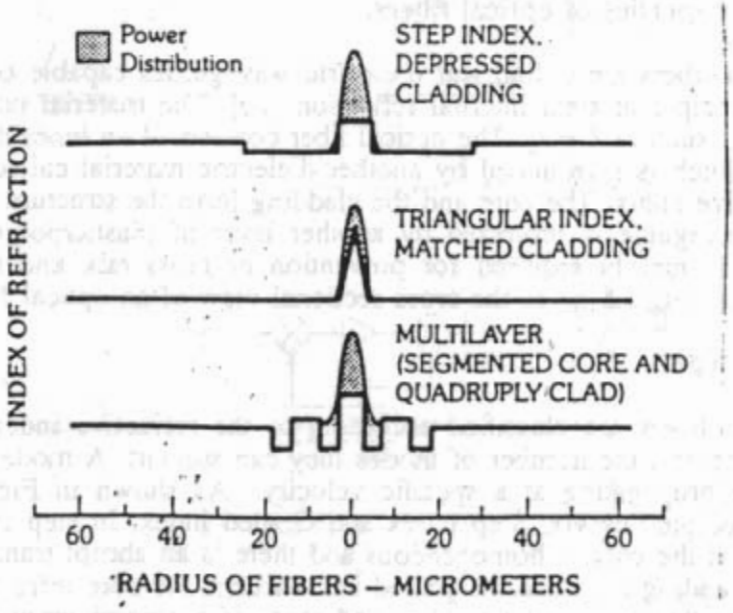

Fig.1.7
Low-dispersion refractive-index profiles for single-mode fibers at 1550 nm.

Multimode fibers:

This type of fiber supports several modes of propagation in addition to the dominant HE_{11} mode or LP_{01} mode[18].Both step index type and graded index type of fibers can support multimode propagation. In step index type of fibers, the core to cladding refractive indices differ by about 1% [17]. Associated with each mode is a direction or an angle which satisfies the condition for total internal reflection. The range of angles is known as the acceptance cone or numerical aperture. This quantity can be derived from fundamental optics, [19]. It is expressed as :

$$NA = \sqrt{n_1^2 - n_2^2}$$

where
n_1 is the refractive index of the core
and n_2 is the refractive index of the cladding

In step index multimode fibers, different partial rays propagate at different angles, resulting in different transit times(refer the section on Dispersion) for different rays. This implies reduction in bandwidth and hence this type of fiber is used only for low bandwidth applications. In the case of graded index fibers, a reduction in the path differences is achieved by a gradual change in the refractive index profile. In such an instance, the optical rays are guided, not by total internal reflection but by distributed refraction similar to what is observed in the mirage effect. As a result, all the modes are confined to be very close to the axis, and this ensures approximately uniform transit times for all the modes. In fact, there exists an optimum profile [18] which gives exactly identical transit times to all the modes. This profile is close to a parabola; slight deviation from this results in significant increase in pulse dispersion or loss of bandwidth. The propagation properties of a fiber are described by its V number, generally referred to as *Normalized frequency*. The V value is an important parameter, because it defines the basic waveguide properties of the fiber [20]. It is defined by

$$V = 2\pi \frac{a}{\lambda} . \sqrt{n_1^2 - n_2^2}$$

where a is the radius of the core
λ is the wavelength of operation and
n_1 and n_2 are the refractive indices of the core and cladding respectively.

Among other things, the V number defines the number of modes a fiber can support. In the case of step index fibers , the relation between the no.of modes N and V number is given by :

$$N = \frac{V^2}{2}$$

General emphasis is on reducing the number of modes in-order to attain higher bandwidths. This implies that the fiber diameter should be small. But this poses practical limitations such as coupling inefficiency due to small dimensions. The multimode fibers typically have core diameters of 50 µm. The types of modes that exist in a cylindrical multimode fiber include a finite number of guided modes and an infinite number of radiation and leaky modes. The guided modes consist of a family of H_{0n} E_{0n} modes and a family of HE_{mn} hybrid modes. In addition, there are TE_{mn} and TM_{mn}

modes [20]. In spite of the poor bandwidth performance, multimode fibers continue to be used in various applications. The reasons include: ease of fabrication, ease of coupling to sources and detectors; compatibility to a wide variety of sources and detectors and availability of economical connectors due to less stringent precision requirements.

Single Mode Fibers :

From the equation relating normalized frequency to fiber parameters, it can be seen that for step index fibers, the number of modes can be reduced by reducing the diameter of the fiber. When the diameter reaches a certain minimum, the fiber supports only one mode. This is known as Single mode fiber and has the highest bandwidth capability and its propagation characteristics are completely determined. It is ideally suited for long haul, high bit rate applications. The single mode fibers carry only the dominant HE_{11} mode. However, due to circular symmetry of the waveguide, all orientations are equivalent, and two orthogonal polarisations of the HE_{11} mode exist in the waveguide. Single mode fibers are designed with core sizes limited to a few wavelengths and the index difference between core and cladding, smaller than 1% . The maximum V number corresponding to single mode operation is found to be 2.405. If the V number exceeds this value, the fiber no longer remains a single mode fiber. An important feature of single mode fibers is their dependence of attenuation on wavelength. This is due to the strong dependence of the V number on wavelength. At higher wavelengths the radiation leaks into the cladding and at lower wavelengths the fiber becomes multimoded. Another important feature of single mode fibers is their insensitivity to microbending losses: losses induced by localized lateral displacement of the fiber from a mean axis [21]. Single mode fibers offer a much higher bandwidth than Multimode fibers primarily due to lack of intermodal dispersion. Let us first analyze the various types of dispersion before discussing dispersion in single mode fibers.

Dispersion:

The width of a pulse propagating through a fiber increases with the distance travelled. The optical pulse consists of several photons each of which has its own velocity. This is due to the fact that there may be many modes supported by a fiber waveguide and the photon may be travelling in any of the modes. Associated with each mode is a direction of propagation and velocity. Let us consider a short duration pulse launched into the fiber. The photons comprising the short pulse take different modes of propagation, and arrive at the other end of the fiber at different times. This increases the duration of the pulse. This phenomenon is known as Dispersion and it is directly dependent on the length of propagation. There are three types of dispersion : a) Intermodal dispersion b) Material and c) Waveguide dispersion

Intermodal dispersion is the dominant source of dispersion in multimode fibers. This arises due to the fact that the velocity of each mode is unique. As a result, modes propagate at different velocities and arrive at different times, although they are all excited simultaneously at the starting end. Graded index profile reduces this problem to a great extent by ensuring that all the modes have approximately same velocity. Refractive index profile can be suitably designed to eliminate intermodal dispersion altogether; but it is practically not feasible to maintain the profile to sub micron accuracy during the manufacturing process. *Material dispersion* is due to the dependence of velocity on wavelength. Radiation at a certain wavelength propagates at a certain velocity different from another wavelength. It causes dispersion even when all the energy is concentrated in one mode. This dispersion is dominant, when the optical source has a broad spectrum. It is observed that glass fibers have nearly zero dispersion at 1300 nm. *Waveguide dispersion* results from the guiding structure and is significant in single mode fibers. The guided energy is divided between the core and the cladding. the propagation velocity is greater in the cladding than in the core. The mode that propagates

in Single mode fiber has a certain distribution of power in the core and the cladding. This distribution determines the effective velocity of the mode. However, the distribution is dependent on the wavelength and the index profile, resulting in waveguide dispersion when there is non mono- chromatic radiation.

Both waveguide dispersion and material dispersion depend on the source spectral width as well as the length of the fiber . They are generally measured in ps/nm/km.(pulse spreading/source spectral width/fiber length).

Dispersion in Single Mode Fibers:

Dispersion in SM fibers is due to the dispersive properties of the fiber material (material dispersion) and to chromatic dispersion inherent to waveguiding processes (waveguide dispersion). Dispersion can be annulled at any wavelength between 1300 and 1700 nm [22]. In this wavelength range, material dispersion has opposite polarity to that of waveguide dispersion in the λ-domain. Single Mode fibers available today have minimum attenuation at 1550 nm. Practical value of attenuation achieved is close to the theoretical minimum (0.16dB/km vs 0.15 dB/km). If dispersion is minimized at this wavelength, then high capacity, long distance communication is easily achieved. For Single mode step index fibers, minimum dispersion occurs at 1300 nm. In order to shift this to a different wavelength or to flatten the dispersion minimum (to sustain for wider wavelengths) several techniques are adopted. These are known as dispersion shifted or dispersion flattened fibers. By modifying the index profile from a simple step index to a more complex one, one achieves dispersion minimum at a different wavelength. Zero dispersion occurs when material dispersion cancels waveguide dispersion. At 1550 nm, material dispersion is larger than at 1300 nm. In order to cancel the higher material dispersion, the index profile is suitably modified to achieve the extra waveguide dispersion. There are may index profiles which can accomplish this. Fig.1.7 illustrates a few examples.

1.2.2 Optical Sources

Optical fiber communication has been made possible by two major technological advances. One of them is the development of a low loss silica fibers and the other is the development of high performance, reliable semiconductor lasers. Originally the operating wavelength of fibers and the laser were at 0.85μm with multimode operation. The next generation systems using laser diodes and singlemode fibers operating at 1.3μm gave rise to longer repeater spacings and higher bandwidths. Even better performance, in terms of repeater spacing is achieved by operating the system at 1.55μm where the fiber loss is minimum. Semiconductor lasers fabricated using InGaAsP material, are used as sources for high bit rate long distance communication systems operating at 1.3 or 1.55μm. For short haul communication system, where the performance requirements are not so critical, light emitting diodes are used.

Laser Diode :

The semiconductor injection laser was discovered in 1962 [24]. Since then it has emerged as a major component in many optoelectronic systems such as long haul communication, Optical recording, optical sensors and guided wave signal processing. The concept of a semiconductor laser diode is based on the principles of quantum electronics and device physics. The basic laser chip consists of two parallel cleaved facets which form the optical cavity (Fig.1.8). The device has a pn junction near the light emitting region (active region) for current injection. The cavity length is typically around 200-400μm. The light/current characteristics of a laser diode is shown in Fig.1.8b. As the current injected is increased beyond a certain value (threshold current), the light output from the facet increases dramatically. Associated with this is a narrowing of the spectral emission from approximately 60 nm below the threshold to about 3-4 nm above the threshold region. The light below the threshold is emitted spontaneously as the electrons and holes recombine in the active region. When the injection current exceeds the threshold, stimulated emission is observed.
Conceptually, the stimulated emission arises from the radiative recombination of electrons and holes in the active region, and the light generated is confined and guided by a dielectric waveguide. The active region has a slightly higher index than the p & n cladding layers and the three layers form a waveguide as shown in Fig.1.9. The cladding layers have a higher bandgap than the active region, thus confining the lasing process only to the active region. The laser structures are often classified into two groups: gain guided and index guided. In the gain guided structure, the width of the lasing optical mode along the junction plane is mainly determined by the width of the optical gain region. The optical gain region is determined by the width of the current pumped region (typ. 5-10μm).Gain guided lasers have undesirable properties such as high threshold current, low differential quantum efficiency and occurrence of light/current kinks at relatively low output powers. In index guided lasers, a narrow central region of relatively higher refractive index (active region) confines the lasing mode to that region. The index guided lasers can be divided into two groups : weakly index guided and strongly index guided. In weakly index guided lasers, the active region is generally continuous and the effective index discontinuity is provided by a cladding layer of varying thickness. The refractive index difference between the active region and the cladding is around 0.01 to 0.03. On the other hand, the strongly index guided lasers employ a buried heterostructure. The active region is bounded by lower index epitaxially grown layers along the junction plane and normal to the junction plane. The refractive index difference in this case is around 0.2. Ridge waveguide and Rib waveguide are typical examples of weakly index guided lasers while the strongly index guided types include MTBH (Mass Transport Buried Heterostructure) and DCPBH (Double Channel Planar Buried Heterostructure) [25, 26].

Single Frequency Lasers :

The above lasers are generally referred to as multi longitudinal mode (MLM) lasers. Several longitudinal modes are supported by the laser cavity, due to the structure of the active region and gain mechanism. In the presence of chromatic dispersion, the undesirable side modes limit the fiber bandwidth. To overcome this problem, semiconductor lasers have been developed that emit light predominantly in one single longitudinal mode. This is achieved by making the laser cavity, frequency selective. Many techniques are used to generate single mode lasers. The most popular ones consist of DFB (Distributed Feedback) and DBR (Distributed Bragg Reflector) lasers. In DFB lasers, the laser feedback is not localized at the cavity facets but is distributed throughout the cavity length. This is done by the use of a grating etched along the

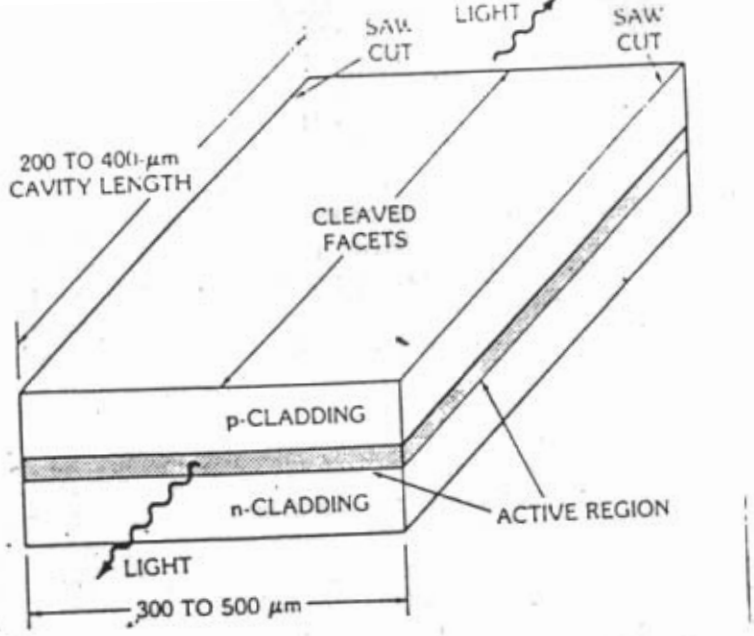

Fig.1.8a Schematic of the basic semiconductor laser diode

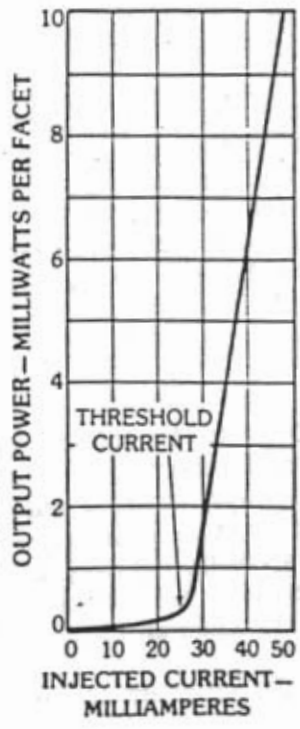

Fig.1.8b
Light emitted from the facet versus the injectedcurrent for a semiconductor injection laser.

cavity length. Mode selectivity of the DFB mechanism results from Bragg's law which states that coherent coupling between forward and backward travelling waves occur for wavelengths such that the grating period, $\Lambda = m\lambda/2$ where λ is the wavelength of the light in the laser cavity and m is any integer. By choosing Λ appropriately, such a device can be made to provide distributed feedback only at a certain wavelength.[27]

Light Emitting Diodes :

Light emitting diodes are closely related to injection lasers. The LED is a spontaneous emission device and its emission characteristics are similar to those of injection lasers below threshold. These devices generally emit low powers and have a broader spectral emission and lower modulation speeds than lasers. The LEDs are generally classified into two groups : Edge emitting LED (ELED) and Surface emitting LED. The ELED structure is similar to that of laser except that the device is operated in the spontaneous emission regime below the threshold. For surface emitting LED, the light is emitted normal to the surface of the wafer. The ELEDs exhibit narrower spectral width and beam divergence than surface emitting LEDs. LEDs are generally used as sources for short distance, multimode fiber transmission systems. However, the small divergence of output from ELEDs makes them a potential candidate for sources for short haul single mode fiber transmission systems [28].

1.2.3 Optical Detectors

Much of the research emphasis on components for optical communication was directed towards sources and the fiber itself. But it is equally important to consider the detectors in estimating the overall performance of the system. In the early work, most components were developed for use at 0.85 μm using silicon materials. Later on the emphasis shifted to 1.3 and 1.55 μm wavelengths and it became important to consider other materials. Ge and GaAs were proved to be suitable material for detector applications at these longer wavelengths.

Basic Photodetector:

In basic photo detection process in a semiconductor material, an incident photon is absorbed and directly excites an electron from a non conducting state to a conducting state. This is done in two ways: intrinsic and extrinsic absorption. In intrinsic photon detection, an electron is excited from the valence band to the conducting band. In extrinsic type of detectors, an electron is excited from the ground state of a neutral donor impurity to the conduction band. Another form of extrinsic photon detection occurs in free carrier photoconductors, when an electron is excited from a given state to one of higher or lower mobility.

Most popularly used photodetectors are of the intrinsic type, due to their fast response and efficient absorption of photons. Intrinsic photodetectors consist of p-n junction in the most basic form (Fig.1.10) and are usually reverse biased, to avoid excess dark current and to reduce the junction capacitance of the device. Dark current is the current flowing in the detector without any incident optical light. Thus the electric field is developed across the high impedance depletion layer sweeping the majority carriers to their respective sides away from the junction. This barrier has the effect of stopping majority carriers from crossing over the junction in the opposite direction to the electric field.

When a photon is incident on the detector surface, with an energy greater than or equal to the band gap energy E_g of the device, (i.e. $h\nu >= E_g$), it will excite an electron from the valence band into the conduction band, leaving an empty hole in the valence band; This phenomenon is known as the photogeneration of an electron hole pair(ehp).

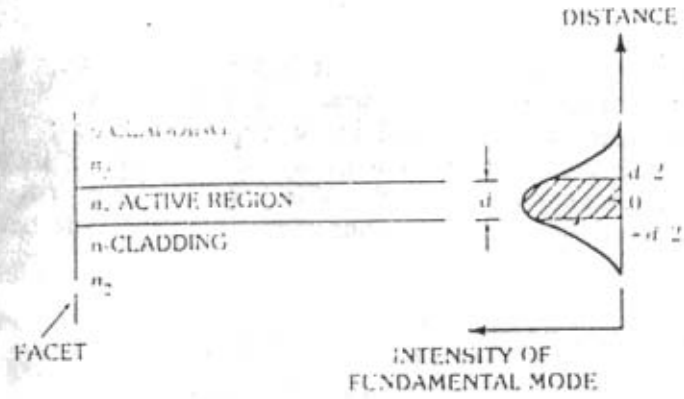

Fig.1.9 The dielectric waveguide of the semiconductor laser

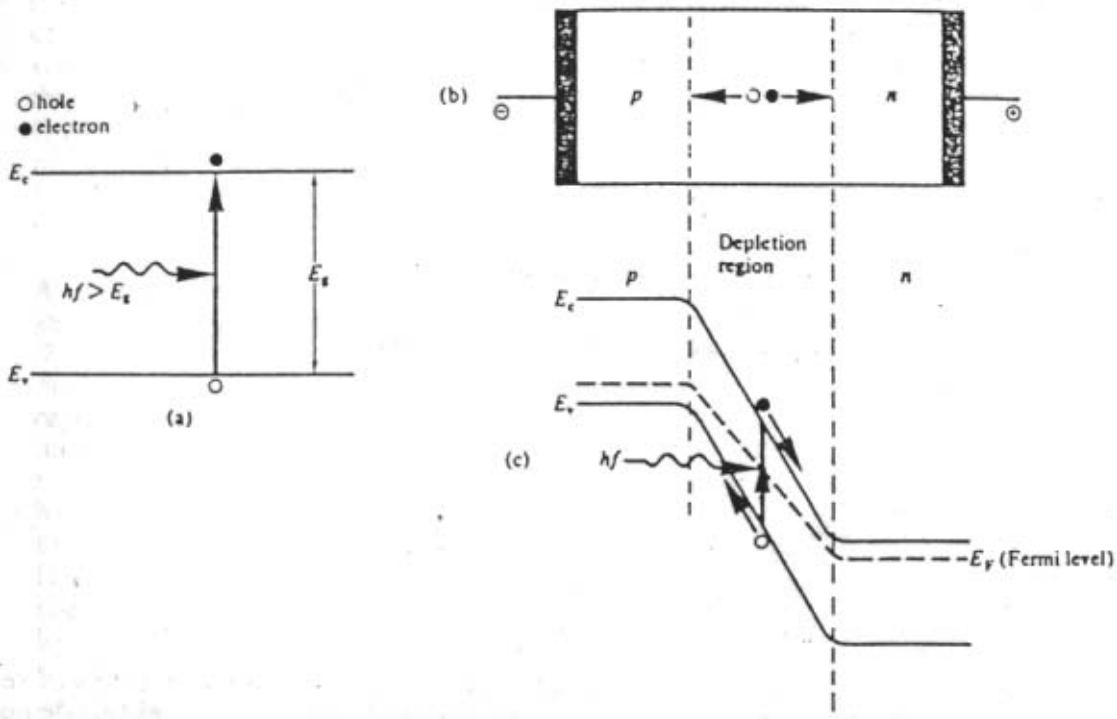

Fig.1.10 Operation of the *p–n* photodiode: (a) photogeneration of an electron–hole pair in an intrinsic semiconductor; (b) the structure of the reverse biassed *p–n* junction illustrating carrier drift in the depletion region; (c) the energy band diagram of the reverse biassed *p–n* junction showing photogeneration and the subsequent separation of an electron–hole pair.

This ehp generated near the junction, is separated and swept under the influence of the electric field to produce a displacement current in the external circuit, which is a result of several photons being absorbed in the depletion region. The depletion region must be sufficiently large to absorb a majority of the photons incident on the material, in order to create maximum ehps. But this leads to long drift times in the region and reduces the speed of operation. Thus there is a trade off between the no.of photons absorbed and the speed of response.

Sensitivity : The absorption of photons in a detector depends on the type of materials used, the width of depletion region and the spectral response of the detector. This is quantified by *Quantum efficiency*, which is denoted by η and given by:

$$\eta = \frac{No.of\ electrons\ generated}{No.of\ incident\ photons}$$

This expression does not include the energy of photons and hence it is difficult to characterize the photo diode performance, by means of η alone. *Responsivity* is another parameter which is often used to determine the detector performance. It is given by :

$$R = \frac{I_p}{P_o} \quad Amps/Watt$$

where
I_p is the photocurrent generated in amperes
and
P_o is the incident optical power in watts

Responsivity and quantum efficiency are related by [29],

$$R = \frac{\eta e}{h\nu}$$

where
e = charge of an electron
h = Planck's constant
ν = frequency of operation

The spectral response of a photo diode is often measured in terms of responsivity, as a function of wavelength. This is determined by the types of materials used and the device structure.

Materials for photodetectors : Silicon and Germanium are the materials which were used in the early communication systems. They absorb light by direct and indirect optical transitions. Silicon has a band gap of 1.14 eV corresponding to indirect absorption [29]. This requires the assistance of a phonon so that energy as well as momentum are conserved. As a result, the indirect transition is less probable than a direct transition, making it less efficient. This explains the low efficiency of Silicon in the spectral range of 0.6 μm to 1.09 μm.
Germanium is another material which has indirect transition during photon absorption. However, it can also absorb light by direct transition at a band gap of 0.81 eV. This makes it attractive for detection at longer wavelengths. Thus Germanium is the only

detector which spans the entire spectrum of (0.6 - 1.6 μm) which is of interest to fiber optic communication systems.
The limitation of Germanium is that it has a high dark current due to its low band gap. This makes the detector very noisy and reduces the sensitivity. This led to the investigation of III-V alloys which are direct band gap materials. These materials are superior to Ge due to larger band gap (1.15 eV and higher) and the flexibility to tune the response to any desired wavelength by changing the relative concentration of the constituent elements.
Ternary alloys such as InGaAs and GaAlSb deposited on GaSb substrates have been used to fabricate photo detectors for the 1.0-1.4 μm wavelength band. Quaternary alloys such as InGaAsP grown on InP and GaAlAsSb grown on GaSb have demonstrated better results. These systems have the advantages of band gap and lattice constant being varied independently.

PIN Photodetectors : At longer wavelengths, the optical light penetrates more deeply into the semiconductor material. In order to absorb all the radiation, the depletion region should be as long as possible. This is achieved by introducing an 'n' type material doped so lightly that it can be considered intrinsic and a heavily doped 'n' type material (n^+) layer to make a low resistance contact. This creates a p-i-n (or PIN) structure as illustrated in Fig.1.11. The width of the depletion layer depends on the type of material used. In silicon detectors, it is between 20-50 μm which gives an efficiency of typically 85% and dark current < 1 nA. Germanium p-i-n photo diodes which span the entire wavelength range of interest are also commercially available, but they are not very popular due to higher dark currents (typ. 100 nA at 20°C)
Quaternary compounds such as InGaAsP grown on InP substrate have remarkably better performance at longer wavelengths. Dark currents of less than 0.2 nA with efficiency above 70% . The response times of less than 100 ps have been reported [30].

Avalanche Photo diodes : Generally known as APDs, these detectors have internal gain, which generates photo current several orders of magnitude higher than the PIN detectors, for identical incident optical power [31]. The device structure is slightly more complicated than PIN devices. It consists of a *Gain region* and an *Absorption region* (Fig.1.12). Similar to the PIN detectors, photons are absorbed in the Absorption region (the depletion layer) and the carriers generated, known as primary carriers, drift under the influence of the external voltage to the Gain region. This region has a very high electric field and the primary carriers acquire sufficiently high energy to generate secondary carriers by means of impact ionisation. The secondary carriers further generate more carriers and the chain reaction continues until the initial impact energy is completely absorbed. This is the well known phenomenon of *Avalanche breakdown* in ordinary reverse biased diodes. The reverse bias voltage required to realize the avalanche gain is of the order of 100 - 400 V. The carrier multiplication factors as high as 10^4 can be obtained by using defect free materials [32].
The speed of these devices is slightly inferior to PIN detectors due to the longer time required for generation of secondary carriers and the resulting diffusion current in the depletion region.
Due to the inherent gain present in the device, APDs are used for high sensitivity applications. However the gain mechanism is unstable and creates excess noise. In addition, the gain is very sensitive to temperature variations.
Currently Ge and Si APDs are commercially available with multiplication gain in the range of 10 and 300(typ) respectively. Quaternary III-V alloys have also been introduced in the market recently with much better noise performance and gain stability [33].

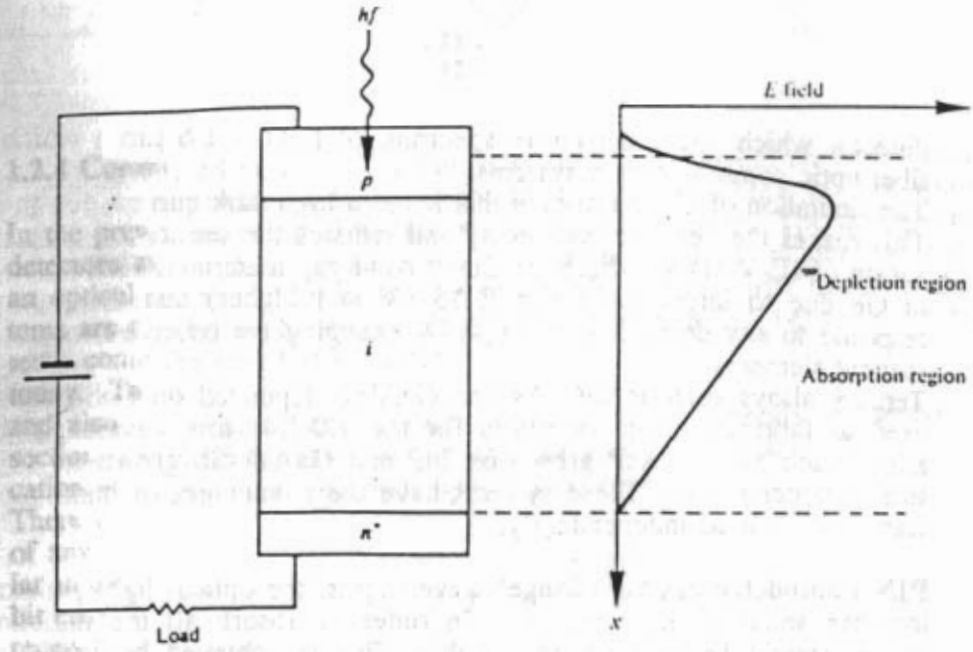

Fig.1.11 *p–i–n* photodiode showing combined absorption and depletion region.

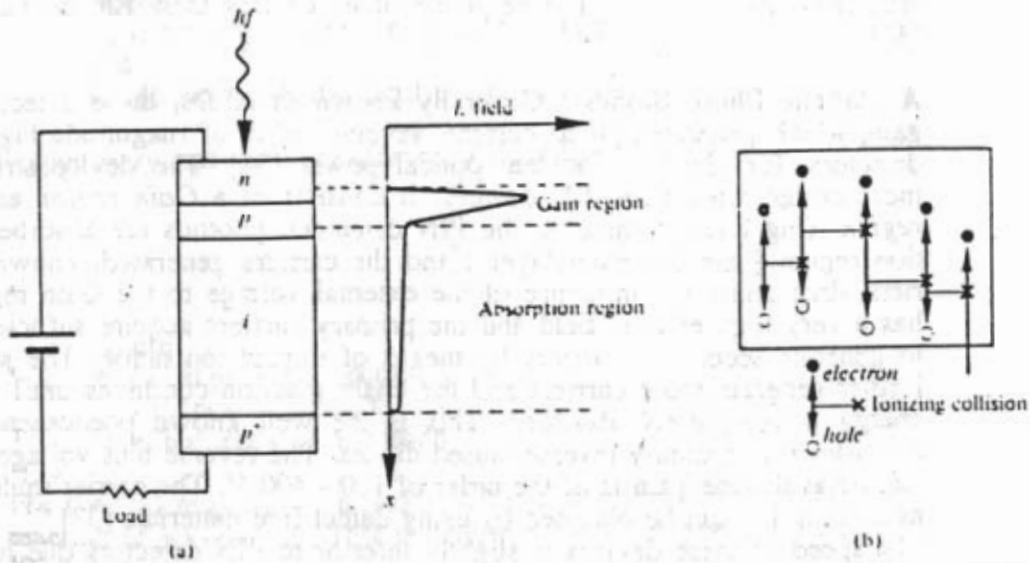

Fig.1.12 (a) Avalanche photodiode showing high electric field (gain) region (b) Carrier pair multiplication in the gain region.

1.2.4 Communication System Design

In the previous sections, a brief description of the optical fiber, the optical sources and detectors and the operating principles were presented. The design and performance of an optical fiber link depends entirely on the choice of these components. Digital systems are most widely used when realizing an optical communication link ; analog systems constitute a very small fraction of the optical communication systems existing today. This is partly due to the robustness of digital systems in the presence of noise and also due to the existing digital technologies in the communication world. In this section a brief description of a typical system design with reference to a digital application is presented, followed by an overview of the emerging technologies in this field. There are many possibilities of component choices available to meet the requirements of any specific communication system. However, the link design methodology is similar in all the systems. The important measure of performance of a digital system is the bit error rate (BER), which is the probability that an error is made in the detection of a received bit. The BER value of $\leq 10^{-9}$ is commonly specified as the tolerance limit in most communication systems. The design procedure aims at meeting the minimum requirement on BER and the accompanying parameters.
System gain analysis (or Power budget) and pulse distortion analysis (or Dispersion budget) are the two important parameters that are considered in evaluating the BER performance of a link. A simplified digital link is illustrated in Fig.1.13, for discussions on the link performance.
The optical transmitter usually consists of an LED or an LD. An optical pulse is generated corresponding to a digital '1' and the absence of the pulse indicates a digital '0'. Important differences between LED & LD include : the amount of optical power, spectral width, and switching speed. The generation of optical pulse is usually accomplished by changing the bias current of the device from the threshold current (in the case of laser diodes) to the peak current.
The optical transmitter is characterized by the following parameters :

- Average output power
- Extinction Ratio
- Operating wavelength
- Optical source spectral width
- Pulse duty cycle
- Line code

The first two parameters indicate the strength of the output signal from the transmitter. However average power corresponds to time averaged values and hence duty cycle information is required to evaluate instantaneous power levels. The extinction ratio is essentially the ratio of the power levels corresponding to the two digital bits ('1'and '0'). More formally, the average power and extinction ratio are given by,

$$P_{ave} = \frac{(P_{max}+P_{min})}{2}$$

$$r_{ex} = \frac{P_{min}}{P_{max}}$$

where

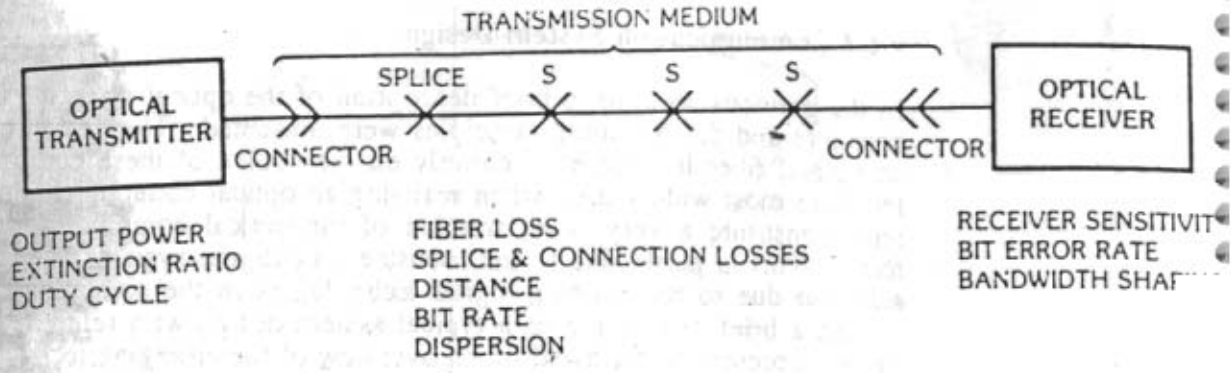

Fig.1.13 Optical digital link model.

P_{ave} = Average optical power
P_{max} = Maximum or peak optical power
P_{min} = Minimum optical power
r_{ex} = extinction ratio

The average power, pulse duty cycle and extinction ratio are required to estimate the receiver power sensitivity. The sensitivity of a detector is defined as the minimum optical power required to detect a digital '1' without any error.
The operating wavelength is an interrelated parameter between all the components of the system. It is important to consider the fiber loss and dispersion characteristics before choosing the operating wavelength of the source.
The spectral width of the source is also a parameter one has to optimize carefully. The linewidths of commercially available devices vary from 50nm (of LEDs) to 2 nm (of LDs).
The component that follows the optical transmitter in the digital optical link is the transmission medium. The important factors that are considered in the link design can be summarized as follows:

- Fiber cable loss
- Splice/Connector insertion loss
- Link distance
- Bit rate
- Fiber dispersion
- Single mode fiber cut off wavelength

These parameters are applicable, in general, to all kinds of fibers. Each of the items contributes to the maximum possible length of the link at a specified bit error rate.
The final constituent of an optical link is the optical receiver as shown in Fig.1.13. This component detects the optical signal and reconstructs an estimate of the signal used to drive the optical transmitter. The most important parameter that is considered in the design is the sensitivity of the detector, which is defined as the minimum optical power required to reconstruct the signal with the specified bit error rate. Although BER gives an indication of the detector's sensitivity, the main factors that influence the sensitivity are : extinction ratio of the source, and the pulse shape of the signals.

System Gain : Using the concepts outlined above, it is easy to describe the link design in terms of the various parameters. In practical terms, a designer is interested in maximizing the link distance, while maintaining the required minimum BER. Physically, the link length consists of a series of component insertion losses. Instead of specifying the physical link length of a link as a measure of performance, it is more useful to define system gain. Then if the total insertion loss in dB/km is known, the link length is easy to compute. The system gain is defined as:

$$G = P_t - P_{rs}$$

where
G = System gain
P_t = The average transmitted power in dBm
P_{rs} = Receiver sensitivity, for a given BER, in dBm

Effectively, the system gain represents the maximum power difference between the

transmitted power and receiver sensitivity figure. If the total insertion loss of the link exceeds the system gain, link BER will deteriorate.
The total insertion loss is actually the attenuation of the optical signal; the attenuation is the aggregate of all loss elements. The total link loss is expressed as the summation of individual fiber lengths, splice insertion loss and optical connector loss. This is given by

$$L = \sum L_s + \sum L_c + \sum \alpha_k . d_k + M$$

where,
L = Total link insertion loss in dB
L_s = individual splice loss, in dB
L_c = individual connector loss, in dB
α_k = attenuation per kilometer of fiber section k, in (dB/km)
d_k = length of fiber section k, in dB km.
M = Power margin or system margin, in dB

The system margin M has been included in the loss expression as a safety factor, to allow for unforeseen losses or system degradation due to aging, increased loss due to cable repairs etc.
Finally, the system designer should ensure that the overall loss L is always below the system gain (while determining the maximum link length). i.e

$$P_t - P_{rs} \geq L$$

where P_t, and P_{rs} are as defined earlier.

Noise limitation The receiver sensitivity is an important parameter that determines the BER of a system for a given link. This can be defined as the ability of the detector to detect an optical pulse in the presence of noise. The various types of noise include those generated at the transmitter, at the detector and in the pre amplifier following the detector. The noise generated in the fiber is usually much smaller than the other sources. The key factors that determine the receiver sensitivity can be summarized as follows:

- Detector responsivity
- APD excess noise
- Pre amplifier noise
- Receiver noise bandwidth
- Detector leakage current
- Inter Symbol Interference (ISI)
- Modal noise (in MM fibers)
- Mode partition noise (in SM fibers)
- Laser mode hopping
- Reflections backward into laser cavity

Dispersion Budget : Analysis of optical receivers has shown that if the product of the bit rate B of the link and the total dispersion σ_t is less than 0.25, then the sensitivity degradation in the receiver is approximately 1 dB [34]. i.e

$$B.\sigma_t \leq 0.25$$

The total dispersion σ_t is the square root of the sum of the squares of the pulse dispersion σ_i of each independent contributor.

$$\sigma_t = \sqrt{\sum_i \sigma_i^2}$$

The contribution from fiber dispersion depends not only on the total length of the fiber but also the source line width, operating wavelength and the type of fiber used. Multimode fibers offer inter modal dispersion whereas intra modal dispersion is predominant in single mode fibers. The total dispersion in a single mode fiber of length L can be represented by the following :

$$\sigma_t = \sigma_\lambda . |D(\lambda)| L$$

where
σ_t = total dispersion in pico seconds
σ_λ = rms spectral width of the source in nanometers
$D(\lambda)$ = Dispersion coefficient in ps/nm/km
L = length of the fiber in km.

A simple relation exists between dispersion and the electrical bandwidth of the system. It can be easily derived if we assume that the pulse spread due to dispersion has a Gaussian profile. i.e

$$P_o(t) = \frac{1}{\sqrt{2\pi}} e^{\frac{-t^2}{2\sigma^2}}$$

where
$P_o(t)$ = Instantaneous power of the optical pulse at time t.
σ = total dispersion in pico seconds

Fourier transform of the above equation gives the spectrum of the optical pulse.

$$P_o(\omega) = \frac{1}{\sqrt{2\pi}} e^{\frac{-\omega^2\sigma^2}{2}}$$

The electrical bandwidth is defined as that point at which the optical power decreases by a factor of $\sqrt{2}$. If we derive this frequency from the above equation it turns out that,

$$f_{3dB} = \frac{133}{\sigma}$$

where
f_{3dB} = 3 dB electrical bandwidth in GHz

1.2.5 Analog systems and Future technologies

In the previous section a brief description of a digital communication system design was presented. Analog systems also need to consider most of the parameters enlisted earlier (Sec.1.2.3). The performance is measured in terms of Signal to Noise Ratio rather than BER. In addition, analog systems need to consider linearity of the communication channel. A typical analog link consists of similar components illustrated in Fig.1.13. Signal amplitude variations are translated into intensity variations by means of modulating the bias current of the laser diode. Similarly, the receiver converts the optical intensity variations into electrical current variations and further processed by electrical circuitry. Fig.1.14 illustrates the analog modulation conceptually. This type of modulation is known as *Direct Modulation* due to the fact that the laser diode is modulated directly by the signal.
The current trend in lightwave systems is to use *external modulation* schemes to attain much higher bandwidths both in the analog and the digital systems. Electro optic modulators, Mach Zender interferometers, and acousto optic devices are currently used to modulate the output of the laser diode externally [35]. Bandwidths and data rates in excess of 10 GHz and 10 Gb/s have been reported using the external modulation schemes [36].

Coherent communication system is another recent technology which is becoming very popular due to its large bandwidth handling capability and long distance communication. Unlike the systems described earlier, which employ direct detection process by converting the optical intensity into electrical signal, heterodyne detection first adds to the optical carrier signal, a locally generated optical signal, the optical local oscillator, and then detects the downconverted signal as shown in Fig.1.15. The downconverted signal is a reproduction of the original modulating signal but shifted down in frequency from the optical carrier, low enough for the signal processing circuits to handle in the electrical domain. This type of detection enhances the sensitivity of the receiver by about 20 dB compared to the state of the art direct detection APDs. In addition, it allows for frequency and phase modulation of the optical carrier rather than just the intensity as in direct modulation systems.

Optical amplifiers is yet another recent phenomenon that has made inroads into the area of regeneration or repeater systems. Based on the well known *laser action* in which the pump mechanism is realized by another laser (which has higher frequency ν, such that $h\nu > E_g$, where E_g is the energy bandgap of the lasing material), stimulated emission is initiated by the incoming optical signal. The optical gain achieved by these amplifiers is in excess of 30 dB. The main advantage of this type of a repeater is its ability to respond to very high frequency signals that is not yet realized by using conventional opto electronic/electro optic repeaters.

A novel phenomenon known as **Soliton propagation** in optical fibers has been reported [37] in the late 80s but it was not practically feasible until the advent of optical amplifiers.
Optical fibers have intensity dependent refractive index at wavelengths longer than 1.3 μm. This is observable at high power levels of the order of a few watts of optical power. The resulting non linear effect gives rise to negative group velocity dispersion, which can be tuned to cancel the dispersion effects of the fiber waveguide, thus maintaining the shape of the optical pulse regardless of the length of the fiber. Optical pulses as short as 100 fs ($1fs = 10^{-15}$) have been transmitted in short lengths of fibers. The emerging technologies cover a wide variety of components and extremely complex systems. Networks such as ISDN, FDDI are paving the way for a *communication super highway*. The emergence of **Photonics** as a separate branch of Lightwave technology is making rapid progress in optical signal processing. The use of optical fibers and related technologies in non conventional applications such as sensors and surgery is

Block diagram

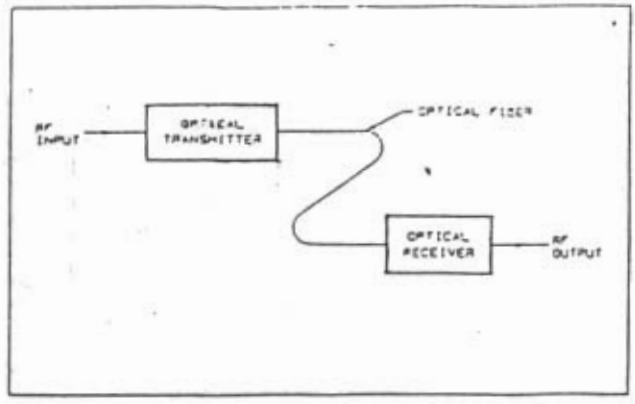

Laser characteristic *The laser converts input current to the output light power . Above the threshold current the output light power is very nearly a linear function of input current*

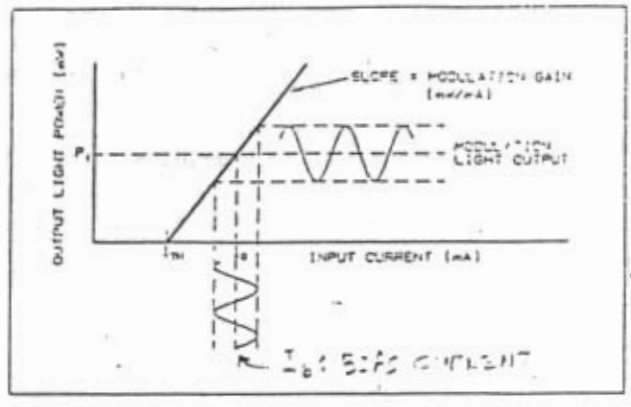

Photodiode REsponsivity *The photodiode converts input light power into electrical current*

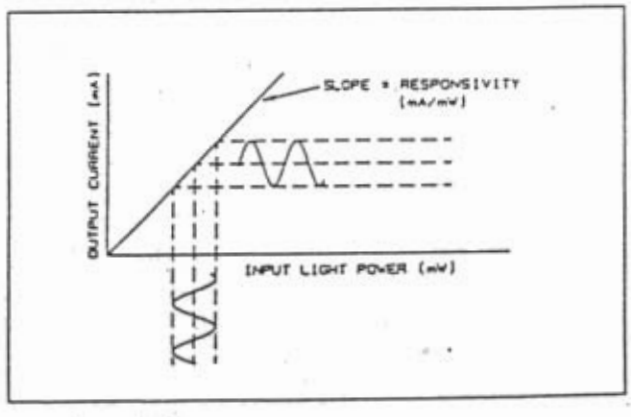

Fig.1.14 Analog Fiber Optic Link and the transfer characteristics

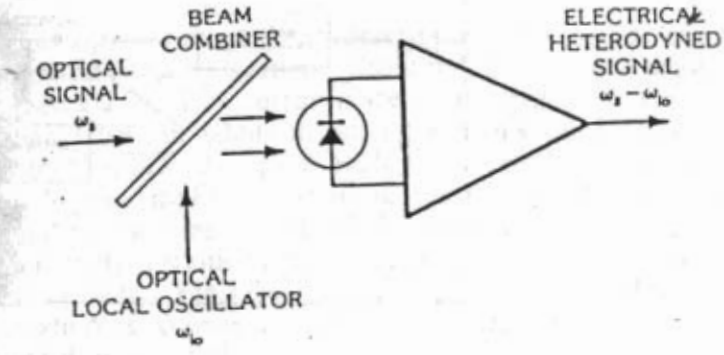

Fig.1.15 Coherent communication system

Optical local oscillator mixes with a received optical signal to produce an electrical frequency equal to the difference between optical frequencies

becoming more diversified. It remains to be seen as to how far the technology can revolutionize the day to day life and its impact on science.

1.3 Aim and Scope of the Thesis

This thesis deals with the design, analysis and implementation of an analog optical fiber communication system for the GMRT. The advantages of optical fiber system and the basic principles of Radio Astronomy were outlined, earlier in this chapter. In the remaining chapters of the thesis, the analog communication system specific to the GMRT is described. An expanded summary of the chapters is given below as an overview of this thesis and for a quick reading.

Chapter 2 briefly describes the communication system for GMRT. Firstly, The communication requirements of the telescope are listed together with the system specifications. Various options available for realizing the communication system are discussed and the final configuration is described in detail. Subcarrier multiplexing is used to combine IF and LO signals and Intensity Modulation is used to modulate the optical carrier in the final system configuration. The components of the system include 2 single mode fibers to each of the 30 antennas, Ridge waveguide lasers(1mW) and low reflection PIN photodiodes operating at 1300 nm.

A comprehensive analysis and system design of the communication system is presented in Chapter 3. In particular, the following parameters are discussed:

1. Noise analysis
2. Linearity
3. Dynamic range
4. Phase stability

Noise analysis: In the GMRT array, antennas receive very faint astronomical signals which can be million times weaker than the system noise due to any background sky radiation, ground leakage and receiver electronics such as polarizers, amplifiers etc. However, due to statistical independence of each of the antennas' noise sources, a cross correlation between any two antennas would eliminate the dc output due to the system noise while retaining the astronomical signal in the form of auto-correlated function (rms noise fluctuations are still present but are minimized by choosing sufficiently long integration time and wide receiver bandwidth). This is due to the fact that all the antennas receive signals from the same source, albeit with different geometrical delays, which can be compensated digitally in the correlator [8].

Thus, the optical fiber generally transmits only the receiver noise with a very tiny fraction of the astronomical signal. The noise of the fiber optic system should not degrade the receiver noise significantly. The major sources of noise in a fiber optic system include: laser intensity noise, shot noise, and thermal noise [38]. The cause of each of these sources is explained in detail in this section. Signal to noise ratio analysis is carried out with respect to each of the noise sources and the effect of fiber optic system on the overall receiver noise is discussed. Brief discussion is also made for the case when either strong astronomical signals are observed or appreciable radio frequency interference is present.

Various combinations of devices are analyzed to study the effect of optical reflections on laser intensity noise. The devices analyzed consist of Ridge waveguide laser of low and medium power, MTBH lasers, low reflection InGaAs PIN photodiodes, high reflection PIN photodiodes, PINFET receivers and Ge APD devices.

Linearity: The linearity of the communication channel is very important from the telescope's observation point of view. Since the signals going through the

communication system consists of broadband noise and several narrow band signals (due to LO, telemetry and RFI due to distant transmitters), it is essential to ensure that spurious products do not interfere with the signals. In this section, the linearity of a typical communication system is discussed with respect to the linear distortion and non linear distortion. Theoretical analysis is carried out to estimate 2nd harmonic and 3rd order intermodulation distortion products. The choice of passband of the communication channel as a result of the distortion produced, is also discussed.

Dynamic range: Dynamic range is an important parameter in the communication system because it gives an estimate of the range of signal levels that the telescope can receive without loss of information. Information may be lost either due to poor signal to noise ratio or high non linearity.
In this section, the analytical treatment of dynamic range is presented and the effects of distortion levels due to broadband noise signals as well as high levels of RFI are discussed.

Phase stability: LO signals are required at each of the antennas to downconvert RF signals received by the antennas to a common IF. For interferometer applications it is required to maintain phase coherence at all the antennas. This requires that the phase of LO signals in each of the signal paths be stable in the time scales of the integration time of the correlator. This implies that the length of the optical fiber is stable in that time scales.($\phi=\omega l/v, \omega$=freq.of LO , l= length of fiber, v= group velocity). The phase variation is mainly due to temperature effects on length and group refractive index of the fiber [39].
The temperature coefficient of phase variation is computed theoretically and the phase variation is studied under actual conditions. This section also describes the phase jitter requirement for interferometry application. The phase jitter translates to an equivalent signal to noise ratio in the communication channel. This aspect is explained in detail and the results are presented.

In Chapter 4, the circuit design of optical transmitter and optical receiver are presented and their performance is evaluated. In the second part of this chapter, measurement results of the parameters discussed in Chapter 4 are given.
Optical transmitter consists of optical power stabilization circuit, temperature stabilization and bias & matching circuits. Each of these sections is analyzed theoretically and the measurements are presented.

Optical receiver consists of photodiode front end along with matching section and a low noise amplifier. Theoretical analysis is carried out to evaluate the performance of the receiver with respect to thermal noise and signal gain. The analysis is compared with actual measurements. The optical fiber cables are used to connect all the 30 antennas of the GMRT array which are spread over a circular area of 14 km radius. The total route distance of the cable is approximately 67 kms. In this section, a brief description of the cable installation and splicing methodology is presented.

In Chapter 5 conclusions and scope for further work are outlined.
References corresponding to each chapter are provided at the end of the chapter.

References

1. R.S.Booth,J.W.Brault and A.Labeyrie, "*High resolution in Astronomy*", 15th Advanced Course,Swiss Society of Astrophysics and Astronomy, SAAS-FEE 1985
2. A.C.Young et al, "*The Optical Fiber System (for AT)*", Journal of EEE,Aust.,I.E Aust.& IREE Aust.,vol.12,No.2, pp.177-181, 1991
3. John D Kraus, "*Radio Astronomy*", McGraw Hill, 1986
4. F.A.Jenkins & H.E.White, "*Fundamentals of Optics*" , 4th edition, McGraw Hill, 1976
5. Ryle M, A.Hewish & J.R.Shakeshaft, "*The synthesis of Large Radio Telescopes by the Use of Radio Interferometry*", IRE Trans.Antennas & Propagation,vol.7,1959,pp.s120-s124
6. M.Ryle, "*The new Cambridge Radio Telescope*", Nature,vol.194,1962,pp.517-518
7. Schwarz, "*Mathematical and Statistical Description of the Iterative Beam Removing Technique*", Jl.of Astronomy & Astrophysics,vol.65,pp.345-356,1978
8. A.Richard Thompson et al, "*Interferometry and Synthesis in Radio Astronomy*", John Wiley Interscience, 1986
9. Weinreb.S,M.Balister et al, "*Multiband Low Noise Receivers for a Very Large Array*", IEEE Trans.MTT,MTT-25, pp.243-248, 1977
10. Archer.J.W et al, " *A broadband UHF mixer exhibiting High Image Rejection over a Multidecade Baseband Freq.Range*", IEEE Jl.of Solid State Circuits,SC-16,pp.385-392, 1981
11. Allen.L.R & R.H.Frater, "*Wideband Multiplier Correlator*", Proc.IEE,vol.117, pp.1603-1608, 1970
12. G.Swarup et al,"*The Giant Metre-wave Radio Telescope*", Current Science, India, Vol.60, No.2, pp.97-105, Jan.1991,
13. Gloge.D, "*Weakly Guiding Fibers*", Applied Optics, Vol.10, No.10, pp.2252-2258, Oct. 1971
14. K.Iwashita, T.Matsumoto et al "*Linewidth requirement evaluation and 290 km transmission experiment for optical CPFSK differential detection,*" Electronics Letters 22, 791-792, 1986
15. N.A.Olsson, J.Hegarty et al "*Transmission with 1.37 Terabit.km/sec capacity using ten wavelength division multiplexed laser at 1.55 μm, Conf.Opt.Fib.Comm.,San Diego, Paper WB6, 1985*
16. A.H.Cherin, "*Introduction to Optical Fibers,*" Auckland McGraw-Hill, 1983
17. H.F.Wolf,"*Handbook of Fiber Optics: Theory & Applications*", New York:Garland STPM Press, 1979.
18. D.Gloge, "*Optical Power Flow in Multimode Fibers*", Bell Sys. Tech. Jl., Vol.51, pp.1767-1783, 1972
19. A.C.Cherin, "*Introduction to Optical Fibers,*" Auckland McGraw-Hill, 1983
20. H.G.Unger, "*Planar Optical Waveguides and Fibers*", Oxford:Claradon Press, 1977.
21. R.Olshansky, "*Microbending loss in Singlemode Fibers*", Proc. 2nd Euro.Conf. on OF Trans., Paris, France, Paper XII p.373, 1976
22. C.T.Chang, "*Minimum Dispersion at 1.55 μm for Singlemode Step Index Fibers*", Elec. Letters, Vol.15, pp.765-767, 1979

23. F.P.Kapron, "*Fiber Optic System Trade-offs*", IEEE Spectrum, pp.68-75, March 1985
24. R.W.Hall et al, "*Coherent Light Emission From GaAs Junctions*", Physics Review. . Letters, Vol.9, pp.336-338, Nov.1962
25. I.P.Kaminow et al, "*Low Threshold InGaAsP Ridge W/G Injection Lasers at 1.3 μm*", IEEE Jl.of QE, Vol.QE-19, p.1312, 1983
26. Z.L.Liau & J.W.Walpole, "*A Novel Technique for GaInAsP/InP Buried Heterostructure Laser Fabrication*", Appl. Phys. Letters, Vol.40, p.568, 1982
27. H.Kogelnik & C.V.Shank, "*Stimulated Emission in a Periodic Structure*", Appl. Phys. Letters, Vol.18, p.152, 1971
28. G.Arnold et al, "*1.3 μm ELEDs Launching 250 μW into a SM Fiber at 100 mA*", Electronics. Letters., Vol.21, p.993, 1985
29. John.M.Senior, "*Optical Fiber Communications: Principles & Practice*", PHI International series on Optoelectronics, Englewood Cliffs, NJ, pp.326-345, 1985
30. C.A.Burrus et al, "*InGaAsP p-i-n Photodiodes with Low Dark Currents and Small Capacitance*", Electronics .Letters., Vol.15(20), pp.655-656, 1979
31. C.E.Hurwitz & J.J.Hsieh, "*GaInAsP/InP Avalache Photo Diodes*", Appl.Phys.Lett., Vol.32(8), pp.487-489, 1978
32. T.P.Lee et al, "*InGaAsP/InP Photodiodes: Microplasma limited Avalanche Multiplications at 1-1.3 μm Wavelength*", IEEE Trans.QE, Vol.QE-15, pp.30-35, 1979
33. G.E.Stillman et al, "*III-V Compound Semiconductor Optical Detectors*", International Symp. on GaAs and Related Compounds, Biarritz, 1984.
34. S.D.Personick, "Receiver Design for Digital Fiber Optic Communication Systems -I", Bell Sys.Tech.Jl., Vol.52, No.6, pp.843-874, July/Aug.1973

Chapter 2

Communication System for GMRT

The electronic system designed to receive astronomy signals with the telescope was briefly described in Sec.1.1.2. Since the antennas are spread over a large area, the communication medium plays a very important role in the receiver system. In the following sections, the requirements of the telescope, for communication purpose are briefly described, followed by the specifications of various parameters as defined by the receiver system. Various options for realizing the communication system using optical fibers are discussed including analog and digital schemes. In conclusion, the analog communication system adopted for the telescope is described in detail.

2.1 System Requirements & Specifications

As described in Sec.1.1, the telescope is expected to detect very faint radio objects (of the order of 10 μJansky). In terms of power levels it turns out to be approximately sub femto watts. Conventional communication media such as coaxial cables, microwave and radio links generate RFI which is several orders of magnitude higher than this power level. Optical fibers are found to be the only inexpensive solution to this stringent requirement. In addition to the RFI requirement, the GMRT receiver requires the following tasks to be carried out by the communication system:

1. The radio astronomy signals received at the RF frequency in two polarisations by the orthogonal feeds at each of the antennas are downconverted to two IFs of 32 MHz bandwidth for each of the two polarisations and transmitted to the centrally located correlator. The communication link between the antenna and the CEB is henceforth referred to as *Downlink*.

2. For interferometry, the LO used for downconversion is required to be synchronous at all the antennas with respect to a central reference oscillator. For this purpose, a reference oscillator signal is sent to each antenna on the communication system and a return LO signal is transmitted back to the central station for round trip phase measurement (described in chapter 3) on the communication channel. The communication link between the CEB and each of the antennas is referred to as *Uplink* hereafter.

3. The earth rotation synthesis described in Sec.1.1 requires that all the antennas track the radio source being observed while the earth rotates. In addition, all the antennas should be capable of changing the direction of observation, whenever required. A high performance Servo control system consisting of DC motors and high efficiency gear system is used for the mechanical control of the antennas with the help of a computer located at each of the antennas. Since the antennas are spread over a vast area, it is virtually impossible to synchronize the antenna movements from the individual locations. Therefore, the communication system is required to convey the control signals to all the antennas from the central computer located at CEB.

4. Monitoring of the electronic systems located at each of the antennas is essential for diagnostic purposes. As it is difficult to manually verify the status of each of the antenna electronics, the monitor signals are sent to CEB over the communication system. It is also desirable to have full duplex voice channel to each location

for installation and maintenance purposes.

To summarize, the GMRT receiver system requirements and communication specifications can be stated as shown below:

1. Transmission of two IF signals each with a bandwidth of 32 MHz either in analog or digital mode.
   In the case of digital, the number of bits/sample should be more than 2 and a BER of $< 10^{-9}$ [1].
   In the analog mode, the Signal to Noise ratio should be better than 20 dB for the farthest antenna.

2. Transmission of LO reference signals so as to maintain a phase error of 3^0 rms at an observation frequency of 1420 MHz.

3. A digital data link, in full duplex mode, to control the antenna movements at a data rate of less than 20 Kbps.

4. A digital data link for voice and monitoring signals at less than 1 Mbps data rate.

2.2 Outline of the Communication System

The requirements of the communication system described above can be realized in many ways. Before analyzing the various options available for the system, it is useful to consider the constituents of the communication system. Shown in Fig.2.1 is the outline of the communication system between CEB and one antenna. In the actual situation, there are 30 such systems required. The communication system can be either digital or analog or a combination of both. The system shown in Fig.2.1 may be considered for both types of communications. In the following section, we consider each of the systems separately.

Digital System The upper half of Fig.2.1 shows the IF signals IF_1 and IF_2 which are downconverted to baseband before being digitized. Similarly, LO signals, Monitor and Voice signals are suitably digitized. The interface unit consists of a data encoder, clock embedding circuits and a channel multiplexer to generate serial data. The Electrical to Optical converter unit converts the data signals to corresponding optical pulses and launches into an optical fiber. At the receiver end, the optical pulses are converted back to serial data stream by the Optical to Electrical converter. The interface unit consists of clock recovery, decoding and data demultiplexing circuits. For the Uplink, the system is similar to the one described above, except that the IF signals are not transmitted. The communication medium may consist of one fiber or two fibers to each antenna. In the case of one fiber/antenna, suitable interfaces are required at each end of the links to isolate the two signal streams flowing in the fiber (in opposite directions). These interfaces may be optical directional couplers with optical isolators or WDM devices. This is elaborated in greater detail in the following sections.

Analog System : In the analog system, the various signals present at the antenna location are first combined at the interface unit, which may consist of a frequency upconverter and power combiner. The combined analog signal modulates the intensity of the optical carrier as discussed in Sec.1.2.5. At the CEB end, the signals are demodulated and appropriately downconverted to the respective frequency bands.
In the case of Uplink, only the LO reference signals control signals and digital audio are transmitted to the remote antenna stations. The digital audio is usually converted to

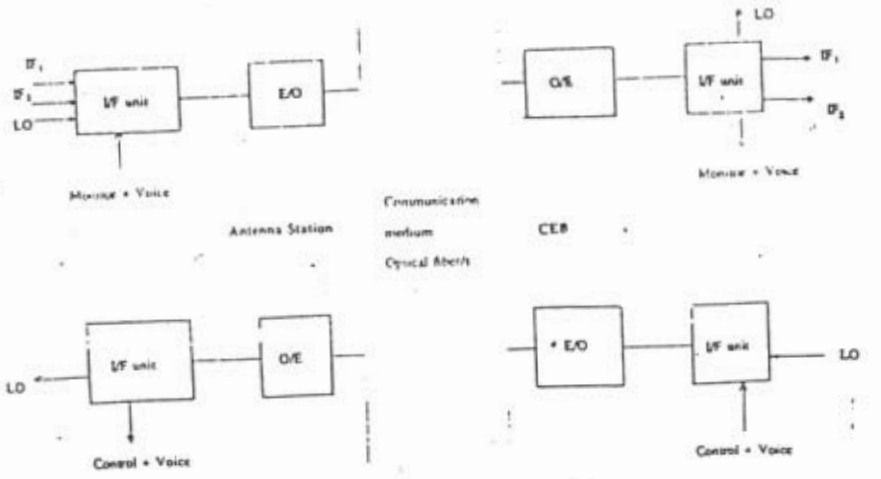

Fig.2.1 Block Schematic of the GMRT communication system for one antenna

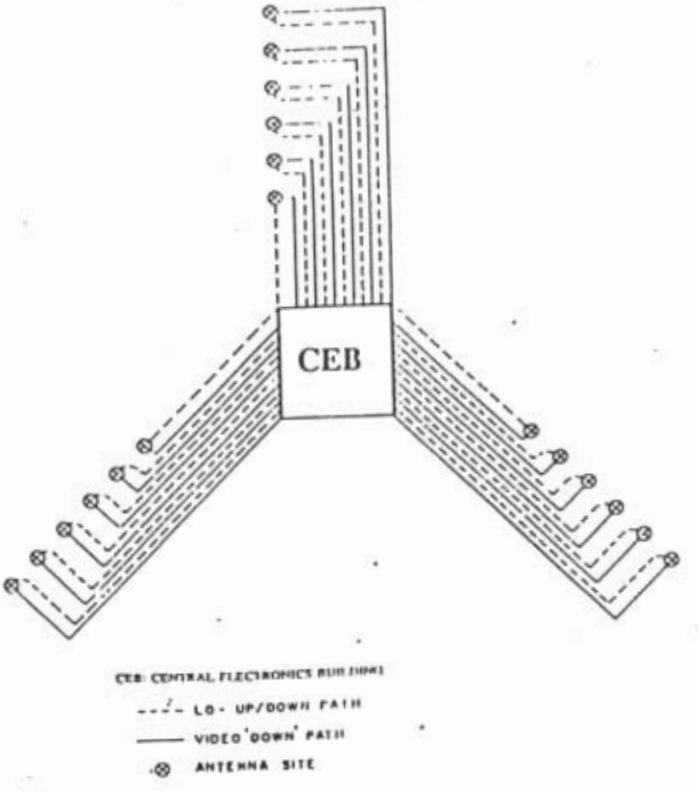

Fig.2.2 Two-Fiber Method

an analog signal by means of a suitable modulation scheme such as FSK or PSK.

2.3 Options Available for implementing the Communication System

There are many possible configurations using optical components and fibers to realize the communication system just described. However, it is advantageous to implement the system with the existing technologies in order to keep the system cost low. In this section, a brief discussion of the alternatives available, with the current technologies, is carried out. First the Y-array with 18 antennas is considered, followed by the Central array consisting of 12 antennas.

Y-array : Three possible configurations of the communication systems for the y-array have been considered and cost comparison was made on the basis of pricing information available at the time of feasibility study of the Project (1987) [2]. Each of the configurations is briefly described below:

i) *Two fibers/each antenna*: In this scheme, one fiber is used for the Uplink of each antenna, consisting of Local Oscillator reference signals, Control signals and voice information. The second fiber is used for transmission of IF signals, LO return, monitor and voice signals on the Downlink (Fig.2.2)

ii) *Two fibers/antenna with Directional Couplers*: The LO reference signals, Control and voice signals are transmitted on a single fiber to all the antennas in each of the Y-arms. In effect, 3 fibers are used to Uplink all the antennas in the Y array (Fig.2.3). A directional coupler is used at each antenna to tap the signals off the fiber. On the Downlinks from the antennas, a separate fiber is used to transmit IF signals, LO return, Monitor and voice signals.

iii) *Bidirectional single fiber /antenna:* In this scheme, a single fiber is used for both Up and Down links. The signals on the Uplink viz. LO reference signals, Control and voice signals are in digital form and so are the signals in the Downlink. Time division multiplexing is employed to isolate the tow links, with the Uplink operating 10% of the time, while 80% of the time is used for the Downlink. The remaining time is used for synchronization purposes. Fig.2.4 illustrates the scheme for one arm of the Y.

There are many variations possible, to realize the multiplexing and demultiplexing of signals in the Uplinks and Downlinks. The amount of electronics involved in each case may vary depending on the modulation scheme, analog/digital complexity etc.; but the optical hardware as outlined in figures 2.2, 2.3 and 2.4 essentially remains the same. Cost analysis was carried out [2] on each of the schemes with the pricing information available in 1987. Table I gives a summary of each of the systems. The prices indicate the upper limit of each of the components operating at 1300nm.

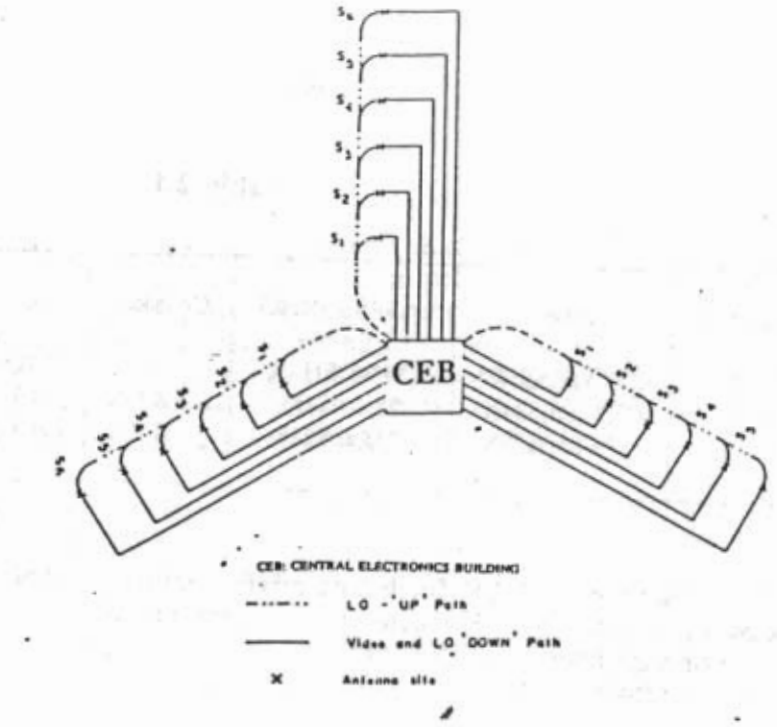

Fig.2.3 Individual Video return, common single LO fiber

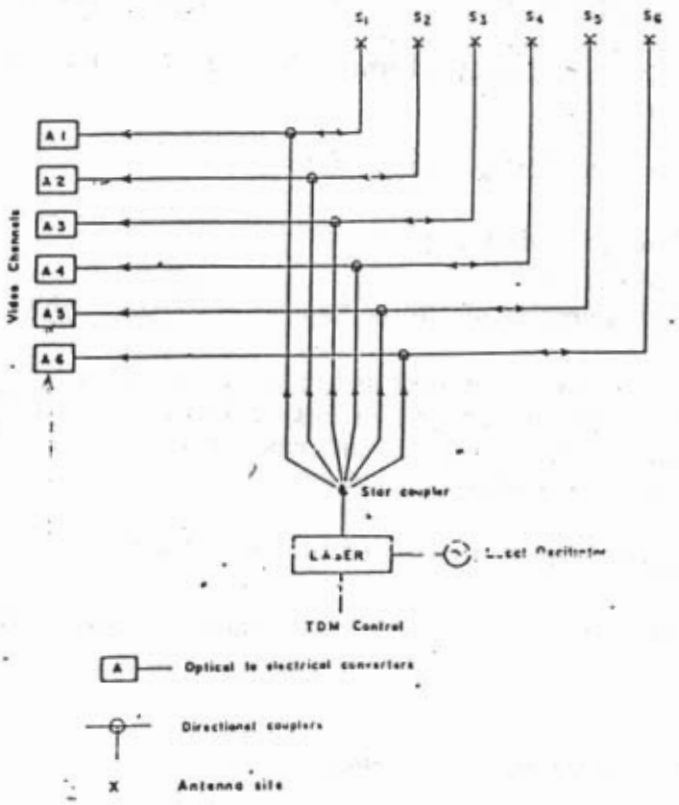

Fig.2.4 'Y' arm : Bi-directional LO/Video Multiplexed Method

Table 2.1

Scheme	Fiber	LASER/PINFET	Couplers	Armouring	Total Cost
I	(378 km)$56K†	(39/36)$114K	-	(54km)$108K	$278K
II	(225 km)$34K	(21/36)$78K	(15)$25K	(54 km)$108K	$245K
III	(189 km)$28K	(21/36)$78K	(18)$30K	(54 km)$108K	$244K

Cost of source = $2.0 K (including driver circuit)
Cost of detector=$1.0 K (including front end circuits)
Cost of bare fiber = $0.15 K per km
Cost of armouring = $2 K per km

The total system cost is approximately in the same range for all the 3 schemes proposed. Due to its simplicity in terms of electronic and optical hardware, scheme I is adopted for the GMRT. We now describe this scheme in greater detail.

Elaboration of Scheme I : In this scheme, each antenna is independently linked to the CEB by 2 fibers. The signals in the Uplink can be either digital or analog. Similarly in the Downlink, the IF signals can be sent directly or after digitization.
In the case of analog, the signals are multiplexed using Frequency Division Multiplexing (FDM). In the case of digital, the signals are Time Division Multiplexed (TDM).
It is more advantageous to implement analog transmission scheme for transmission of IF signals than digital scheme. Some salient points in favor of analog scheme are shown below:

Advantages of Analog transmission:

- Low bandwidth requirement
- Less complex electronic systems at remote stations
- Low cost transmitters and receivers. A typical analog transmitter that can support transmission up to 20 km. distance costs approximately US $ 1200/. The corresponding receiver may cost approximately US $ 300/ including the demodulator and downconversion circuits.
- There is no RFI produced by the analog electronic circuits
- Easy to transmit reference LO signals without additional circuitry

Disadvantages of Analog transmission:

The disadvantages of the analog system may be summarized as below:

† K indicates 1000

- Non linearity of the analog system due to the laser device is predominant. Harmonic distortion and intermodulation produced as a result of non linearity restricts the transmission bandwidth to only one octave. This is due to the fact that 2nd order distortion products resulting from non linearity are more prominent than 3rd order products. If the passband is restricted to one octave, the 2nd order products fall outside the passband. However, with the advances in device technology, the linearity of laser diodes has improved considerably.

- There is a very limited dynamic range [Refer Sec.3.3] available from an analog system. This limitation is due to the limited range of modulation current of the laser diode and the intrinsic noise of the laser [Sec.3.1.1].

- Analog systems are very sensitive to optical reflections. Reflections along the transmission path may severely affect the linearity and sensitivity of the system.

On the other hand digital transmission system suffers from many serious disadvantages. First we'll consider the advantages.

Advantages of Digital transmission:

- High noise immunity

- Insensitive to intrinsic laser noise and optical reflections

- No intermodulation or cross talk between channels

Disadvantages of Digital transmission:

- High level of RFI due to high frequency sampling of IF signals.

- High data rates are required for IF transmission. Two IF channels each of 32 MHz bandwidth and 4 bits/sample require a data rate of 2 X 2 X 32 X 4 = 512 Mbits/sec.
  A digital transmitter operating at 565 Mbps may cost approximately US $ 2000/ while the corresponding receiver may cost approximately US $ 1000/ including clock recovery, decision circuits etc.

- Complex circuitry is required for phase synchronization of LO signals.

- Digital transmission scheme requires that most of the receiver electronics be located at the remote antenna sites except the correlator [Ref. Fig.1.4, chapter 1]. This reduces reliability of the system and increases maintenance costs.

Central Array : In the central array 12 of the antennas are located within 1 km distance from CEB. This places a less stringent requirement on the communication system in terms of power budget and dispersion budget. Two different schemes were considered for this array as shown in Fig.2.5. The bidirectional fiber method makes use of a single high power laser and a star coupler to realize the Uplinks on a single fiber going to each of the antennas. The same fiber is used to convey Downlink signals in a

- Non linearity of the analog system due to the laser device is predominant. Harmonic distortion and intermodulation produced as a result of non linearity restricts the transmission bandwidth to only one octave. This is due to the fact that 2nd order distortion products resulting from non linearity are more prominent than 3rd order products. If the passband is restricted to one octave, the 2nd order products fall outside the passband. However, with the advances in device technology, the linearity of laser diodes has improved considerably.

- There is a very limited dynamic range [Refer Sec.3.3] available from an analog system. This limitation is due to the limited range of modulation current of the laser diode and the intrinsic noise of the laser [Sec.3.1.1].

- Analog systems are very sensitive to optical reflections. Reflections along the transmission path may severely affect the linearity and sensitivity of the system.

On the other hand digital transmission system suffers from many serious disadvantages. First we'll consider the advantages.

Advantages of Digital transmission:

- High noise immunity

- Insensitive to intrinsic laser noise and optical reflections

- No intermodulation or cross talk between channels

Disadvantages of Digital transmission:

- High level of RFI due to high frequency sampling of IF signals.

- High data rates are required for IF transmission. Two IF channels each of 32 MHz bandwidth and 4 bits/sample require a data rate of 2 X 2 X 32 X 4 = 512 Mbits/sec.
  A digital transmitter operating at 565 Mbps may cost approximately US $ 2000/ while the corresponding receiver may cost approximately US $ 1000/ including clock recovery, decision circuits etc.

- Complex circuitry is required for phase synchronization of LO signals.

- Digital transmission scheme requires that most of the receiver electronics be located at the remote antenna sites except the correlator [Ref. Fig.1.4, chapter 1]. This reduces reliability of the system and increases maintenance costs.

Central Array : In the central array 12 of the antennas are located within 1 km distance from CEB. This places a less stringent requirement on the communication system in terms of power budget and dispersion budget. Two different schemes were considered for this array as shown in Fig.2.5. The bidirectional fiber method makes use of a single high power laser and a star coupler to realize the Uplinks on a single fiber going to each of the antennas. The same fiber is used to convey Downlink signals in a

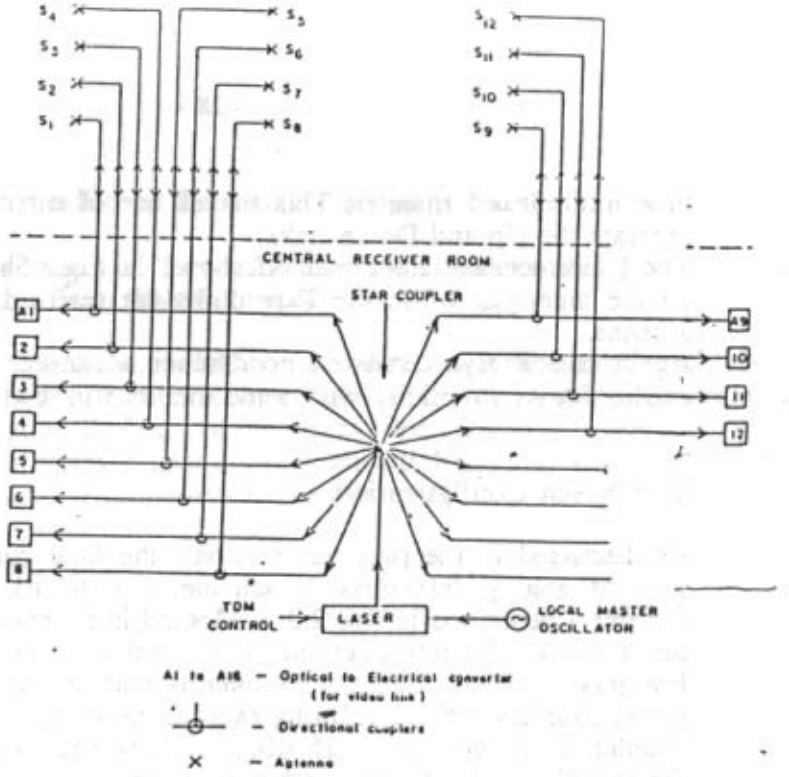

(a)

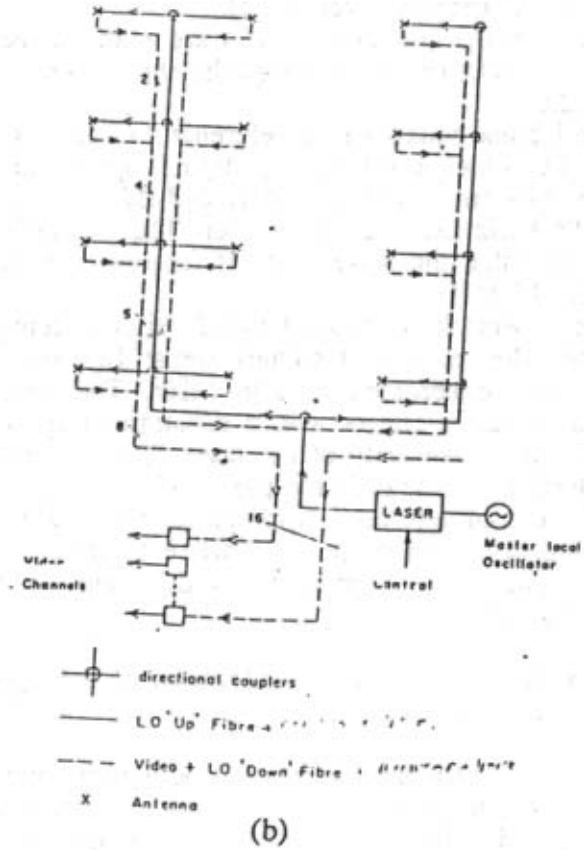

(b)

Fig.2.5 Central Square : (a) Bi-directional Fiber Method
(b) Uni directional Fiber Method

time multiplexed manner. This makes use of directional couplers at the CEB end to separate the Up and Down links.
The Unidirectional fiber method shown in Fig.2.5b consists of 2 fibers for Uplinking all the antennas while the Downlinks are realized using individual fibers from each antenna.
Again cost analysis showed no distinct advantage in either scheme and the latter is chosen for its simplicity with some modifications as explained later.

2.4 Chosen Configuration

As discussed in the previous sections, the final configuration chosen for GMRT consists of analog transmission scheme, due to its simplicity and cost effectiveness. Scheme I described in Sec.2.3 is adopted in its entirety for both Up and Down links of the Y array. The unidirectional fiber method is employed for the central array with a few modifications. The star coupler is realized using a combination of optical directional couplers (of 1:1 splitting ratio at the output). The insertion loss of a 1 x 16 star coupler is approximately 15 dB, including excess loss due to coupling. This exceeds the power budget of the system as described in chapter 3. Therefore two lasers have been incorporated in the Uplinks of the central array to keep the system margin. A combination of directional couplers have been configured as 2 star couplers of 1 X 8 configuration and separate fibers (instead of a common fiber) are used for each antenna.

For the Y array, the Uplinks for nearby antennas which have sufficient system margin are realized using directional couplers. A detailed analysis of the Uplink configuration for the Y array is given in [3].
Both the Up and Down links are realized using analog modulation, with sub carrier multiplexing of various signals; the channel spectra of both the links are shown in Fig.2.6.
The Uplink consists of 2 reference LO signals at 106 and 201 MHz. Control and voice signals, which are basically digital signals, are converted into analog signals using an FSK Modem with f_0= 4 MHz and Δf= 1 MHz. The FSK signals are then upconverted to 18 MHz using a sub carrier. The second stage of upconversion is necessitated by the fact that the lower cut off frequency of the pass band of the optical fiber link is about 15 MHz.
The Downlink consists of two IF signals centered at 130 and 175 MHz, each 32 MHz wide. The return LO signals are at 105 and 200 MHz, while the Monitor and voice signals are centered at 208 MHz. The spectrum in the Downlink is restricted to approximately one octave, a constraint imposed by the non linearity of the laser device. The nonlinearity of the laser device is such that it produces very strong 2nd order distortion products. If the passband is limited to one octave, these products fall outside the band of interest. Appropriate filtering techniques are then used to eliminate the strong distortion products. This restriction is not applicable in the case of Uplinks as the signals have narrow bandwidths and the distortion products can be eliminated by proper filtering.

Finally, the technical specifications of the optical transmitter and receiver used in the Up and Downlinks are summarized in Table 2.2 and Table 2.3 respectively.

The optical transmitter has a modulation bandwidth of nearly 1.0 GHz. The frequency response, mentioned in Table 2.2, indicates a variation of ± 2 dB in the passband compared to the midband frequency response.
The equivalent input noise is indicated only for the laser transmitter. As described in

Sec.3.1.6, the thermal noise in the receiver accounts for the total noise present in the link.
The DC parameters listed in Table 2.2 are typical values and a variation of around 10% is likely to occur from device to device.

Table 2.3 gives the specifications of the optical receiver. The photodiode element has a very low back reflection, which is essential for analog systems for maintaining low intensity noise and good linearity of the lasers (Sec.3.1.1).
The passband of the receiver shows a low cut off frequency of 15 MHz which is due to the design of low noise amplifiers in the circuit.

TABLE 2.2

Specifications of Optical Transmitter

[Laser diode : Lasertron make , Part No.: QLM3S860SPEC]

RF Parameters

1.Modulation bandwidth	: 60 KHz - 1.0 GHz
2.Frequency response	: ± 2 dB
3.Input impedance	: 50Ω
4.Input 1-dB Compression point [*measured with 32 MHz wide, noise source centered @ 175 MHz*]	: > + 10 dBm
5.Input Third order intercept point [*measured at 70 MHz*]	: > + 18 dBm
6.Equivalent input noise [*Laser noise*]	: ≤ -135 dBm/Hz

DC Parameters

1.Slope efficiency [*Slope of Power vs Current curve*]	: ≥0.04 mW/mA
2.Optical output power	: ≥ 0.5 mW
3.Peak optical wavelength	: 1300 ± 10 nm
4.Spectral width (rms)	: < 1.5 nm
5.Maximum DC power requirement	: +5V @ 1 A [T_{amb}= 65°C]
	+5V @ 80 mA [T_{amb}= 25°C]
	-12V @ 80 mA

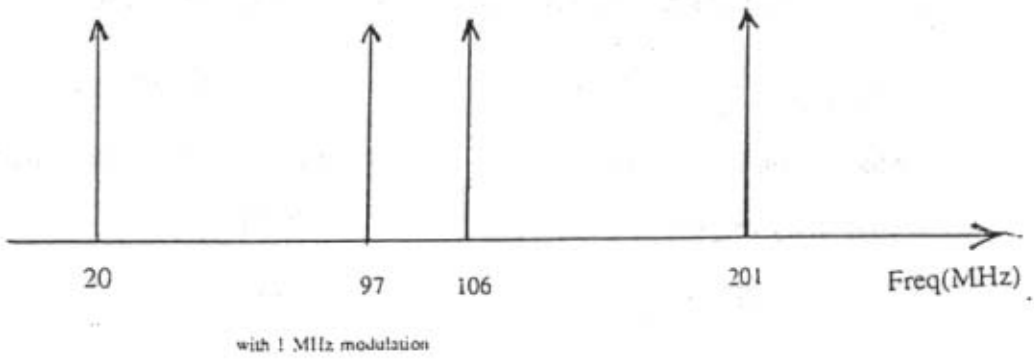

Up link frequencies

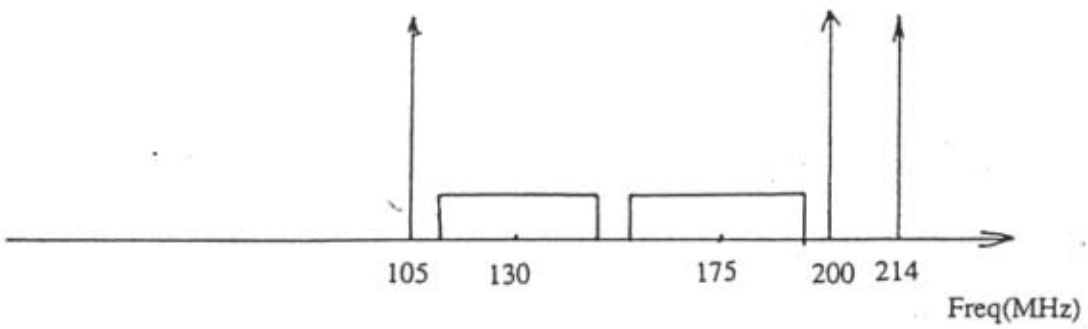

Down link frequencies

The down link is restricted to one octave bandwidth to avoid 2nd order distortion products

Fig.2.6 Channel Spectrum in the Up link and Down link

TABLE 2.3

Specifications of Optical Receiver

[Photodiode : Epitaxx make , Part No.: ETX75FJ-SLR]

RF Parameters

1.Modulation bandwidth	: 7 MHz - 870 MHz (min.)
2.Frequency response	: ± 2 dB
3.Input impedance	: 50Ω

DC Parameters

1.Responsivity	: ≥ 0.8 mA/mW
2.Operating wavelength	: 1100 - 1600 nm
3.Optical return loss	: > 45 dB
4.Maximum DC power requirement	: 12V @ 90 mA

References

1. S.Vivek, "*A note on the GMRT Correlator*", Appendix 7, GMRT Project Report, Bangalore, 1986

2. S.Vivek & Viraf.K.H, "*A note on the Optical Fiber System for GMRT*", Appendix 6, GMRT Project Report, Bangalore, 1986

3. D.S.Sivaraj, " *A new configuration for GMRT Fiber Optic Uplinks*", *NCRA Technical Memo, No. DSS/05/0892, Aug.1992*

Chapter 3

System Design and Analysis

The performance of any communication channel depends on its ability to maintain all the characteristics of the signal being conveyed. Ideally, all statistical and deterministic properties present at the input are transmitted unaltered to the output. But the noise in the channel and non linear properties of the medium invariably alter the signal characteristics during transmission. The channel performance is usually measured in terms of the amount of noise present in the channel, the degree of linearity of the medium and the dynamic range (the range of minimum to maximum signal amplitudes that the channel can transmit without significantly altering the signal properties). In the following sections, these parameters are described in detail. In addition, the phase stability of LO signals is also described.

3.1 Noise Analysis

The significance of channel noise depends on the type of signals being transmitted. Although, in general, all the sources of noise present in the channel contribute to the overall signal degradation, some sources are insignificant in certain types of modulation method. As described in chapter 2. analog communication system is adopted for GMRT, and the types of noise sources that play a significant role can be listed as below:

- Laser intensity noise
- Shot noise
- Thermal noise

3.1.1 Laser intensity noise:

The operating principle of a typical laser diode was described in Sec.1.2.2. From the characteristic curve it can be seen that for a bias current above the threshold, stimulated emission of radiation is produced. But the output power does not remain at a constant level even when the bias current is perfectly stabilized. This phenomenon, known as intrinsic noise, is due to the quantum processes inside the laser cavity [1]. These processes include the shot noise of the injection current, spontaneous recombination of the carriers within the active layer, absorption and scattering of radiation and the stimulated emission. Theoretical analyses by Haug showed that the quantum intensity noise peaks at the laser oscillation threshold where spontaneous emission dominates stimulated emission.
This can be written as follows [2]:

$$RIN \propto \left(\frac{I_b}{I_{th}} - 1\right)^{-3} \qquad (1)$$

RIN is the Relative Intensity Noise given by :

$$RIN = \frac{\langle \Delta P^2 \rangle}{\langle P^2 \rangle} \qquad (2)$$

where,

I_b is the bias current of the laser
and

I_{th} is the threshold current of the laser
<P> is the average laser light intensity
<ΔP> is the mean square intensity fluctuation spectral density of light output

This effect is more pronounced in index guided lasers than in gain guided lasers [3]. It is due to the fact that in gain guided lasers, the transition between lasing and non lasing modes is much smoother than in index guided lasers. However, index guided lasers exhibit lower noise than gain guided lasers above threshold. Apart from spontaneous emission there are other factors contributing to laser noise. In the following sections, some of them are examined in detail.

Partition Noise: The laser cavity supports several lasing modes and the output power is distributed among the modes in a time varying fashion. As a result the output spectrum of the laser varies from time to time. Added to this, the material dispersion of the fiber alters the power in each mode in a random manner. This phenomenon is known as *Mode partition noise*. This is observed in multimode lasers, (where partition of optical power takes place among the longitudinal modes in a random manner) as well as in single mode lasers such as DFB or DBR lasers. In the latter case, the partition noise occurs between the lasing mode and "non lasing mode" [4]. But the amount of noise due to mode partitioning is much smaller in the case of single mode lasers. It is also observed that when the laser has a large number of longitudinal modes, the partitioning noise is reduced drastically [3]. The material dispersion of fiber can aggravate the problem of partition noise by introducing non uniform delays between the modes. The deterioration can be as much as 20 dB [5]. The dispersion effect can be avoided by operating near the zero dispersion wavelength of the fiber.

Reflection induced noise: When a laser diode's optical output power is launched into a fiber, there will be a small portion of the light reflected back to the laser cavity, due to a fiber connector or some discontinuity along the optical path. Due to this reflection, an additional lasing cavity is formed, with light amplification being confined to the original laser cavity. This cavity, known as *external cavity* introduces additional modes. The interaction between these two cavities may lead to severe alteration of laser performance. Change of emission spectrum, non linear behavior of laser device, increased intensity noise are some of the negative effects due to external reflections. Reflections occurring within a few centimeters from the laser cavity and those occurring from a few kilometers away, have considerably different effects and need to be considered separately.

Near End Reflections: In the case of single longitudinal mode lasers, mode stabilization occurs if the external cavity mode has the same lasing wavelength. This will lead to considerable narrowing of spectral width. Linewidths as narrow as 100 kHz have been reported using this technique [6].

On the other hand, if one of the cavity lengths is changing, either due to temperature or due to mechanical instability, the lasing mode changes and mode locking takes place at a different wavelength; thus leading to fluctuations in the light output.

Due to the near end reflections, low frequency noise occurs whose frequency extends up to several kilo hertz [7].

The effect of near end reflections is very prominent in the case of single mode laser. But in the case of multimode lasers, the interaction of the external cavity mode with each of the laser cavity modes produces an averaged result, which is not so severe as in the former case.

Far End Reflections: Reflections from distances longer than the coherence length of the laser are of particular importance when considering far end reflections. In this

situation, sub-modes corresponding to the external cavity modes are generated. The spectral emission is altered and periodic peaks corresponding to the sub modes are observed. The spacing between the peaks $\Delta\nu$ corresponds to the round trip time of the external resonator [8]. If the submodes are sufficiently strong, mode locking may occur, giving rise to peaks in the output spectrum at a frequency corresponding to the inverse of the round trip time and its harmonics extending up to the relaxation resonance frequency [8].
The amount of reflection required to alter the output spectrum as described above, depends on the type of laser and the type of fiber. In general, if the amplitude of the reflected wave is smaller than the relative amount of spontaneous emission, then it is sufficient to avoid the excess noise. When using single mode lasers and single mode fibers, the limit on the reflection is worked out to around -80 dB to -60 dB [3]. This is smaller than the Rayleigh back scattering of fibers, thus necessitating the use of optical isolators with single mode lasers. For multimode lasers (which are used for the GMRT project), the requirement is less stringent: -50 dB to -30 dB. In this case, an optical isolator need not be used.
Optical isolators are non reciprocal devices which transmit light in one direction but forbid it in the other direction. Based on the well known principle of "Faraday rotation", it consists of an input polariser, a Faraday material such as a YIG crystal and an output polariser. The input polariser converts the incident light into a linearly polarised light. The Faraday material rotates the polarisation by 45^0 (as a result of appropriate design) and the polarisation axis of the output polariser is aligned to transmit maximum power at the output. Any back reflections through the output polariser will undergo an additional 45^0 rotation through the Faraday material and become orthogonally polarised to the input polariser. Thus the back reflections are not isolated from the source of radiation.

3.1.2 Shot noise : The generation of photocurrent is a sequence of discrete events that includes the electron hole pair (ehp) and the motion of these charges under the influence of the applied electric field . Each ehp will result in a pulse of current . The total current is the sum of many pulses . The total current is not a smooth continuous flow, but has variation about an average value . This variation is called shot noise.
It is observed that when a photodetector is exposed to a certain no.of photons N, the generated photocurrent indicates an equivalent no.of photons n which is not necessarily equal to N. Because this is a statistical phenomenon, the probability distribution function which defines the probability of detecting n photons when N photons are incident on the detector is found to be

$$P(n) = \frac{N^n . e^{-N}}{n!} \tag{3}$$

This is a Poisson distribution with mean and variance equal to N.

The mean squared value of the shot noise associated with the photo current is

$$\langle i_{sh}^2 \rangle = 2\, e\, I\, B \tag{4}$$

where

$$I = I_d + I_{ph} \tag{5}$$

I_d is the dark current
I_{ph} is the photocurrent due to incident light .

e is the charge of an electron
and
B is the noise bandwidth

3.1.3 Thermal Noise :

Thermal noise was first observed by J.B.Johnson in metallic resistors as early as 1928, which is why it is sometimes referred to as *Johnson noise*. Thermal noise results from the random motion of electrons, in conducting media. The random motion is mainly due to temperature. From the well known kinetic theory, the kinetic energy of electrons at a temperature T is given by kT, where 'k' is Boltzmann's constant.
When a resistance of value R is at a temperature T, random motion of electrons within the resistor produces a noise voltage v(t) at the two terminals of the resistor. From central limit theorem it can be shown that v(t) has Gaussian probability distribution with zero mean and variance σ given by [9],

$$\sigma^2 = \langle v^2(t) \rangle = \frac{2(\pi kT)^2 R}{3h} \tag{6}$$

where, h = Planck's constant.

The power spectral density of thermal noise is

$$N_{th}(f) = 4RkT \qquad Volts^2/Hz \tag{7}$$

This indicates that thermal noise has a flat frequency spectrum. However it does not imply that there is infinite energy available from the resistor. Eqn.7 is only an approximation; at frequencies near the infrared, the spectrum falls off gradually towards zero.
In circuit analysis of noise sources, it is more convenient to define the rms voltage and rms current sources of the thermal noise rather than the noise spectrum. From the above discussion, a Thevenin equivalent circuit and a Norton equivalent circuit of thermal noise can be constructed. As shown in Fig 3.1a the Thevenin circuit consists of a noiseless resistor and a noise voltage source. Similarly, the Norton circuit consists of a noise current source and a noiseless resistor (Fig 3.1b).
The noise power delivered to a load depends upon the load resistance. From the maximum power transfer theorem, it is known that maximum power is delivered when the noise source resistance is perfectly matched to the load resistance. This is known as the maximum available noise power. For worst case noise analysis, this value is usually considered. Mathematically, it is shown to be

$$N_{th}(f) = \frac{1}{4R}.(4kTR) = kT \qquad Watts/Hz \tag{8}$$

which is independent of resistance.

When thermal noise is amplified by an amplifier, additional noise is produced at the output due to the internal noise present in the amplifier. This is quantified by *Noise factor* of the amplifier defined by

$$Noise factor,\ F = \frac{Noise\ power\ at\ the\ output}{Gain\ x\ Thermal\ noise\ at\ the\ input} \tag{9}$$

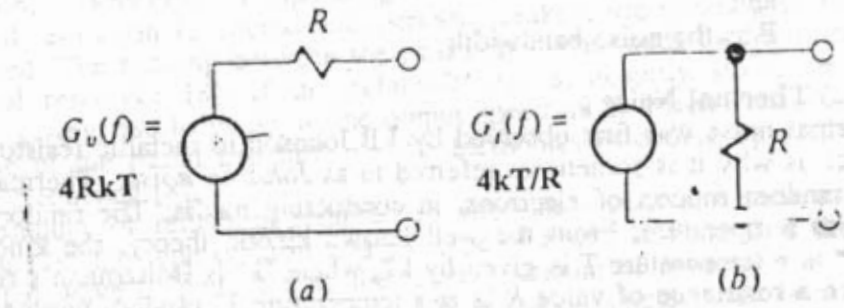

Fig.3.1 Thermal Noise Source (a) Thevenin equivalent circuit
(b) Norton equivalent circuit

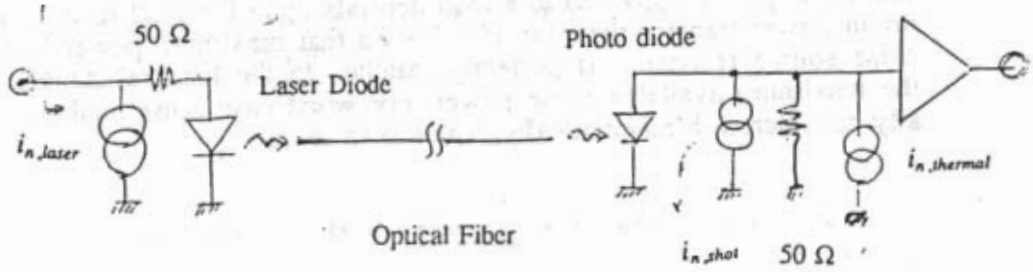

Fig.3.2 Noise sources present in a fiber optic link

Thermal noise at the laser end is ignored as it is small when compared to the laser noise. $i_{n,thermal}$ at the receiver consists of noise due to the resistor as well as the amplifier

Deterioration in thermal noise due to amplifier can be evaluated from the above equations. It can be shown that noise power at the input of the amplifier is given by,

$$N_{th}(f) = (F-1)kT \qquad Watts/Hz \tag{10}$$

where, $N_{th}(f)$ is the aggravated thermal noise due to amplifier with a noise factor F.

3.1.4 Noise Equivalent Bandwidth:

In the preceding sections, the noise sources described, have a flat frequency spectrum. Since the spectrum extends over a wide frequency range, the total noise power is minimized by including bandpass/low pass filters in the bandwidth of the signals of interest, at the receiving end of the channel. The noise spectrum integrated over the passband of the filter gives the total noise power present at the receiver. Noise equivalent bandwidth, a mathematical quantity, defined for ease of calculations, is given by:

$$B = \int_0^\infty \frac{|H(f)|^2 . df}{|H(f)|^2_{max}} \tag{11}$$

In the foregoing sections, the noise equivalent bandwidth is used to calculate the total noise power.

3.1.5 Signal to Noise Ratio :

Before evaluating the optical fiber system shown in Fig.3.2 for Signal to Noise ratio, it is convenient to electrically model all the noise sources in the system .
The intensity variations of optical light can be viewed as corresponding variations in the bias current of the laser . This contributes towards noise in the transmitter and can be equated to some equivalent noise at the input of the laser (EIN_{laser}). If the input circuit, including the laser diode, has an input impedance R_i then EIN_{laser} can be defined as :

$$EIN_{laser} = \langle \Delta I^2 \rangle R_i \tag{12}$$

where ΔI indicates the current fluctuations corresponding to the intensity fluctuations .
The quantities ΔP and P of eqn.2, Sec.3.1.1 can be expressed with the help of the laser characteristic curve, Fig.1.14b, as:

$$\Delta P = S . \Delta I \tag{13}$$

$$P = S.(I_b - I_{th}) \tag{14}$$

where S is the slope of the laser characteristic curve.

The Relative Intensity Noise, RIN can be redefined using the above equations:

$$RIN = \frac{\langle \Delta I^2 \rangle}{(I_b - I_{th})^2} \tag{15}$$

$$i.e \quad \langle \Delta I^2 \rangle = RIN.(I_b - I_{th})^2 \tag{16}$$

Substituting for ΔI in eqn.12, we obtain

$$EIN = RIN(I_b - I_{th})^2 R_i \tag{17}$$

When the laser is biased at some operating current I_b, and modulated by a signal of power RF, the rms signal current, normalized to 50 Ω (i.e R_i = 50 Ω), is given by :

$$\langle i_s \rangle = \sqrt{\frac{RF}{50}} \tag{18}$$

Similarly, the rms laser noise current is given by

$$\langle i_{n,laser} \rangle = \sqrt{\frac{EIN_{laser}.B}{50}} \tag{19}$$

These currents are converted into optical light by the laser . The laser output is given by

$$S.(\langle i_s \rangle + \langle i_{n,laser} \rangle) \tag{20}$$

where S is the slope of the laser characteristic curve. This can be rewritten as :

$$\langle P_{opt} \rangle = S.(\sqrt{\frac{RF}{50}} + \sqrt{\frac{EIN.B}{50}}) \tag{21}$$

The optical output of the laser can be divided into signal and noise components in the optical domain, i.e

$$\langle P_s \rangle|_{opt} = S.\sqrt{\frac{RF}{50}} \tag{22}$$

$$\langle P_{n,laser} \rangle|_{opt} = S.\sqrt{\frac{EIN.B}{50}} \tag{23}$$

The optical output, P_{opt} is coupled to the optical fiber and as it travels through the fiber it undergoes an attenuation proportional to the length of the fiber . If α is the total attenuation of the fiber of a given length L, then the power received at the receiver turns out to be

$$\langle P_{rec} \rangle = \langle P_{opt} \rangle.\alpha \qquad Watts \tag{24}$$

This power is converted into electrical current by the photodiode according to the following relation :

$$\langle i_{ph} \rangle = \langle P_{opt} \rangle.\alpha.R \qquad Amp \tag{25}$$

where R is the responsivity of the photodiode (measured in Amp/Watt).

The photodiode is terminated by a 50 Ω resistor for matching purpose . Due to this only one fourth the power is delivered to the amplifier, following the photodiode (see Fig.3.2) . Now, the power delivered to the amplifier is given by

$$\frac{1}{4}< i_{ph}^2 >.50 = \frac{1}{4}(RF + EIN.B).(SR\,\alpha)^2 \qquad Watts \qquad (26)$$

This consists of signal power as well laser noise power, i.e

$$<P_s> = (RF).(\frac{1}{2}SR\,\alpha)^2 \qquad Watts \qquad (27a)$$

$$<P_{n,laser}> = (EIN.B).(\frac{1}{2}SR\,\alpha)^2 \qquad Watts \qquad (27b)$$

The shot noise at the input to the amplifier is

$$<P_{n,sh}> = \frac{1}{4} < i_{sh}^2 >.50.B \qquad Watts \qquad (28)$$

or

$$<P_{n,sh}> = \frac{1}{2} .e. (RP_0\alpha + I_d)50.B \qquad Watts \qquad (29)$$

where

P_0 = Ave.optical power corresponding to the dc bias of the laser
e = Charge of an electron
B = Noise equivalent bandwidth

The thermal noise present at the input of the amplifier is the sum of noise power of the matching resistor, given by eqn.8, and that of the amplifier, given by eqn.10. Therefore, the effective thermal noise at the input of the amplifier integrated over the noise bandwidth B is:

$$<P_{th}> = F.k.T.B \qquad Watts \qquad (30)$$

The total noise contribution from all the noise sources is

$$<P_{n,total}> = <P_{n,laser}> + <P_{n,sh}> + <P_{th}> \qquad Watts$$

$$= [EIN_{laser}.(\frac{1}{2}SR\,\alpha)^2 + 25.e.(RP_0\alpha + I_d) + FkT].B \qquad Watts \qquad (31)$$

This noise is present at the input of the amplifier .

The signal to noise ratio is given by

$$\frac{S}{N} = \frac{RF.\left[\frac{1}{2}SR\,\alpha\right]^2}{\left[EIN_{laser}(\frac{1}{2}.SR\,\alpha)^2 + 25e\,(RP_0\alpha + I_d) + FkT\right]B} \qquad (32)$$

When the laser noise is the dominant source of noise, the expression reduces to :

$$\frac{S}{N} = \frac{RF}{EIN_{laser}.B} \tag{33}$$

which is independent of optical loss .

When thermal noise is the dominant source of noise, the expression changes to

$$\frac{S}{N} = \frac{RF(\frac{1}{2}.SR\,\alpha)^2}{FkTB} \tag{34}$$

which indicates that

$$\frac{S}{N} \propto (\alpha)^2 \tag{35}$$

When shot noise is dominant, the equation takes the following form :

$$\frac{S}{N} = \frac{\left(\frac{1}{2}SR\,\alpha\right)^2.RF}{25.e.(RP_0\alpha + I_d).B} \tag{36}$$

The variation of S/N is plotted in Fig.3.3, elucidating the effect of the three noise sources. It can be seen from this graph that for an optical loss of 10 dB, which is the worst case situation for GMRT, the SNR is approximately 28 dB. The noise power as referred at the input of the amplifier given by eqn.30, when α.L =-10 dB, B = 100 MHz, is -172 dBm/Hz.

3.1.6 Effect of SNR on Telescope's sensitivity

Due to the high level of laser noise and thermal noise, the noise figure of the optical fiber link is very high [typ. 60 dB]. The effect of this can be analyzed theoretically as shown below :

Let EIN_{OFS} represent the equivalent noise of optical fiber system at its input. This quantity can be evaluated by using eqn.31, where the total noise in the optical fiber system is referred at the input of the amplifier (refer Fig.3.2). To translate this quantity at the input of the laser, one can use eqn.27b and replace EIN_{laser} and $\langle P_{n,laser} \rangle$ by EIN_{OFS} and $\langle P_{n,total} \rangle$ respectively. Solving for EIN_{OFS}, we obtain

$$EIN_{OFS} = EIN_{laser} + \frac{\left[25.e.(RP_0\alpha + I_d) + F.k.T\right]}{\left(\frac{1}{2}SR\,\alpha\right)^2} \tag{37}$$

Eqn.37 indicates that the equivalent input noise of the optical fiber system is a function of optical loss. This is shown in Fig.3.4. Accordingly, the noise figure of the optical link varies from antenna to antenna. The high noise figure of the optical link has a pronounced effect on the sensitivity of the telescope receiver as will be shown in the

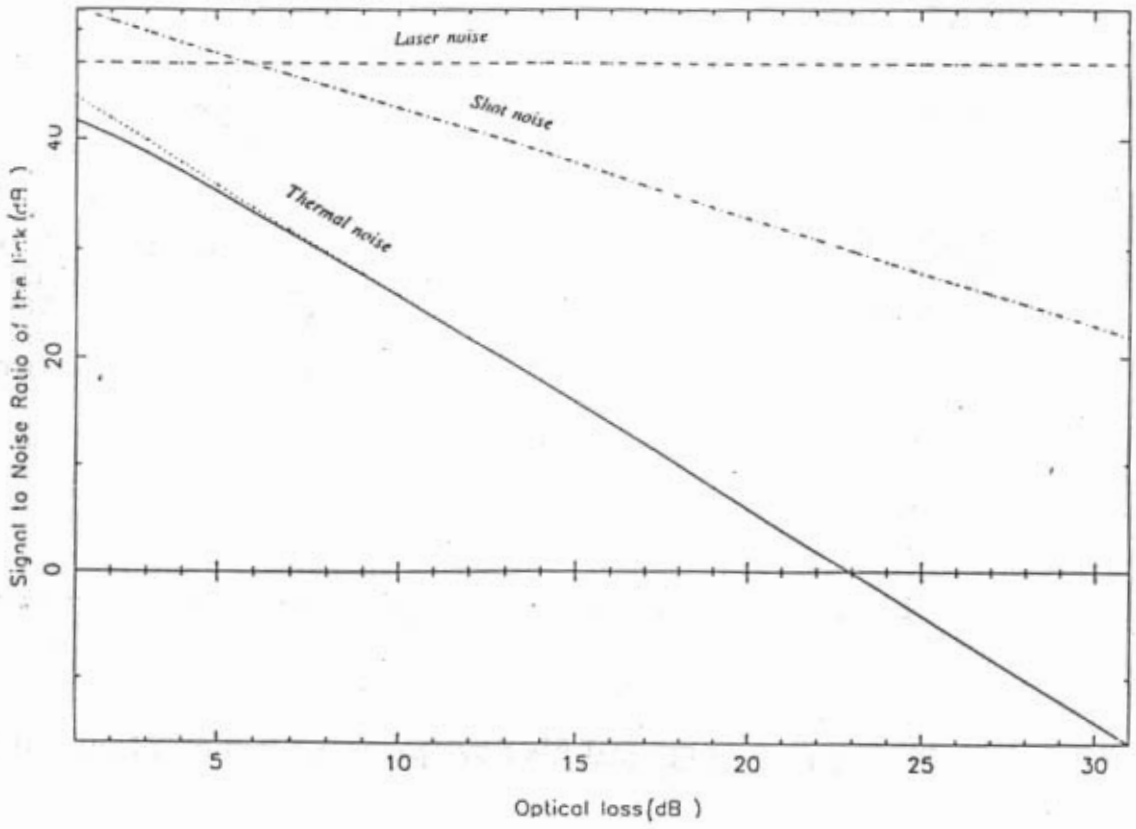

Fig.3.3 Variation of SNR due to various noise sources as a function of optical loss

Table 3.1 Parameters used in Fig.3.3

Signal power, RF	-10 dBm
EIN_{laser}	-137 dBm/Hz
Laser slope S	0.047 mW/mA
Photodiode Responsivity R	0.8 mA/mW
Photodiode Dark current I_d	5 nA
Laser Power P_0	0.5 mW
Amplifier Noise Figure F	2 dB
Noise Bandwidth B	100 MHz

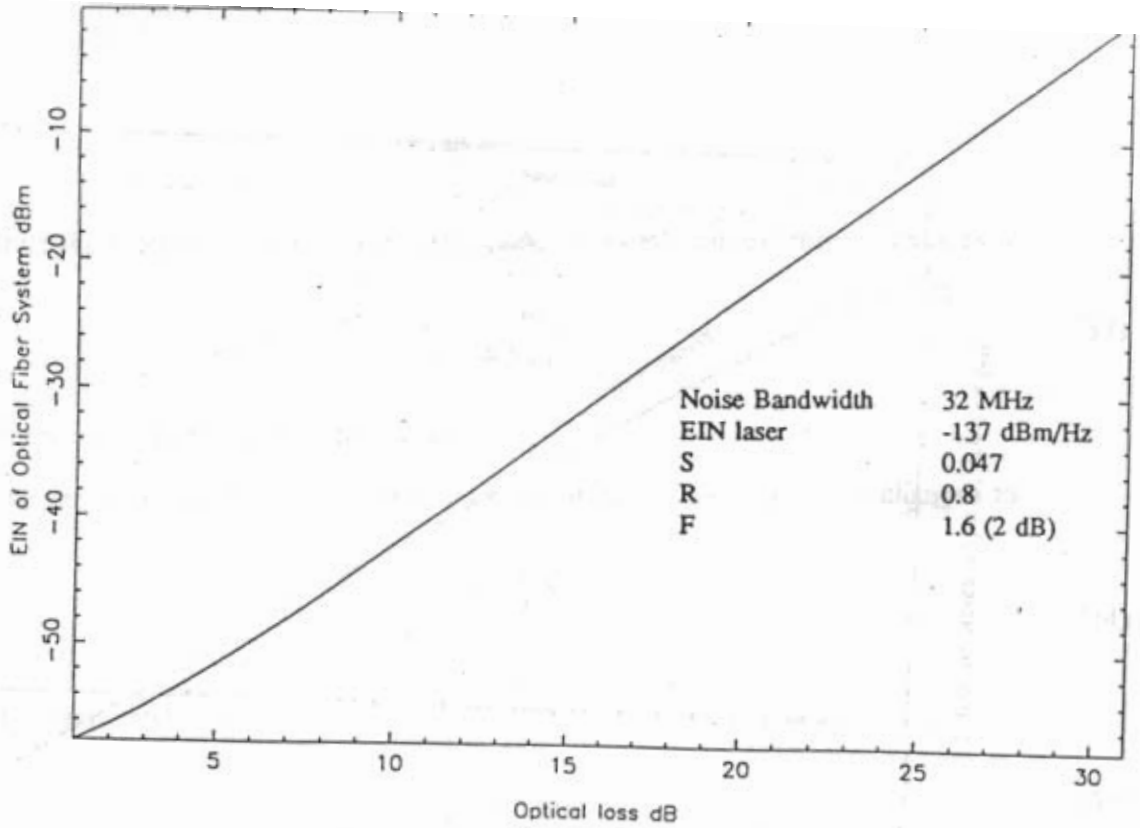

Fig.3.4 EIN of Optical fiber system as a function of optical fiber loss

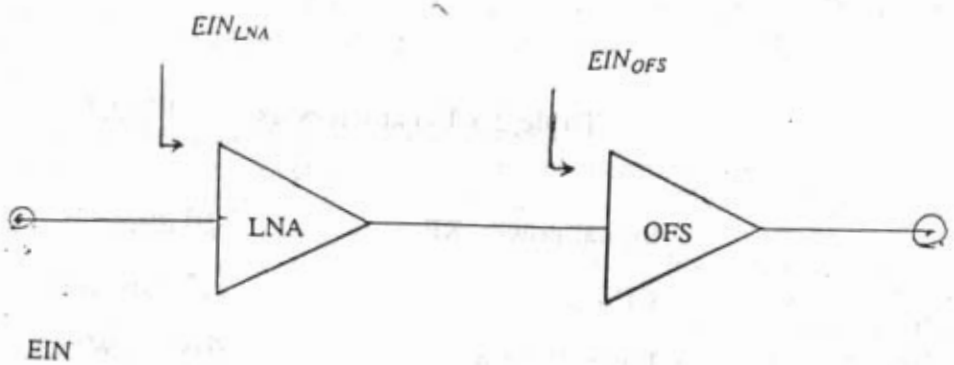

Fig.3.5 The equivalent picture of noise sources in the communicaiton system

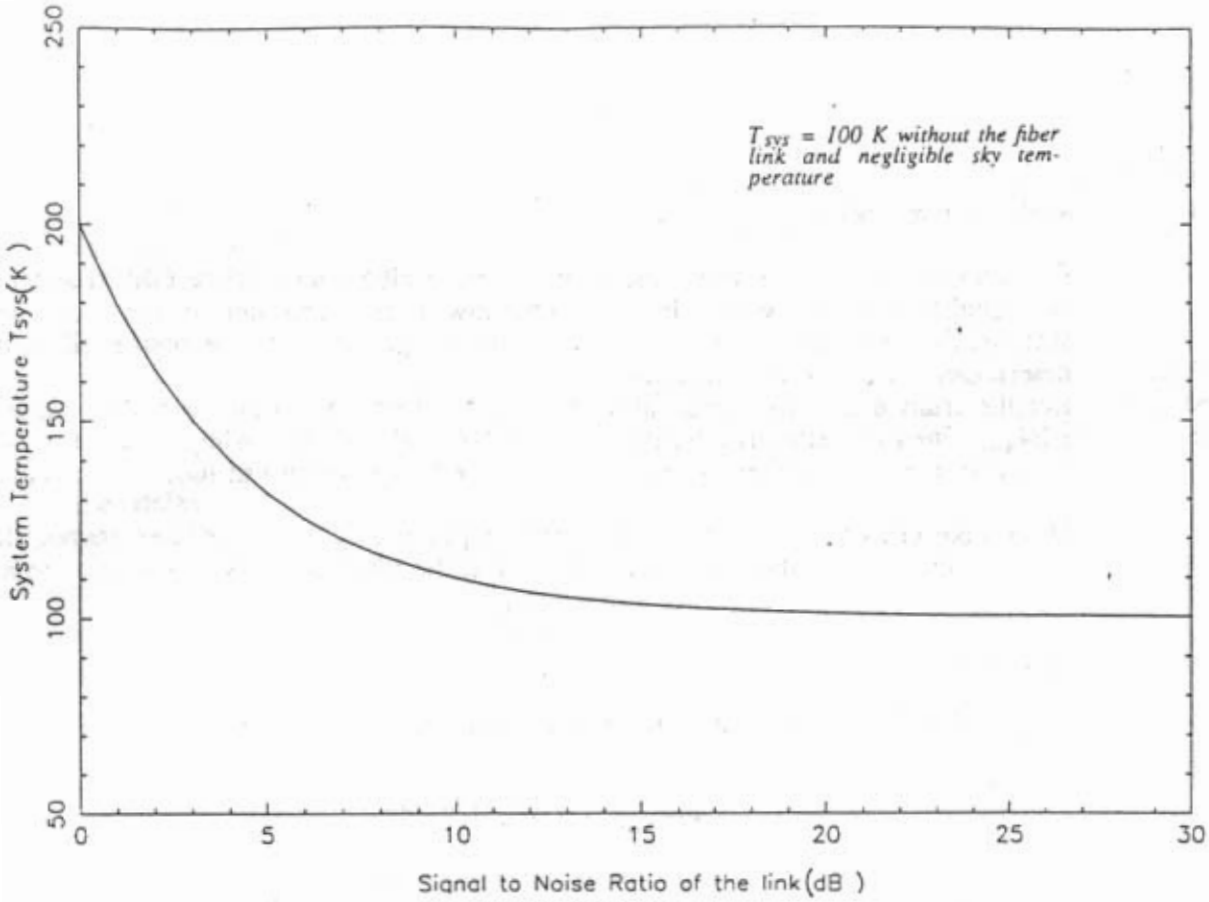

Fig.3.6 The effect of SNR on receiver sensitivity

analysis given below.

From the noise point of view, the entire receiver electronics of the GMRT antenna can be simplified as shown in Fig.3.5. The low noise amplifier at the front end has sufficiently high gain, so that the over all noise figure (up to the optical fiber link) is determined by the front end alone .
Let the front end noise temperature (T_{LNA}) correspond to an equivalent input noise, EIN_{LNA} when the effective output of the LNA and the succeeding stages are not connected to the optical fiber system but terminated by a resistor at room temperature.

If we take G as the gain of the front end amplifier and the succeeding stages, then the noise of the optical fiber system as referred at the input of LNA can be written as :

$$\frac{EIN_{OFS}}{G} \tag{38}$$

The total noise at the input of the LNA is given by

$$EIN_{Total} = EIN_{LNA} + \frac{EIN_{OFS}}{G} \tag{39}$$

In most cases, the antenna is looking at faint radio sources, whose power levels are below the noise power of the front end . As a result, the signal that is present at the input of the optical fiber system consists of the noise power of the LNA amplified by G . This can be formulated as :

$$\frac{S}{N} = \frac{EIN_{LNA}.G}{EIN_{OFS}} \tag{40}$$

The overall sensitivity is determined by the equivalent input noise of the entire system, given by EIN_{Total} .This can be rewritten as :

$$EIN_{Total} = EIN_{LNA} + \frac{EIN_{LNA}}{S/N} \tag{41}$$

This is depicted graphically in Fig.3.6.
In order not to degrade the sensitivity of the receiver system, the lower limit on S/N is arbitrarily fixed at 20 dB (100). This figure corresponds to a degradation in the sensitivity by 1 % for the case when receiver temperature of the RF front end including sky and ground contribution is 100 K.

It is interesting to note that in the GMRT array, the antennas receive very faint astronomical signals which can be millions of times weaker than the system noise due to any background sky radiation, ground leakage and receiver electronics such as polarisers, amplifiers etc. However, due to statistical independence of each of the antennas' noise sources, a cross correlation between any two antennas would minimize the rms fluctuations due to the system noise (if the bandwidth of the receiver is large and the integration time is sufficiently long) while retaining the astronomical signal (in the form of auto-correlated function). This is due to the fact that all the antennas receive signals from the same source, albeit with different geometrical delays, which can be compensated digitally in the correlator [3].
Thus, the optical fiber generally transmits only the receiver noise with a tiny fraction

of the astronomical signal. The signal power referred to in Sec.3.1.5 is actually the noise power of the front end system amplified by the overall gain of the system extending up to the fiber optic link.

3.2 Linearity

A communication system is said to be linear if the input phase and amplitude are preserved at the output. Quantitatively, given an input x(t), the system is said to be linear, if the output, y(t), differs from the input only by a scaling factor and a finite time delay.
Analytically,

$$y(t) = K.x(t-t_d) \tag{42}$$

where K and t_d are constants . In the frequency domain, the output spectrum is

$$Y(f) = K.e^{-j\omega t_d} . X(f) \tag{43}$$

where X(f) is the Fourier transform of x(t) .

If we define the transfer function of the communication channel as

$$H(f) = \frac{Y(f)}{X(f)} \tag{44}$$

then it turns out that

$$H(f) = K.e^{-j\omega t_d} \tag{45}$$

This implies that the channel should have a constant amplitude response and a negative phase shift i.e
$|H(f)| = K$ and $\angle H(f) = -2\pi f t_d \pm m$

Practically it is not feasible to obtain such an ideal frequency response . Generally the channel spectrum is studied only in the pass band of the input spectrum .
Depending upon the variations of the frequency response, several types of distortion are defined . The three major types of distortion usually considered are :

1. $|H(f)| \neq K$, called amplitude distortion

2. $\angle H(f) \neq -2\pi f t_d \pm m.\pi$, known as phase distortion

3. Non linear distortion caused by non linear elements present in the system.

The first two types can be grouped under 'linear distortion' which can be well defined, based on the transfer function of a linear system . The third type of distortion

precludes the existence of a transfer function .

3.2.1 Linear Distortion :

Linear distortion includes any amplitude or delay distortion associated with a linear transmission system . Amplitude distortion means that the output frequency components are not in correct proportion . Since this is caused by |H(f)| not being constant with frequency, amplitude distortion is sometimes called frequency distortion .

The most common forms of amplitude distortion are excess attenuation or enhancement of extreme high frequencies or low frequencies in the signal spectrum . Less common, but equally bothersome, is disproportionate response to a band of frequencies within the spectrum .

Delay distortion is another kind of linear distortion in which the phasé shift of the signal frequencies is not linear . This results in different frequencies undergoing different amounts of time delay, causing delay distortion . The time delay can be expressed analytically

$$t_d(f) = \frac{-/H(f)}{2\pi f} \tag{46}$$

which is independent of frequency only if /H(f) is linear with frequency .
One of the most important effects of delay distortion is pulse dispersion. This leads to an upper limit on the transmission bandwidth .
Linear distortion can be eliminated - theoretically, and to a good approximation, practically - by using equalisation networks . These networks are connected in cascade with the distorting transmission channel and correct for the variations in the passband of the signal, thus providing a distortionless signal . The transfer function is given by

$$H_{eq}(f) = \frac{K.e^{-j\omega t_d}}{H(f)} \tag{47}$$

The overall transfer function $H_{eq}(f).H(f)$, produces $K.e^{-j\omega t_d}$, which is the required response .

3.2.3Nonlinear Distortion

A system having non linear elements cannot be described by a transfer function in frequency domain . Instead, the instantaneous values of input and output are related by a curve or function y(t) = T{x(t)}, commonly called the transfer characteristic. Fig.3.7 is a representative transfer characteristic; the flattening out of the output for large input excursions is the effect due to saturation or cut off of the system .
In this chapter, we will consider only memoryless nonlinear devices, which can be completely described by the transfer characteristic .
The transfer characteristic of Fig.3.7 is in general approximated by a polynomial of the form,

$$y(t) = a_1x(t) + a_2x^2(t) + a_3x^3(t) + \cdots \tag{48}$$

The higher powers of x(t) give rise to the non linear distortion . If we look at the frequency spectrum,

$$Y(f) = a_1X(f) + a_2X(f)*X(f) + a_3X(f)*X(f)*X(f) + \cdots \tag{49}$$

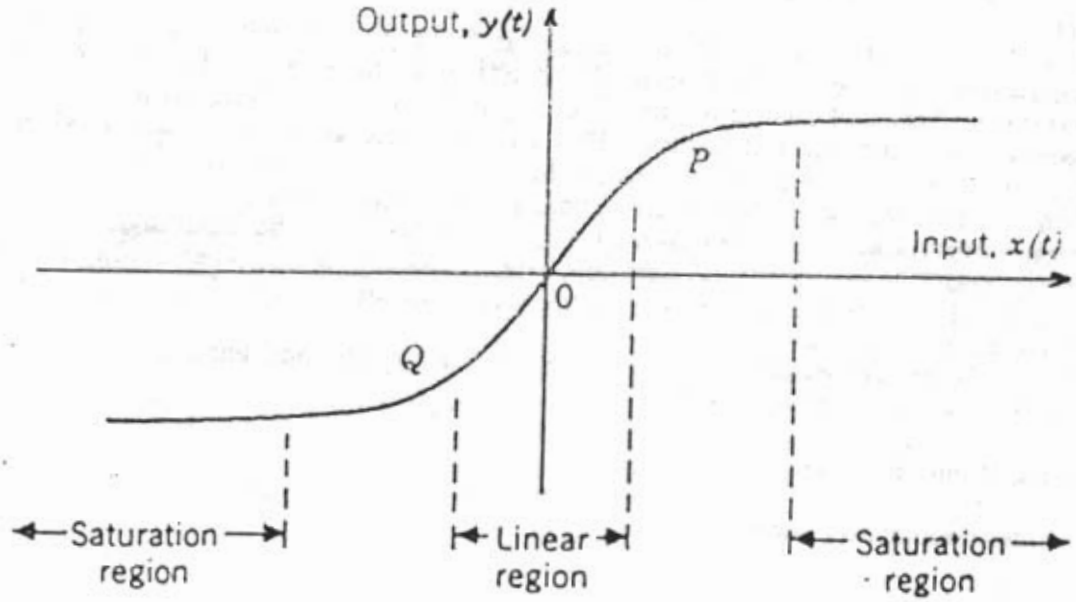

Fig.3.7 Transfer characteristic of a non linear device

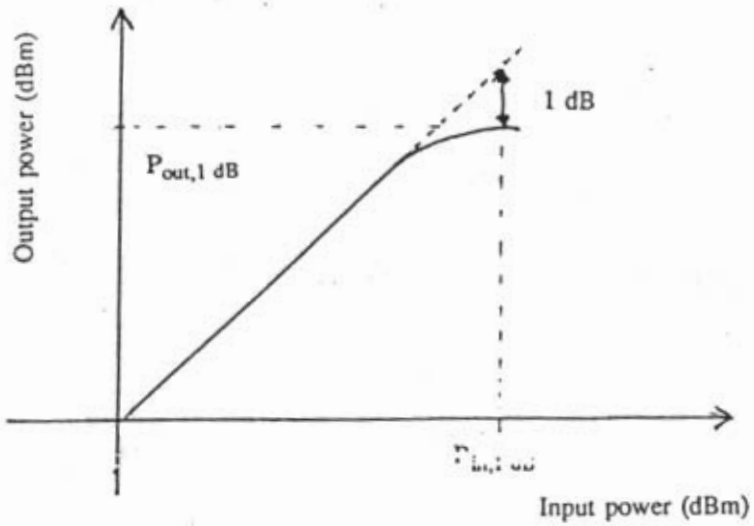

Fig.3.8 1-dB Compression Point

where X(f)*X(f) denotes convolution .
This clearly indicates that a transfer function of the form Y(f)/X(f) is difficult to obtain.
A closer look at equation 49 indicates that for a given bandlimited input signal of bandwidth W, the product term X(f)*X(f) will have a bandwidth of 2W and X(f)*X(f)*X(f) will have 3W etc . The output Y(f) can be filtered to include only the bandwidth of the input spectrum . This will eliminate all the distortion products outside the passband . But the spectra of higher order terms overlap with X(f), creating non linear distortion . There is no simple way to eliminate this distortion . There have been some solutions to circumvent this problem, wherein, the input signal is made to pass through a pre distorting network, whose characteristics, when multiplied by the transfer characteristics of the system, produces a linear characteristic . These are called 'Linearizing networks' .

There are several parameters used to quantify the non linear distortion ; Of the more important ones, we have,

1.Harmonic distortion

1.Intermodulation distortion

3.1-dB compression point

4.Third order Intercept Point (TOI).

Harmonic Distortion: Harmonic distortion occurs when the input consists of a single frequency and the corresponding output consists of all the harmonics of the signal . If $x(t) = \cos \omega_o t$, then from eqn.48, we have,

$$y(t) = a_1 \cos\omega_0 t + a_2^2 \cos^2\omega_0 t + a_3^3 \cos^3\omega_0 t + \ldots\ldots \tag{50}$$

Further simplification yields,

$$y(t) = (\frac{a_2}{2}+\frac{3a_4}{8}+\ldots) + (a_1+\frac{3a_3}{4}+\ldots)\cos\omega_0 t + (\frac{a_2}{2}\frac{+a_4}{4}+\ldots)\cos 2\omega_0 t + \ldots. \tag{51}$$

Second harmonic distortion is defined as the ratio of the second harmonic to the fundamental :

$$\textit{Second harmonic distortion} = \frac{(\frac{a_2}{2}+\frac{a_4}{4}+\ldots)}{(a_1+\frac{3a_3}{4}+\ldots)} \tag{52}$$

Similarly Third harmonic distortion and higher harmonic distortions are defined as the ratio of the respective harmonic amplitude to that of the fundamental .

Intermodulation Distortion:Now let's consider x(t) which consists of 2 frequency components :

$$x(t) = A_1 \cos \omega_1 t + A_2 \cos \omega_2 t \qquad (53)$$

Inserting this in eqn.48, we get a complex output which can be summarized as follows :

1.The second term $a_2x^2(t)$ of eqn.48 produces a dc and a second harmonic component as seen earlier . But it also produces new components at f_1+f_2 and f_1-f_2 that are the sum and difference frequencies respectively . Such components are referred to as Second order intermodulation products .

2.The third term $a_3x^3(t)$ produces the expected fundamental and third harmonic components . In addition, it gives rise to intermodulation products of its own, at the frequencies : $2f_1 \pm f_2$ and $2f_2 \pm f_1$, which are referred to as Third order intermodulation products. Table 3.2 gives a summary of the frequencies and the corresponding amplitudes of the various second and third order products.

TABLE 3.2

Summary of Intermodulation Products

Types of Intermodulation Distortion	Frequency	Amplitude
Second Order		
	f_1+f_2	$a_2.A_1.A_2$
	f_1-f_2	$a_2.A_1.A_2$
Third Order		
	$2f_1+f_2$	$\frac{3}{4}.a_2A_1^2.A_2$
	$2f_1-f_2$	$\frac{3}{4}.a_2A_1^2.A_2$
	$2f_2+f_1$	$\frac{3}{4}.a_2A_1.A_2^2$
	$2f_2-f_1$	$\frac{3}{4}.a_2A_1.A_2^2$

1-dB Compression Point : If we plot the output power against the input power of a linear (time invariant) system, we expect to see a graph similar to Fig.3.8 (dotted line). However, when the system is nonlinear, the output power will not increase at the rate as the input power. This is shown in Fig.3.8 (solid line). For sufficiently small levels of input power, the system may look linear, but at higher power levels, the response deviates from the linear graph. 1-dB compression point is defined as that point at which the deviation from the linear graph is 1 dB measured at the output.

Third Order Intercept Point: If we take a signal of a single frequency and allow it to pass through a non linear system, the output will consist of second harmonic, third harmonic and higher harmonic signals in addition to the fundamental frequency . If the power levels of each of the harmonics were observed as a function of the input power, it would look similar to Fig.3.9 .
From eqn.48 it can be seen that if x(t) = Acosωt then the output

$$y(t) = a_1x(t) + a_2x^2(t) + a_3x^3(t) + ...$$
$$= a_1A\cos(\omega t) + a_2A^2\cos^2(\omega t) + a_3A^3\cos^3(\omega t) + ... \quad (54)$$

The harmonic levels are given by :

Fundamental $= A\, a_1 + A^3.a_3/2$

2nd harmonic amplitude $= \frac{1}{2}\, a_2.A^2$

3rd harmonic amplitude $= \frac{1}{4}\, a_3.A^3$

If the output and input are plotted on a log-log scale, it is easily seen that the fundamental will have a slope of 1, 2nd harmonic will have a slope of 2 and the 3rd harmonic will have a slope of 3 as shown in Fig.3.9.

From a similar argument it can be shown that the variations of 2nd and 3rd order IMD products are similar to 2nd and 3rd harmonic levels respectively. The third order intercept point is defined as the power level at the output, at which the 3rd order IMD product intersects with the fundamental frequency component .

3.3 Dynamic Range

Dynamic range of any system is the range of signals which the system is capable of handling without distorting the signal quality perceptibly . Depending on the kind of distortion considered, various types of dynamic ranges exist :

1.Spurious free dynamic range : This parameter quantifies the range of input signal levels, in which spurious products are insignificant . It is measured with respect to the 3 rd order intercept point at the output . Analytically,

$$SFDR = \left[\frac{P_{out,int}}{N_{out}}\right]^{2/3} \quad (55)$$

where,
$P_{out,int}$ = Third order intercept point measured at the output
N_{out} = Noise power at the output

2.Compression dynamic range : This is the most commonly used parameter, in which the saturation level is considered as the upper limit .

$$CDR = \left[\frac{P_{in,sat}}{N_{in}}\right] \quad (56)$$

where,
$P_{in,sat}$ = 1 dB compression point measured at the input

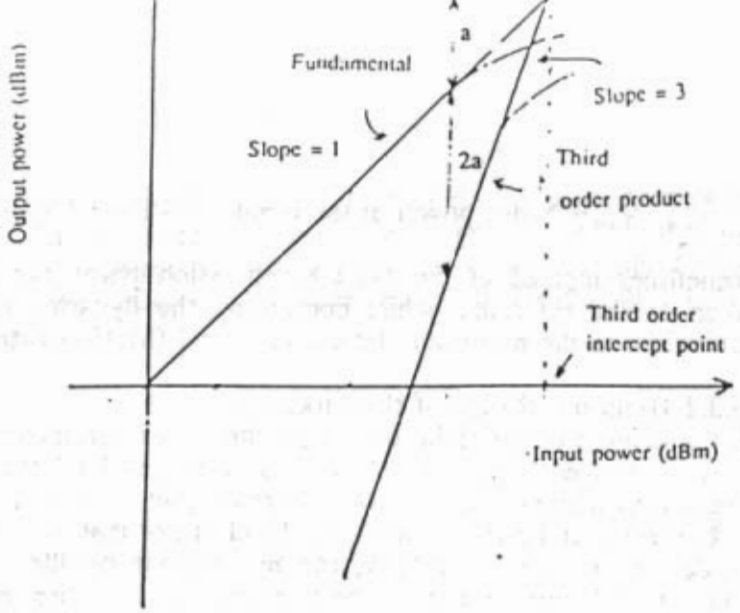

Fig.3.9 Third Order Intercept point

For a non linear system, the third order intermodulation products will be twice as much below the fundamental level as the fundamental is below the input third order intercept point (TOI) e.g if the output power for fundamental decreases by **a** *dB from TOI, the 3rd order product will decrease by* **3a** *dB*

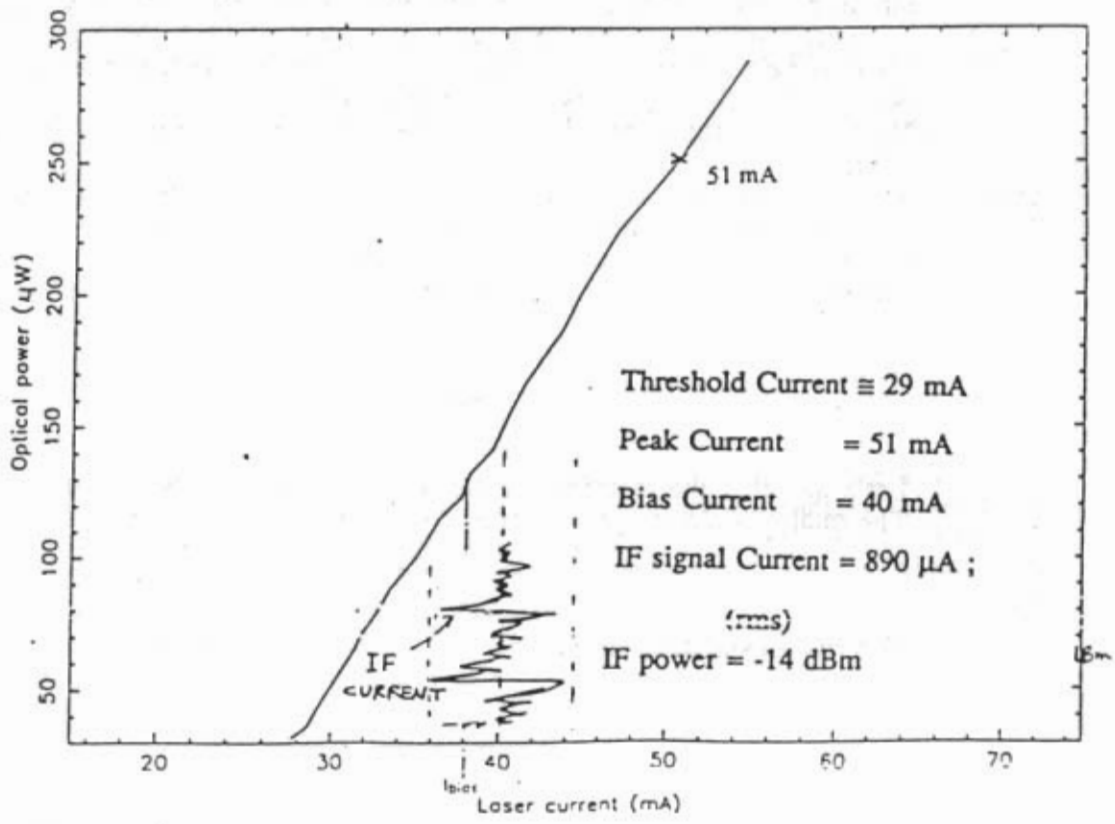

Fig.3.10 Laser diode characteristics and the operating conditions for IF signal transmission

N_{in} = Noise power at the input

Sometimes instead of the 1-dB compression point, the third order intercept point is taken as the reference while computing the dynamic range. The lower limit N_{in} is equivalent to the minimum detectable signal (MDS) of the system.

3.3.1 Dynamic Range of the link:

In the context of the radio telescope, the above parameters cannot be used to define the dynamic range of the link . As discussed in Sec.3.1.5 the minimum signal level is constrained to maintain S/N = 100. Therefore, when considering the dynamic range of the link, the lower limit on the signal level is not that of the noise present in the channel as defined earlier. Similarly, the upper limit on the signal level is defined by the amount of distortion that can be tolerated by the entire telescope system. There are two cases one has to consider while determining the tolerable distortion : 1.Radio frequency interference and 2.Observation of Strong astronomical sources. In the following sections we will analyze each of the cases separately.

Radio Frequency Interference: Due to the high sensitivity of the telescope, unwanted radio frequency signals such as Police wireless, UHF/VHF Television carriers are received by the antennas. These interference signals are usually stronger than the system noise and the astronomical sources. In order to eliminate the effect of interference, the corrective action is taken at the correlator end where the FFT output is examined for strong interference signals in each of the output channels. Whenever interference is present in one or more of the channels, it is blanked out by resetting the respective output channels. This eliminates the primary affect of interference signals; but due to the non linearity in the communication channel, 3rd IMD products are generated. Measurements have shown (Chapter 4) that the resulting non linear products are about 60 dB below the signal levels (i.e front end noise levels).

Now, we consider the maximum level of the interference signal that the link can tolerate.

The laser characteristic curve shown in Fig.3.10 indicates the operating power levels of the communication system when the telescope is observing weak sources. In the IF channel, the total power, say P_{IF} is -14 dBm in 32 MHz.

The corresponding rms signal current is

$$\langle I_{rms} \rangle = \sqrt{\frac{P_{IF}}{50}} \tag{57}$$

Let's say that the interference signal is a simple sinusoid with a power level of P_i. The total modulation power level is then given by

$$(P_{IF} + P_i) \tag{58}$$

The rms modulation current is

$$i_m = \sqrt{\frac{P_{IF}+P_i}{50}} \tag{59}$$

It may be noted that P_{IF} has a Gaussian distribution while P_i is quasi sinusoidal. Assuming that $P_i >> P_{IF}$, the peak current is

$$i_p = \sqrt{2}.(i_m) \tag{60}$$

The threshold current $I_{th}$and the peak current I_p determine the maximum peak to peak excursions of the modulation current. If these limits are exceeded, the signals are clipped and the resulting spectrum is garbled. Therefore the maximum value of the peak to peak current is the difference between the peak current and the threshold current of the laser diode.
i.e

$$i_p = \frac{(I_p - I_{th})}{2} \tag{61}$$

For typical values, we will consider Fig.3.10 : P_{IF}= -14 dBm, I_p = 51mA, I_{th} = 29mA ; Substituting these values in eqn.s 59,60 and 61, we get,

$$\frac{11mA}{\sqrt{2}} = \sqrt{\frac{-14dBm + P_i}{50}} \tag{62}$$

This corresponds to P_i = 4.75 dBm.
The maximum permissible power of the interference signal at the output of the IF chain $P_i$is therefore limited to 4.75 dBm i.e 18.75 dB (4.75 -(-14 dBm)) above the input receiver noise, for the operating conditions shown in Fig.3.10

2.Strong astronomical sources: The astronomical sources are Gaussian random processes emitting radiation over a wide frequency spectrum. When observing strong sources, the power received at the front end amplifier is significantly higher than the EIN_{LNA}.
We will now evaluate the required power level to reach the peak modulation current allowed by the laser.
As shown in the previous section, the maximum peak peak current excursion is

$$i_p = (I_p - I_{th}) \tag{63}$$

If P_{IF} is the signal power, then the rms modulation current is

$$i_m = \sqrt{\frac{P_{IF}}{50}} \tag{64}$$

The peak to peak current of this signal cannot be quantitatively defined because it is a Gaussian random process. In principle the signal has a finite probability to reach an infinite amplitude (the probability is infinitesimally small however). But for practical considerations 5 times the rms signal amplitude is taken as a safe margin for the peak to peak variation. This approximation ensures that the signal amplitudes fall within these limits with a probability of 0.99 .
Therefore the peak to peak current is given by,

$$i_{p-p} = 5.\sqrt{\frac{P_{IF}}{50}} \tag{65}$$

In the limiting case,

$$(I_p - I_{th}) = i_{p-p} \tag{66}$$

For the typical case mentioned earlier, P_{IF} works out to 0 dBm.
Thus, the dynamic range is 14 dB [0 dBm - (-14 dBm)]
However, when observing strong sources, such as the Sun, the input signal power will not be limited by LNA, but will depend on antenna temperature. For example, for the relatively quiet Sun at 327 MHz, the power flux is approximately 10^{-21} Watts $m^{-2}Hz^{-1}$ for which the antenna temperature T_A = 30000 K. Hence, one would have to decrease the sensitivity of the receiver by inserting a solar attenuator in the RF signal path. It can be shown that for a 10% degradation of the input receiver noise, we can reduce the IF output power level to -32 dBm (which is due to background sky radiation and receiver noise), thus increasing the dynamic range to 32 dB (0 dBm - (-32 dBm).
However, it has been planned to monitor the IF power levels through the telemetry system and with the help of Microprocessor controlled attenuator switches, included in the IF signal path,the average power level at the input of the optical fiber system is maintained at a relatively uniform value. Additional attenuation is added in the IF signal path whenever an increase of 8 - 10 dB is detected in the IF signal power. By this process, the dynamic range of the telescope can be extended to 40 dB or more.

3.4 Phase Stability For interferometry applications, the coherence of the source radiation needs to be preserved, as discussed in Sec.1.1. The RF signal received at the antenna is converted to the IF using a Local Oscillator (LO). To maintain coherence of the RF signals, it is important to keep the phase of the LO signal stable. Moreover, since there are several antennas situated at different locations, they need to have phase synchronous LO signals at the respective locations. In the following sections, a brief description of the scheme for the above requirement is carried out, followed by the effect of the communication channel on the phase stability.

3.4.1 Phase stable LO distribution: Synchronization of the LO signals at different antennas is achieved by phaselocking them to a reference frequency which is transmitted from a central master oscillator to all the antennas. The phase of the reference frequency needs to be stable, requiring the transmission path to be located underground to minimize temperature related variations. This is dealt with in greater detail in Sec.3.4.2.
Transmission path length variations alter the phase of the reference frequency. These variations can be determined by transmitting and monitoring the phase of a signal of known frequency on the channel. It is necessary to measure the phase in two directions i.e. from the master oscillator to the antenna and back from the antenna to the master oscillator, since all phase measurements must be made with respect to the reference frequency. This technique is know as "Round Trip Phase Measurement". The phase changes at the antennas can be corrected in real time or by introducing appropriate delays in the data analysis at the correlator.
Several methods are available for round trip phase measurement - one of the first was devised by Swarup and Yang [10]. In this scheme, a fraction of the reference signal is reflected back to the master oscillator and the relative phase of the reflected signal is measured using a detector. In order to differentiate from other sources of reflection along the transmission path, the reflected component at the antenna is modulated by a low frequency signal and synchronous detector is used at the master oscillator to detect the reflected component.
A slight variation of this scheme known as *Frequency offset Round trip system* is popularly used in radio astronomy. As shown in Fig.3.11, the signals traveling in opposite directions in transmission path are slightly different frequencies f_1 and f_2, which allows them to be separated easily. A detailed analysis of this scheme is described below:
A reference frequency f_1 and a difference frequency (f_1-f_2) are transmitted to an

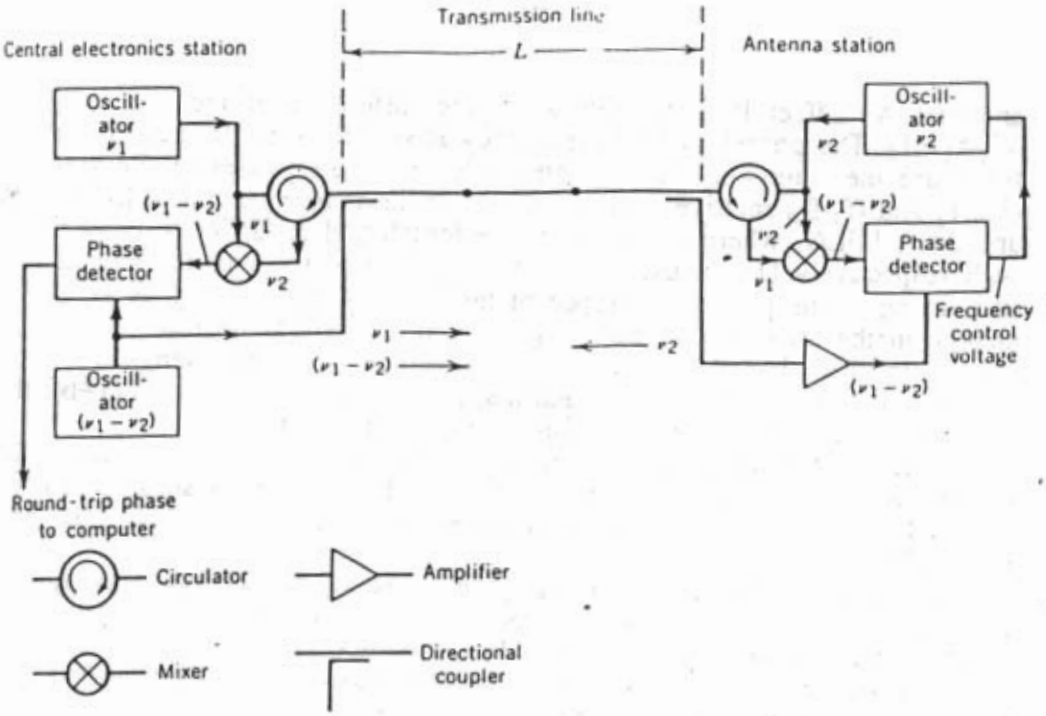

Fig.3.11 Offset Frequency Round Trip Phase Measurement Scheme

antenna; An offset PLL phaselocks to the difference of the tow frequencies viz. f_1 -$(f_1-f_2)=f_2$. The phaselocked f_2 frequency is sent back to the master oscillator location for phase measurement. At the antenna location, the phases of the signals at frequencies f_1 and (f_1-f_2) relative to their phases at the master oscillator location are $2\pi f_1 L/v$ and $2\pi(f_1-f_2)L/v$, where L and v are the length and group velocity of the transmission path respectively.The phase of the f_2 oscillator at the antenna is constrained by the PLL to equal the phase difference of these two signals, which is $2\pi f_2 L/v$. the phase change in the signal f_2 in traveling back to the central location is $2\pi f_2 L/v$. Thus the round trip phase is $4\pi f_2 L/v$. If there is a change in the path length by a small fraction say from L to $L(1+\beta)$,then the measured round trip phase in $4\pi f_2 L(1+\beta)$; the correction required is half the additional change measured i.e. $2\pi f_2 L\beta$.
Due to reflections along the transmission path and other circuit systems, the round trip phase may include erroneous measurements. The frequency separation can be suitably adjusted to take care of unwanted reflections if the actual points of reflections are known [11].
Another way of circumventing this problem is to use separate transmission paths for the two directions, if the transmission paths have identical characteristics with respect to path length variations. For the GMRT, two fibers placed in the same cable are used for the two directions. Studies by Sarma [12] showed that fibers within the same cable have closely matching characteristics of path length variations, to the accuracy required for radio astronomy applications.

3.4.2 Phase Stability in Optical fibers

The phase of LO signal traversing the fiber is affected mainly by the path length variations and the noise present in the transmission medium. We will consider each of the effects separately.

Path length variations: The optical fiber has a certain thermal expansion coefficient due to which the length varies due to temperature variations. The phase change introduced due a length of fiber L with group refractive index N in a signal at a frequency f is given by:

$$\phi = \frac{2\pi f.N.L}{c} \tag{67}$$

where c is the velocity of light in air.
If we differentiate eqn.67 with respect to temperature, T, we get

$$\frac{d\phi}{dT} = \frac{2\pi f}{c}\left(L.\frac{dN}{dT} + \frac{N.dL}{dT}\right) \tag{68}$$

$$i.e \quad \Delta\phi = \frac{d\phi}{dT}.\Delta T = \frac{2\pi f}{c}\left(L.\frac{dN}{dT}.\Delta T + \frac{N.dL}{dT}.\Delta T\right) \tag{69}$$

$$= \frac{2\pi f}{c}.(L.\Delta N + N.\Delta L) \tag{70}$$

Therefore,

$$\frac{\Delta\phi}{\phi} = \frac{\Delta N}{N} + \frac{\Delta L}{L} \tag{71}$$

But,

$$\frac{\Delta N}{N} = -k \cdot \frac{\Delta L}{L} \tag{72}$$

which is due to Photo elastic effect; k is a constant.

Therefore eqn.71 changes to

$$\frac{\Delta \phi}{\phi} = (1-k). \frac{\Delta L}{L} \tag{73}$$

For silica fibers $k == 0.22$.

Therefore,

$$\frac{\Delta \phi}{\phi} = 0.78 \frac{\Delta L}{L} \tag{74}$$

The thermal expansion coefficient of length α_{eff} is defined as

$$\alpha_{eff} = \frac{1}{L} \cdot \frac{dL}{dT} \tag{75}$$

Therefore,

$$\frac{\Delta \phi}{\phi} = 0.78\, \alpha_{eff}\, .\Delta T \tag{76}$$

$\alpha_{eff} = 1.1 \times 10^{-5}/°C$

$= 8.6 \times 10^{-5}\, \Delta T$

Effect of noise on Phase stability: The noise present in the communication system (described in Sec.3.1) affects the phase stability of LO signals. The in phase component of noise contributes towards amplitude variations while the quadrature component generates phase variations. A detailed analysis of phase noise is carried out by Robin [13].
The phase error generated due to the noise of the link can be quantified in terms of SNR [13]. This is given by

$$\phi_{error} = \frac{1}{2(S/N)^2} \tag{77}$$

where N is the double sided noise bandwidth. This expression is arrived at, with the assumption that the noise spectrum is uniformly flat.
Experiments conducted by Logan, Lutes et al [14] indicate that the noise spectrum of the link need not be uniformly flat as of white noise; especially when the laser is modulated by a single frequency such as an LO signal. With single mode lasers, Logan, Lutes et al observed that the noise spectrum has 1/f roll off in the vicinity (about 1 Hz up to several KHz) of the single frequency modulation signal, contributing to much larger phase error than the one obtained by using eqn.77.
Experiments were carried out with a similar set up used in [14], but with multimode lasers. The observed results showed no such roll off and confirmed eqn.77 as regards phase stability [15].

References

1. D.E.McCumber, "*Intensity fluctuations in the output of CW laser oscillators*", Phys.Rev., vol.141, pp306-322, Jan.1966

2. H.Haug, "*Quantum Mechanical rate equations for semiconductor lasers*", Phys.Rev., vol.184, pp.338-348, Aug.1969

3. Klaus Petermann & G.Arnold, "*Noise and Distortion Characteristics of Semiconductor Lasers in OFC systems*", IEEE Journal of Quantum Electronics, vol. QE-18, No.4, pp.543-555, April 1982

4. H.Melchior, "*Noise in Semiconductor Lasers*", Proc.of Conference on Integrated and Guided wave Optics, Incline Village, NV, paper MA2, Jan.1980

5. Y.Okano et al, "*Laser Mode Partition noise evaluation for Optical Fiber Transmission*", IEEE Trans.on Communications, vol.COM-28, pp.238-243, Feb.1980

6. S.Saito & Y.Yamamoto, "*Direct Observation of Lorentzian lineshape of Semiconductor Laser and Linewidth reduction with external grating feedback*", Electronics Letters, vol.17, pp.325-327, April 30, 1981

7. O.Hirota & Y.Suematsu, "*Noise properties of injection lasers due to reflected waves*", IEEE Journal of Quantum Electronics, vol.QE-15, pp.142-149, Mar.1979

8. I.Ikushima & M.Maeda, "*Lasing spectra of semiconductor laser coupled to an optical fiber*", IEEE Journal of Quantum Electronics, vol.QE-15, pp.844-845, Sept. 1979

9. J.B.Johnson, "*Thermal agitation of Electricity in conductors*", Physics Review, vol.32, pp.97-109, 1928

10. G.Swarup and K.S.Yang, "*Phase adjustment of Large antennas*", IRE Trans. on Antennas and Propagation, AP-9, pp.75-81, 1961

11. A.Richard Thompson et al, "*Interferometry and Synthesis in Radio Astronomy*", John Wiley Interscience, 1986

12. N.V.G.Sarma, "*Optical Fiber Links for Reference Frequency Distribution*", AT Technical Report AT/23.2/020, 1988

13. W.P.Robins, "*Phase noise in Signal sources* ", IEE Telecom series, No.9, Peter Peregrinus, 1982

14. R.T.Logan, Jr. G.F.Lutes et al,"*Design of a Fiber Optic Transmitter for Microwave Analog Transmission With High Phase Stability*",TDA Progress Report 42-102,Jet Propulsion Laboratory,Pasadena,California ,pp.27-38, August15,1990 .

15 D.S.Sivaraj, "*Phase stability of GMRT LO system through the optical fibers*", NCRA Technical Reports, to be reported.

Chapter 4

Circuit Design and System Evaluation

4.1 Introduction

Single mode optical fiber has a very high bandwidth. The optical transmitter and optical receiver usually limit the overall frequency response of the link. In this chapter, the transmitter and receiver systems for the GMRT are described in detail. The design aspects of transmitter and its frequency response are presented followed by those of the optical receiver and the electronic systems following it.
The system performance is evaluated and the measurements of the analog parameters enlisted in chapter 3 are presented. The concluding part of the chapter includes a discussion on the results and scope of further work.

4.2 Design and Circuit Analysis

In the design of an analog optical communication system, the circuit designer has to consider the linearity and SNR parameters in addition to matching the devices for high frequency response. In the following sections, a complete analysis of each of the sub systems is carried out.

4.2.1 Optical Transmitter: The laser diode is the central element in the optical transmitter. Commercially available laser diode packages have in-built photo detectors to monitor the optical power of the laser chip and thermistors to monitor the temperature of the device. Also included in the package is a thermoelectric cooler to stabilize the operating temperature of the laser chip. It has been observed that InGaAsP laser devices are very sensitive to temperature variations [1]. Fig.4.1 indicates the optical power output of a typical laser diode due to temperature variations at a fixed bias current. In order to stabilize the output optical power, the temperature and the bias current of the device should be kept stable. This is achieved by control circuitry using the temperature and optical power sensors.
As shown in Fig.4.2, the analog optical transmitter consists of optical power control, temperature control and bias and matching sections. The optical power control consists of a photodetector which senses the output optical power and generates a feedback signal. This is compared against a reference and the resulting error signal is used to adjust the bias current of the laser.
The temperature control section uses the thermistor to sense the temperature and the generated feedback signal is used to drive the thermoelectric cooler to cool the laser chip.
The detailed circuit diagram is shown in Fig.4.3. We will now consider each of the sections separately.
Automatic Power Control: This section consists of the monitor photodiode and an error signal generator. If we assume that P_{opt} is the optical power of the laser, corresponding to a bias current I_L then the monitor photodiode gives a photo current I_{ph} given by,

$$I_{ph} = \alpha \, . \, P_{opt} \qquad (1)$$

where α (amp/watt) is a constant determined by the responsivity of the photodiode and the coupling efficiency.

P_{opt} is related to the bias current of the laser, I_L by

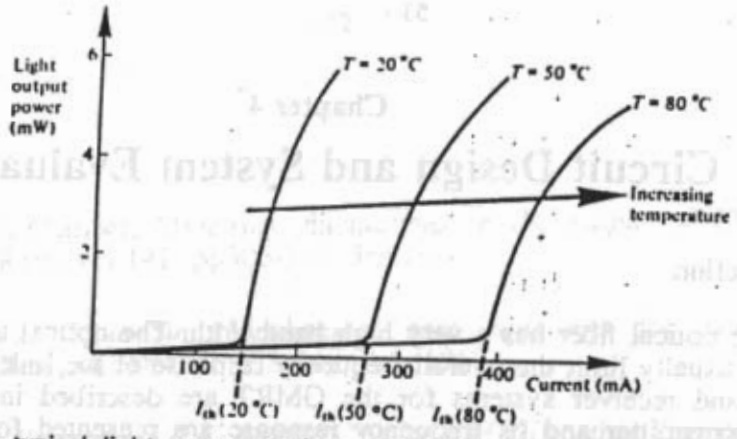

Fig.4.1 A typical light output against current characteristic for an injection laser showing the variation in threshold current with temperature.

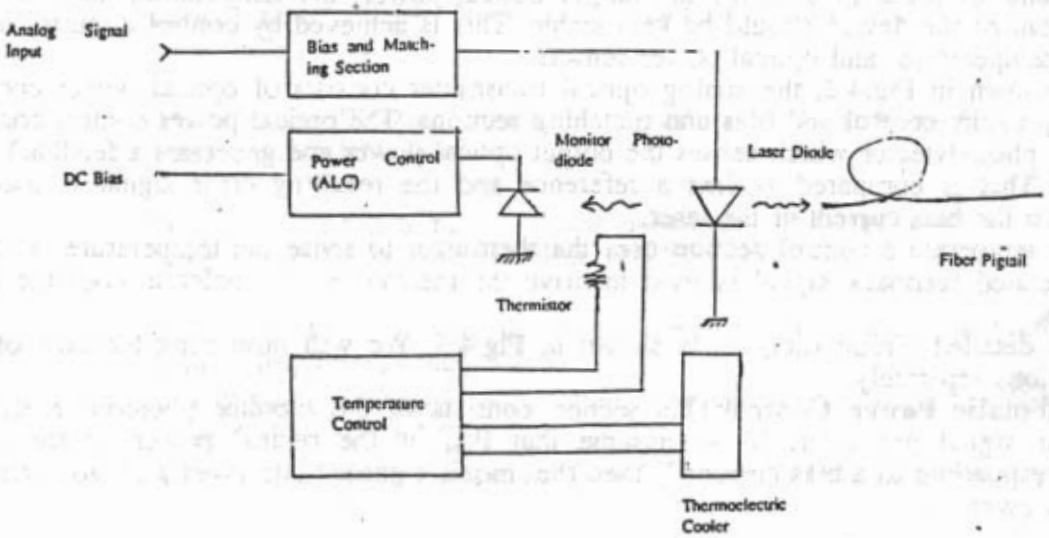

Fig.4.2 Block diagram of Optical Transmitter

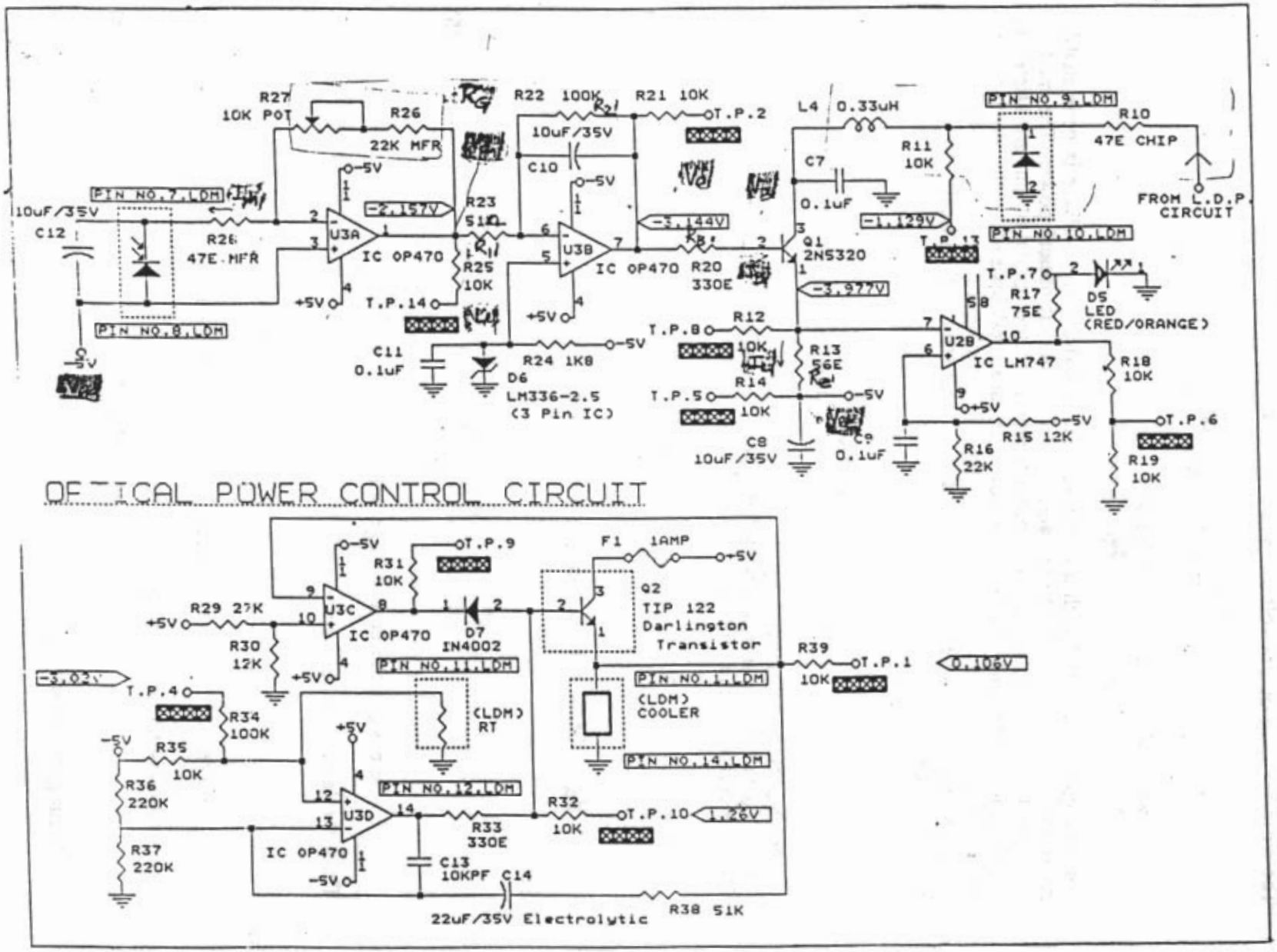

Fig.4.3 Laser Diode Driver - Circuit details

$$P_{opt} = (I_L - I_{th}).S \quad (2)$$

where, S is the slope of the laser characteristic curve (Watts/Amps).
The corresponding output voltage, V_{ph} is given by

$$V_{ph} = R_G I_{ph} + V_{ee} \quad (3)$$

where R_G is the feedback resistor
and V_{ee} is the negative supply voltage

This voltage is compared with a reference voltage and an error voltage is generated by the control circuit according to the variation of the output optical power. The modulation signals and high frequency components present in the optical output are filtered by a capacitor so that only the average power is measured instead of the instantaneous optical power.
For convenience, we will consider only the dc conditions of the circuit.
V_e is given by :

$$V_e = (1+\frac{R_2}{R_1}).V_{ref} - \frac{R_2}{R_1}.V_{ph} \quad (4)$$

where V_{ref} is the reference voltage
and V_{ph} is the output of the amplifier U3A
The base current in the transistor

$$I_B = \frac{I_L}{\beta_{dc}} \quad (5)$$

β_{dc} is the dc current gain of the transistor

But,

$$I_B = \frac{(V_e - V_B)}{R_B} \quad (6)$$

where V_B is the base voltage with respect to ground.

Thus, the laser current is given by

$$I_L = \frac{(V_B - V_\gamma) - V_{ee}}{R_e} \quad (7)$$

where V_γ is the base to emitter voltage of the transistor.

By rearranging the terms in eqn.7, we get

$$V_B = (R_e I_L + V_{ee} + V_\gamma) \quad (8)$$

Substituting this in eqn.6 ,

$$I_B = \frac{V_e-(R_e I_L+V_{ee}+V_\gamma)}{R_B} \quad (9)$$

From eqn.5 we have ,

$$\frac{I_L}{\beta_{dc}} = \frac{V_e-(R_e I_L+V_{ee}+V_\gamma)}{R_B} \quad (10)$$

$$i.e \qquad V_e = \frac{R_B}{\beta_{dc}} I_L+R_e I_L+V_{ee}+V_\gamma \quad (11)$$

$$= (\frac{R_B}{\beta_{dc}}+R_e) I_L+V_{ee}+V_\gamma \quad (12)$$

Substituting for V_e from eqn.4 we get,

$$(1+\frac{R_2}{R_1}).V_{ref}-\frac{R_2}{R_1}.V_{ph} = (\frac{R_B}{\beta_{dc}}+R_e) I_L+V_{ee}+V_\gamma \quad (13)$$

Replacing V_{ph} by RHS of eqn.3,

$$(1+\frac{R_2}{R_1}).V_{ref}-\frac{R_2}{R_1}.(R_G I_{ph}+V_{ee}) = (\frac{R_B}{\beta_{dc}}+R_e) I_L+V_{ee}+V_\gamma \quad (14)$$

From eqns.1 and 2 we get an expression for I_{ph} in terms of I_L, which is

$$I_{ph} = \alpha.S.(I_L-I_{th}) \quad (15)$$

Eqn.14 can then be rewritten as

$$[(1+\frac{R_2}{R_1}).V_{ref}-\frac{R_2}{R_1}.(R_G.\alpha.S(I_L-I_{th})+V_{ee}) = (\frac{R_B}{\beta_{dc}}+R_e) I_L+V_{ee}+V_\gamma \quad (16)$$

$$[(1+\frac{R_2}{R_1}).V_{ref}-\frac{R_2}{R_1}.V_{ee}-V_\gamma] = [\frac{R_B}{\beta_{dc}}+R_e+\frac{R_2}{R_1}.R_G.\alpha.S] I_L-\frac{R_2}{R_1}.R_G.\alpha.S I_{th} \quad (17)$$

If $(R_2/R_1) >> R_e$ and R_B, then eqn.17 reduces to:

$$(\frac{R_2}{R_1}).(V_{ref}-V_{ee}) = (I_L-I_{th}).\frac{R_2}{R_1}.R_G.\alpha.S \quad (18)$$

i.e.

$$(I_L-I_{th}) = \frac{\frac{R_2}{R_1}(V_{ref}-V_{ee})}{\frac{R_2}{R_1}.R_G.\alpha.S} = \frac{(V_{ref}-V_{ee})}{R_G.\alpha.S} \quad (19)$$

Therefore, from eqn.2, we get

$$P_{opt} = \frac{(V_{ref} - V_{ee})}{R_G.\alpha} \tag{20}$$

This implies that, irrespective of the slope variations of the laser characteristic curve due to temperature variations, the optical power remains stable at a constant value determined by V_{ref}, V_{ee}, R_G and α.
The optical power was monitored at various chip temperatures and it was observed to be constant.
The optical power was also monitored for 24 hour periods for several days and it was observed to be within 0.05 dBm as measured by an optical power meter with a resolution of 0.01 pW.
Theoretically, the stability of the optical power can be determined by evaluating the effect of temperature coefficients of the parameters enlisted in eqn.20. (The operational amplifiers have much lower temperature drifts than the variables listed in eqn.20).

Assuming that α is independent of temperature variations, we can evaluate the change in optical power for a change in temperature, ΔT as given below:

If we differentiate eqn.20 w.r.t temperature,

$$\frac{dP_{opt}}{dT} = \frac{1}{R_G.\alpha}\frac{d}{dT}(V_{ref} - V_{ee}) + \frac{(V_{ref} - V_{ee})}{\alpha}.\frac{d}{dT}\left(\frac{1}{R_G}\right) \tag{21}$$

$$\Delta P_{opt} = \frac{dP_{opt}}{dT}.\Delta T = \frac{1}{R_G.\alpha}\frac{d}{dT}(V_{ref} - V_{ee}).\Delta T + \frac{(V_{ref} - V_{ee})}{\alpha}.\frac{-1}{R_G^2}.\frac{dR_G}{dT}.\Delta T \tag{22}$$

Assuming worst case deviation in the error analysis, we get

$$\Delta P_{opt} = \frac{1}{R_G.\alpha}\left[\frac{d}{dT}V_{ref} + \frac{d}{dT}V_{ee} + \frac{1}{R_G}(V_{ref} - V_{ee}).\frac{dR_G}{dT}\right].\Delta T \tag{23}$$

From the data sheets [2,3,4],

$$\frac{dV_{ref}}{dT} = 5X10^{-5}V/°C \quad (20ppm/°C)$$

$$\frac{dV_{ee}}{dT} = 5X10^{-5}V/°C \quad (10ppm/°C)$$

$$\frac{dR_G}{dT} = 1\Omega/°C \quad (100ppm/°C \text{ at } R_G = 10k\Omega)$$

$$\alpha = 0.3A/W$$

From these values, the expected variation turns out to be

$$\Delta P_{opt} = 0.12\mu W/°C = 140ppm/°C \quad (24)$$

when $P_{opt} = 0.833$ mW
$R_G = 10$ kΩ
$V_{ref} = -2.5$ V
and $V_{ee} = -5$ V

Temperature Control
The laser diode package consists of a thermistor and a thermoelectric cooler to provide temperature stabilization. The temperature control section senses the temperature of the laser chip by means of the thermistor. A Wheatstone's bridge consisting of R35, R36, R37 and the thermistor is used to generate the feedback signal. The bridge is balanced at the desired chip temperature. Any change in this temperature alters the thermistor value, and an unbalance is created in the bridge. Amplifier U3D is used to generate the required error signal. The thermoelectric cooler is driven by the error signal with the help of a Darlington transistor Q2 to compensate for the unbalance. The circuit is designed such that, at 25°C of laser chip temperature, the Wheatstone bridge is balanced and there is no error voltage generated at the output of the error amplifier(U3D).If the laser chip gets heated due to the current flow in the device, an error signal is generated by the amplifier U3D and the power transistor pumps the extra current needed to cool the device.
The principle of operation of this section is similar to the Power Control circuit. Theoretical analysis of this circuit shows that the temperature stability is approximately 0.1°C.

Bias and Matching Section:
The RF signals which modulate the laser diode originate from 50-Ω systems and hence it is required to match the optical transmitter to 50 Ω to ensure maximum power transfer. The dynamic impedance of the laser diode (when forward biased) is usually of the order of 5 Ω. The reactive part of the impedance is generally very low and at frequencies below 1 GHz, it is ignored. Impedance transformation techniques are used at high frequencies to match the dynamic impedance of the diode to 50 Ω. At lower frequencies it is adequate to add a series resistance along with the laser diode for matching purpose. This implies that most of the RF signal power is absorbed in the series resistor. But this is not a serious issue, as the laser device is sensitive to signal current rather than signal power. In other words, there is no degradation in SNR despite the loss of signal power at the matching interface.

The laser diode is forward biased at a bias point using a dc current source consisting of transistor Q1. At quiescent state, the output of the amplifier U3B corresponds to the steady state of the control loop. This voltage drives the transistor and according to eqn.7, current I_L flows through the emitter of the transistor. The collector current of Q1 is very nearly the same as the emitter current and this is the bias current of the laser diode. Inductor L4 and capacitor C7 (cf.Fig.4.3) are used to filter out high frequency components present in the modulation current.

4.2.2 Optical Receiver The photocurrent generated by the optical signal described in Sec.3.1.5, is generally converted into a voltage before being amplified and processed further. Usually a resistance of appropriate value serves this purpose; higher value resistance will enhance the signal gain but frequency response is reduced due to large RC time constant, where C is the junction capacitance of the photodiode. Smaller values of resistors will increase the frequency response, but will also increase the thermal noise current (ith= 4FkTB/R). When both high frequency and low thermal noise

are required, two popular schemes are adopted: High impedance and Transimpedance front ends.
In High impedance front end (refer block diagram in Fig.4.4), the load resistance R_L is very high. The capacitance C which includes the input capacitance of the amplifier, junction capacitance of the detector and any other stray capacitance.
Assuming that the amplifier has a flat frequency response in the frequency range of interest, the frequency response of this front end at V_1, is given by

$$\frac{V_1(\omega)}{I_s(\omega)} = \frac{AR_L}{1+j\omega R_L C} \tag{25}$$

Because R_L is chosen to be very large, the thermal noise contribution is very small. However, the $R_L C$ time constant is very high and the frequency response is limited to $1/R_L C$ order of 1- 50 MHz. (Refer Fig.4.5a). An equaliser is therefore required to extend the bandwidth to the required range of interest. Because $R_L C$ network tends to integrate the signal, a differentiator is used as an equalizer to compensate for the frequency response. Fig.4.5b gives the frequency response of such an equaliser. This network may be passive as in Fig.5b or active with some gain.
The transfer function of a passive equaliser (Fig.4.6) is given by

$$\frac{V_2(\omega)}{V_1(\omega)} = \frac{R_2}{(R_1+R_2)} \cdot \frac{(1+j\frac{\omega}{\omega_1})}{(1+j\frac{\omega}{\omega_2})} \tag{26}$$

where

$$\omega_1 = \frac{1}{R_1 C_1} \tag{27}$$

$$\omega_2 = \frac{(R_1+R_2)}{R_1 R_2 C_1} \tag{28}$$

For ideal equalisation, ω_1 should equal $1/ R_L C$. With this equalisation, the bandwidth is extended to ω_2 . The overall frequency response after equalisation is shown in Fig.4.5c. It should be noted that the effective gain is reduced due to attenuation of lower frequency signals by the equalizer. Thus, the amplifier gain A has to be significantly large, not only to maintain adequate signal strength, but also to reduce the effect of noise present in the succeeding stages, following the equalizer. Because R_L is very large, the signal voltage is large; this coupled with the high gain of the amplifier reduces the overall dynamic range of the receiver.
Active equalization reduces this problem to some extent due its inherent gain, but a transimpedance front end eliminates this problem altogether because it does not require any equalisation.
Transimpedance front end: The transimpedance amplifier is a shunt feedback amplifier shown in Fig.4.7a. The feedback resistor R_f has a stray capacitance C_f. While the capacitor C includes the amplifier input and the detector's junction capacitances. R_b consists of the bias resistance and the detector's dynamic impedance. The transfer function of this amplifier can be shown to be [5],

$$\frac{V_2(\omega)}{I_s(\omega)} = -\frac{R_f}{1+\frac{R_f}{AR_b}+j\omega R_f(C_f+\frac{C}{A})} \tag{29}$$

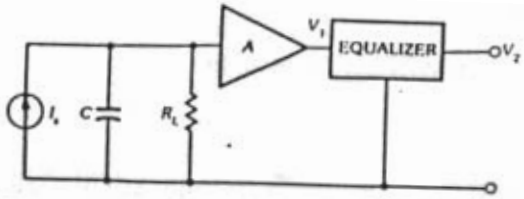

Fig.4.4 Hig-impedance receiver amplifier

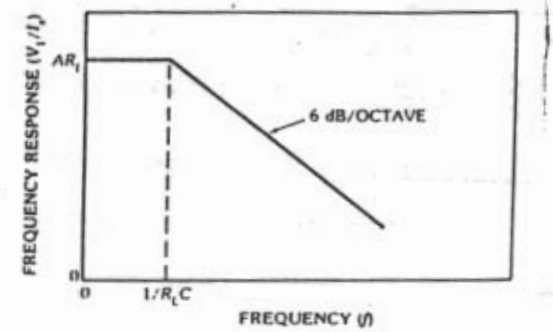

(a) Front end.

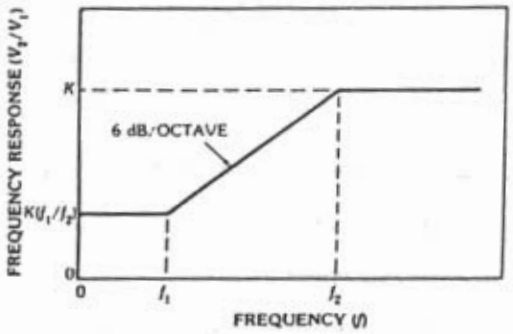

(b) Equalizer.

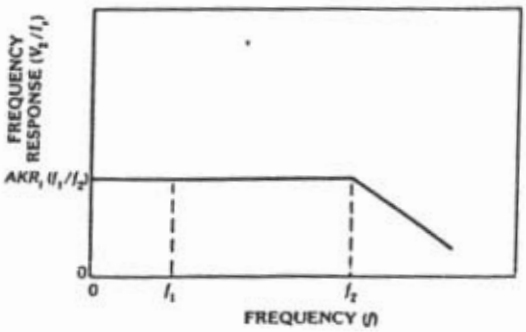

(c) Complete receiver amplifier.

Fig.4.5 Frequency responses in the high impedance receiver amplifier

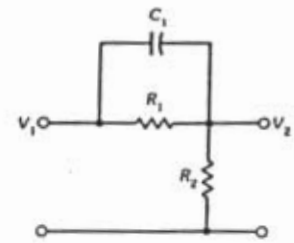

Fig.4.6 Passive *RC* equalizer.

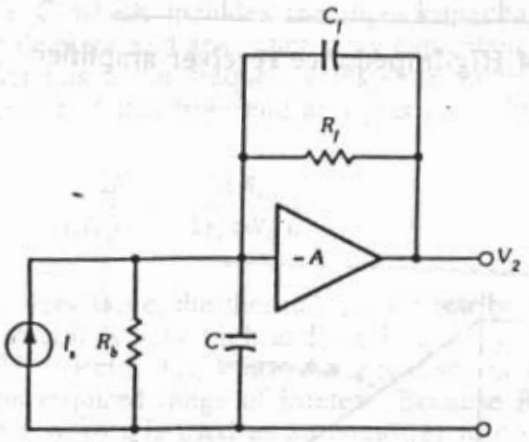

(a) Circuit diagram.

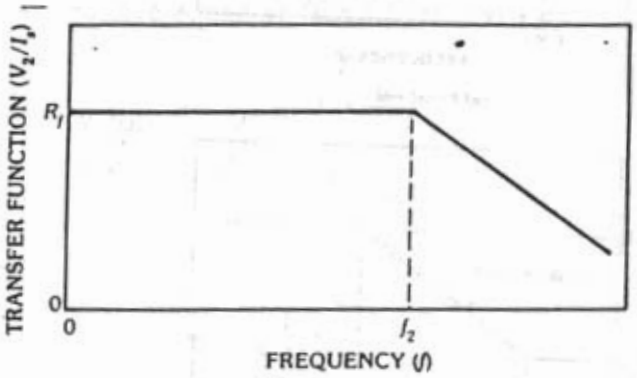

(b) Frequency response.

Fig.4.7 Transimpedance receiver amplifier and response.

Table 4.1

Technical Specifications of the cable used for GMRT

Modefield diameter of fiber	: 10 μm
Cladding diameter	: 125 μm
Primary coating material	: UV cured Acrylate
Primary coating diameter	: 250μm
No.of fibers	: 4,6,8,10,12 or 14
Cable outer diameter	: 12.8 ± 0.8 mm
Minimum bending radius	: 10 times the outer diameter
Cable weight	: 126 kg/km
Tensile strength	: 126 kgf

In practice, R_b is designed to be greater than R_f and A >>1. If the value of C_f is much smaller than C/A (which is practically feasible), then the 3-dB frequency will be

$$f_{3dB} = \frac{A}{(2\pi R_f C)} \tag{30}$$

This shows an improvement of a factor of A over the high impedance front end. The dynamic range of transimpedance front end is also better than high impedance system due to the fact that there is no equalization. As a result low frequencies are not attenuated as in the case of high impedance front end. The improvement in the dynamic range can be worked out, considering this fact; it turns out that the ratio of the two dynamic ranges is a factor of A.

GMRT Optical Receiver: In the case of GMRT, the laser noise is the predominant source of noise. As a result no attempt has been made to reduce thermal noise contribution from the front end; instead, high frequency response is enhanced by including a low value resistance of 50Ω, so that the succeeding high frequency amplifiers are matched. The block diagram of the optical receiver is shown in Fig.4.8
Let's now proceed with the circuit analysis with the help of the circuit diagram in Fig.4.8b.

The received optical power at the photodetector P_{rec} is converted into electrical current; this current flows in the direction of the electric field which is due to the bias voltage. This current is given by

$$i_{ph} = P_{rec}.R \tag{31}$$

where,

$$P_{rec} = P_{opt}.\alpha \tag{32}$$

$$P_{opt} = \textit{Optical power at the transmitter} \tag{33}$$

$$\alpha = \textit{Optical loss incl. cable and connector's insertion loss} \tag{34}$$

The generated photocurrent is equally divided between the load resistor and the amplifier because the input impedance of the amplifier is also 50Ω.
Power delivered to the amplifier is

$$(\frac{1}{2}.i_{ph})^2 \tag{35}$$

If G_{amp} is the power gain of the amplifier, then the power delivered at the output of the amplifier is

$$P_{out} = (\frac{1}{2}.i_{ph})^2.50.G_{amp} \tag{36}$$

The SNR performance of the receiver is treated exhaustively in chapter 3.
The amplifier in the receiver circuit consists of a single stage or two stage Bipolar MMIC, INA 02186/02170. This device is a broadband low noise amplifier. It operates on a single voltage with a bias current of 40 mA.. As shown in Fig.4.8b, the biasing circuit is a simple resistor connected to +12V. The frequency response of the amplifier is shown in Fig.4.8c and the specifications are summarized below:

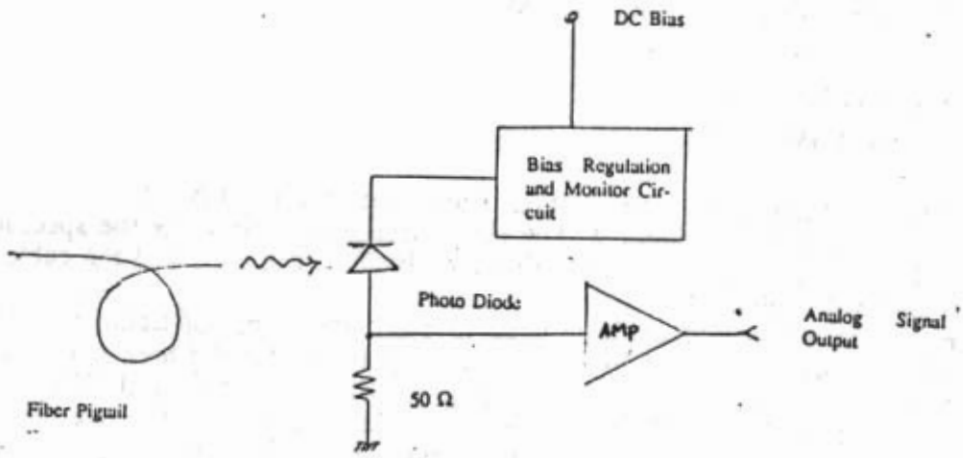

Fig.4.8a Block diagram of Opitcal Receiver

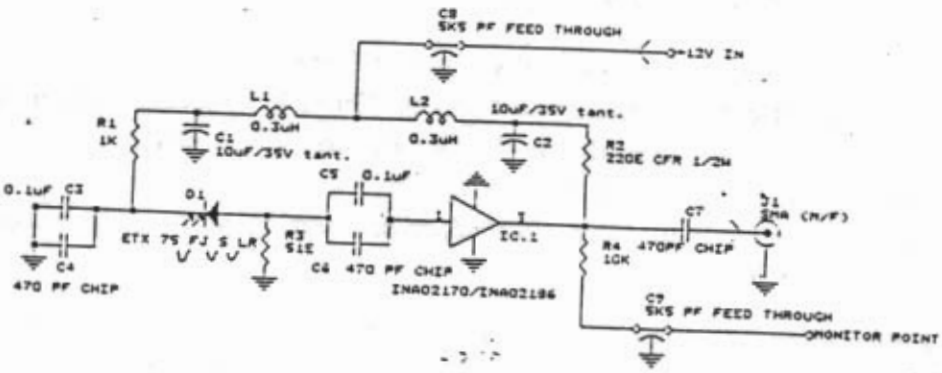

Fig.4.8b Optical Receiver - Circuit details

Specifications of MMIC Amplifier INA 02170

- Frequency response : DC-1000 MHz
- Noise figure : < 1.8 dB
- Input VSWR :<1.6
- Output VSWR :<1.6

4.2.3 Optical fiber cable: The optical fiber cable for the GMRT consists of several sections as outlined in chapter 2. The cable design was made for the specific application of GMRT. The details of the cable are given in Table.4.1 and the cable construction is outlined in Fig.4.9.
The non metallic type of cable is used to avoid the effect of lightning. The central strength member is made of FRP which is responsible for the high tensile strength of the cable. The slotted core member is a high density polyethylene (HDPE) with helical groves cut into it. Optical fibers are located in these groves; each grove can accommodate up to 4 fibers. The groves are filled with a non hygroscopic petroleum jelly to prevent the ingress of moisture- moisture contains OH ions which severely degrade the attenuation performance of optical fibers [6].
The outer coating is a Nylon sheath which is resistant to abrasion. This makes the installation procedure very simple.

Cable installation: As discussed in chapter 3, the optical fiber is required to be buried underground, where temperature variations are minimized, in order to maintain a stable phase of the LO. Unfortunately non metallic cables are prone to attacks from rodents and there have been many instances of non metallic cables being completely gnawed through by rodents. The Telecommunications Engineering Center at Delhi have recommended several installation procedures to overcome this problem. However, these procedures worked out to be very expensive and could not be implemented within the budget of the project. A cheaper alternative was worked out to circumvent this problem, which can be summarized as follows:

1. Dig a cable trench to a depth of more than 5 feet.
2. Pour cement concrete and make a slot of 30mm X 30 mm throughout the section.
3. After curing, place the cable in the slot and cover with sand.
4. Pour cement concrete and allow it to cure.
5. Cover the trench with sand and mud, after inserting warning signs about the cable at 1 meter depth.

In the case of crossing small canals and rivulets, the procedure is carried out 1 meter below the river bed. In cases where the cable runs below a road, pre fabricated reinforced concrete channels were used and hume pipes of 400 mm dia are placed over the concrete channels to prevent excess stress on the cables.

Cable insertion loss: The fiber used in the cable is a single mode type with zero dispersion wavelength centered at 1310 nm. The dispersion is measured to be 3.5 ps/nm/km as given by the manufacturer. The average fiber loss is 0.36 dB/km as measured by OTDR (Fig.4.10).
A typical optical fiber communication system to any of the antennas, as installed at the site is illustrated in Fig.4.11. It consists of uplink and downlink. The uplink carries only the control and monitor signals and reference LO signals. While the downlink consists of IF signals in addition to return LO and telemetry signals. There is a low reflection

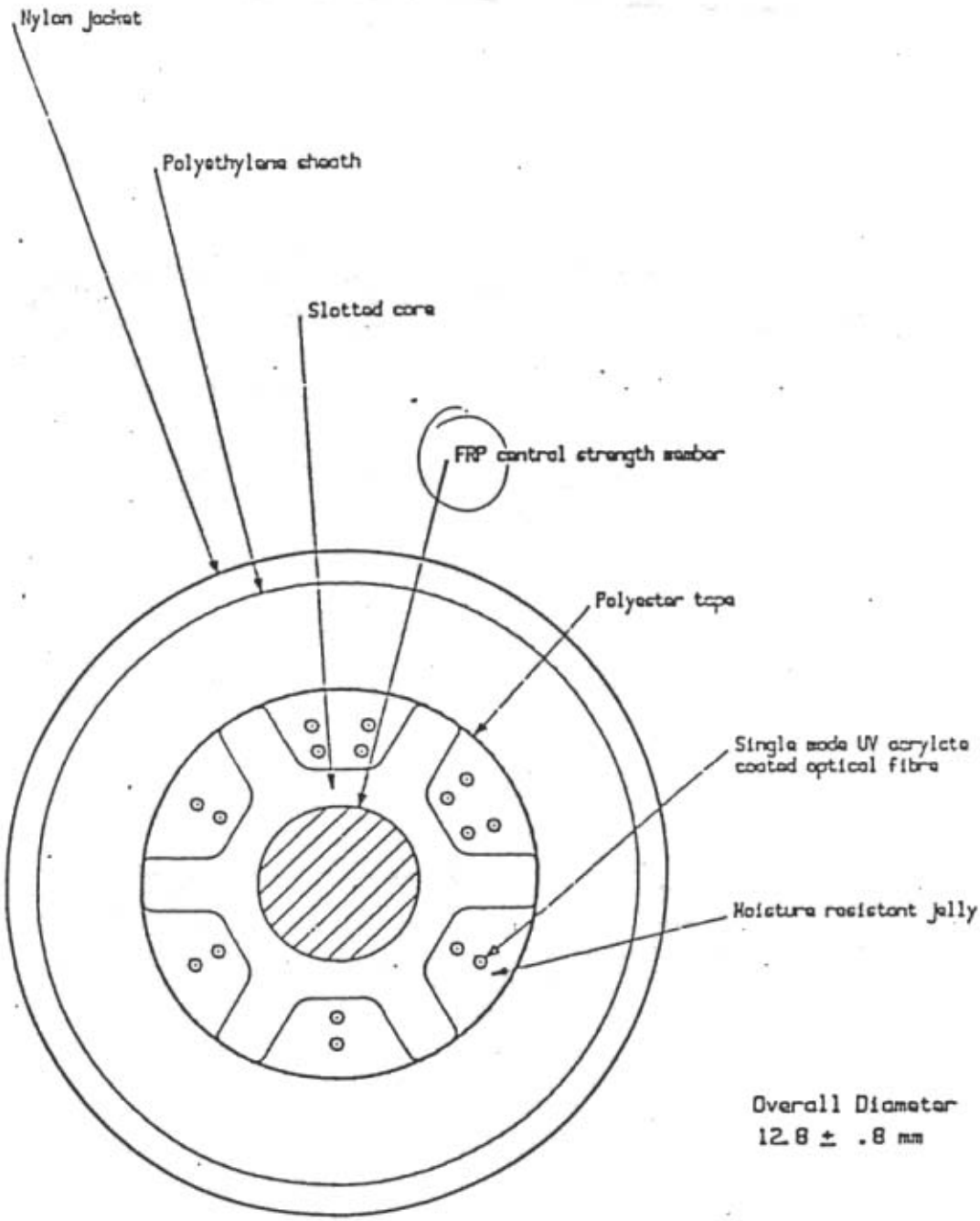

Fig.4.9 Construction of Cable used for GMRT

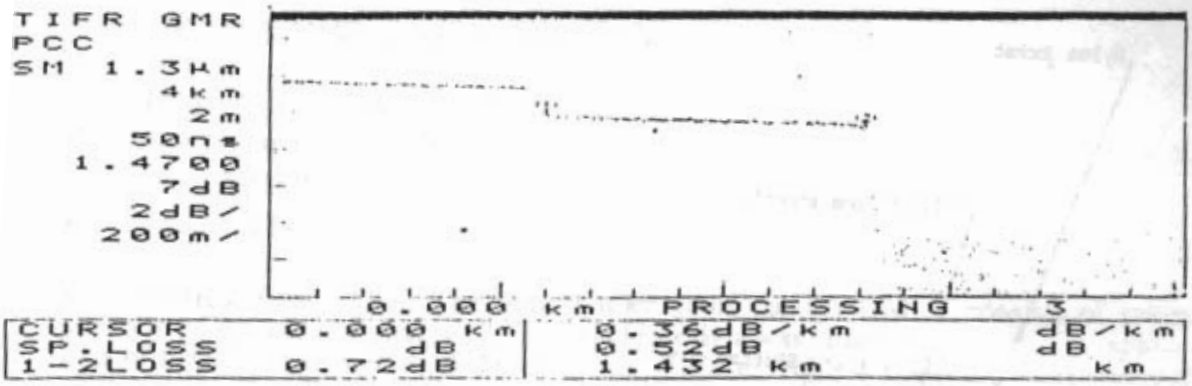

Fig.4.10 Loss measurement of Optical Fiber Cable using OTDR

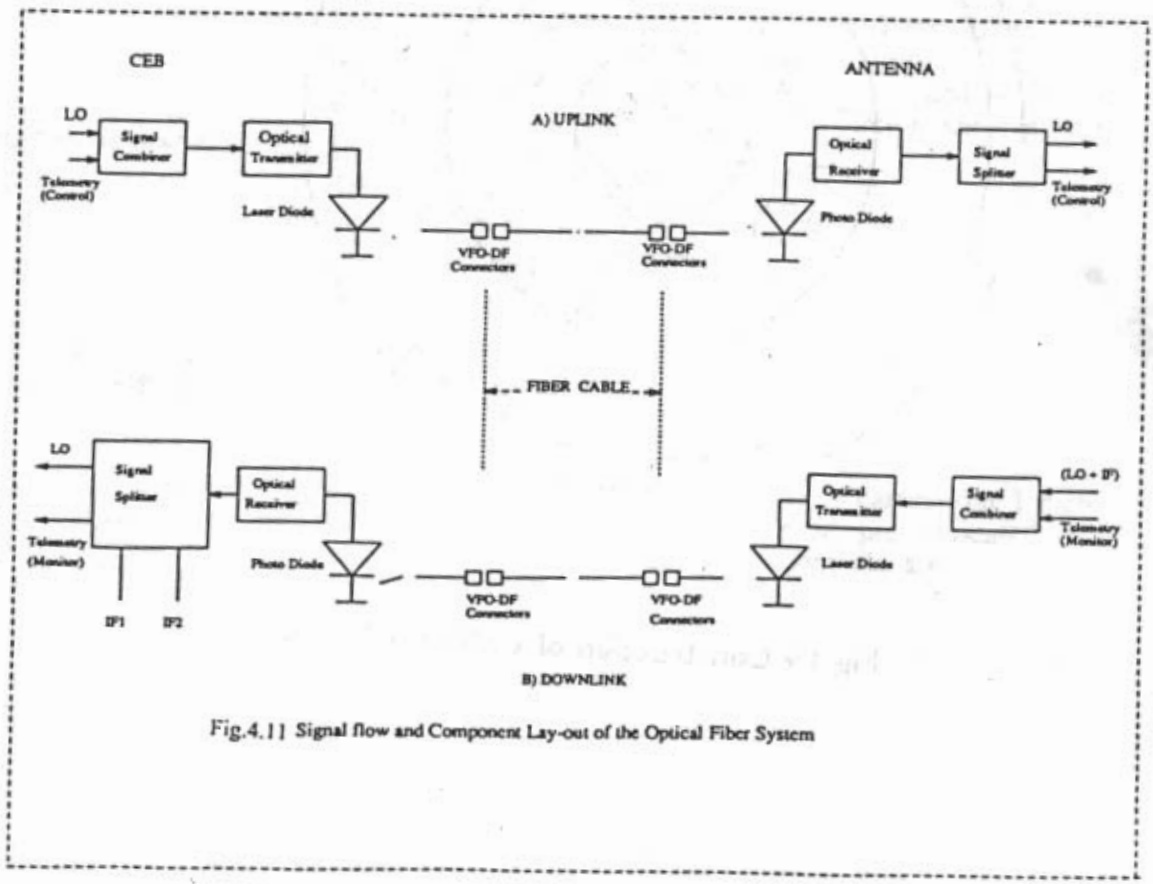

Fig.4.11 Signal flow and Component Lay-out of the Optical Fiber System

VFO-DF connector at the end of each transmitter both in the up and down links. This is required for maintenance purposes. Single ended measurements with OTDR can be performed to check the continuity of the fiber in any link without disturbing the set up. The connector uses the principle of angled facets of fibers to achieve a very low back reflection (< -55dB). The insertion loss of the connectors varies from 0.4 dB to 1.0 dB. The optical receivers also are terminated by VFO-DF connectors for ease of replacement.

4.3 Measurements

The theoretical description of the analog system is presented in chapter 3. The analog parameters have been analyzed thoroughly and their effect on the performance of the telescope is also presented. The analog parameters considered in chapter 3 include:

- SNR
- Linearity
- Dynamic Range
- Phase stability of LO signals

Experiments were carried out to quantify each of these parameters very rigorously. In the following sections, a brief description of the experiments performed and their measurement accuracies are presented in the following sections.

4.3.1 Signal to Noise Ratio : The experiment set up used to measure SNR is shown in Fig.4.12. The optical transmitter and optical receiver circuits are described in Sec.4.2. The optical attenuator has HMS-10/HP connectors at the input and output interfaces. These connectors have a back reflection of -40 dB. The attenuation setting can be adjusted from 0 dB to 80 dB in steps of 0.1 dB. The instrument has an insertion loss of 1.56 dB..
A single tone at a frequency f_0 and a fixed power level is used as the signal at the input of the optical transmitter. Spectrum analyzer TEK 2710 is used to measure the noise and signal power levels with the resolution bandwidth as indicated in Fig.4.13.
The experiment is carried out with various combinations of sources and detectors as shown below:

1. 1 mW RWG LASER + Low reflection PIN photodiode
2. Low power RWG laser + PINFET (back reflection : -30 dB)
3. Low power RWG laser + High reflection PIN photodiode (back reflection : -17dB)

The measurement results are graphically depicted in Fig.4.13
The first of the above combinations showed higher SNR levels due to the absence of strong reflections. PINFET receiver has higher sensitivity and the SNR performance is close to the shot noise regime. Theoretical calculations match very closely with the observed results.

Fig.4.14a shows the experimental set up for measuring the effect of reflection on laser noise. A 2 x 2 directional coupler is used to introduce the required back reflection and the optical attenuator HP 8157A is used to control the amount of back reflection. The specifications of the directional coupler are summarized below:

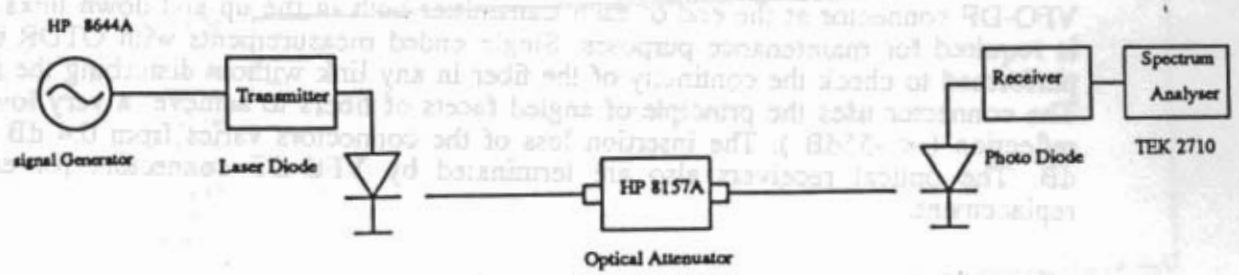

Fig.4.12 Measurement Set up for SNR

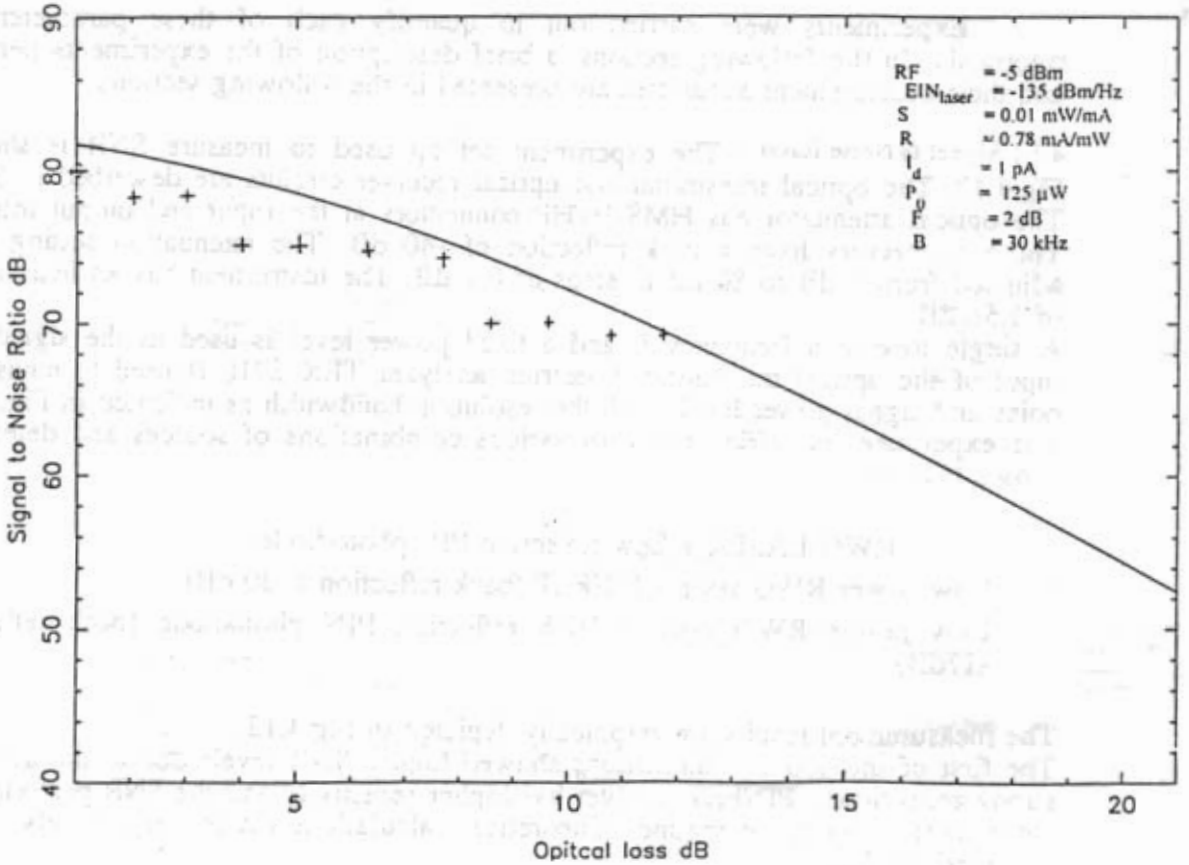

Fig.4.13a Low Power RWG laser + PINFET receiver (back reflection : -30 dB)

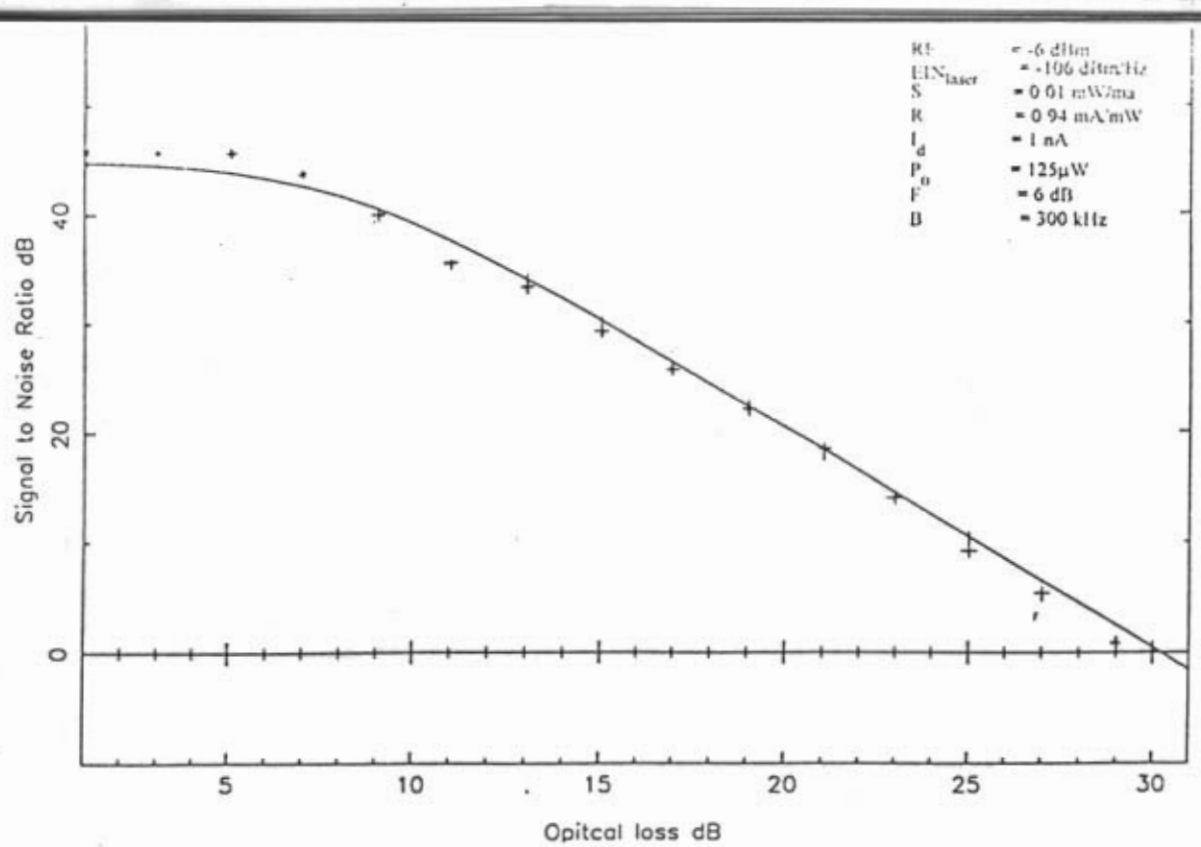

Fig.4.13b Low Power RWG laser + High reflection (-17 dB) PIN detector

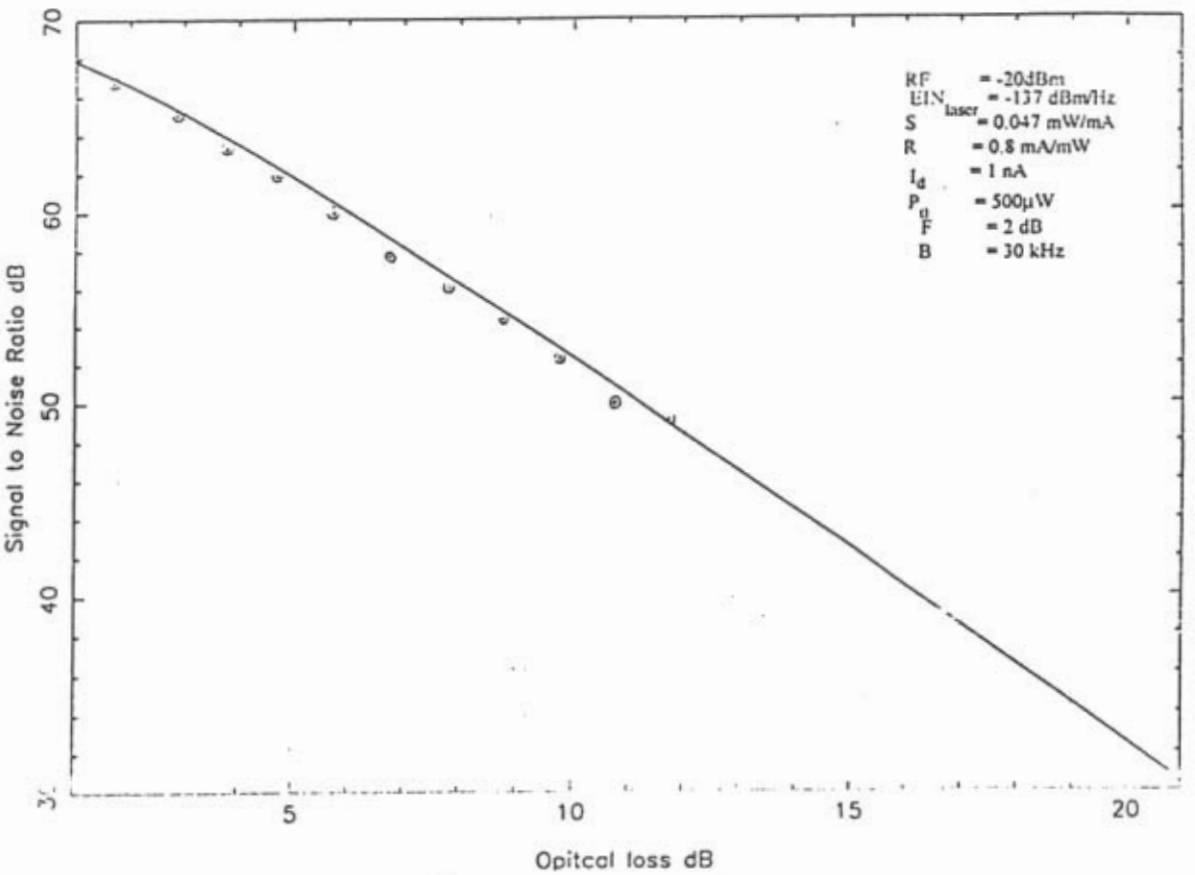

Fig.4.13c 1 mW RWG laser + Low reflection (-55 dB) PIN detector

Fig.4.13 SNR measurement results

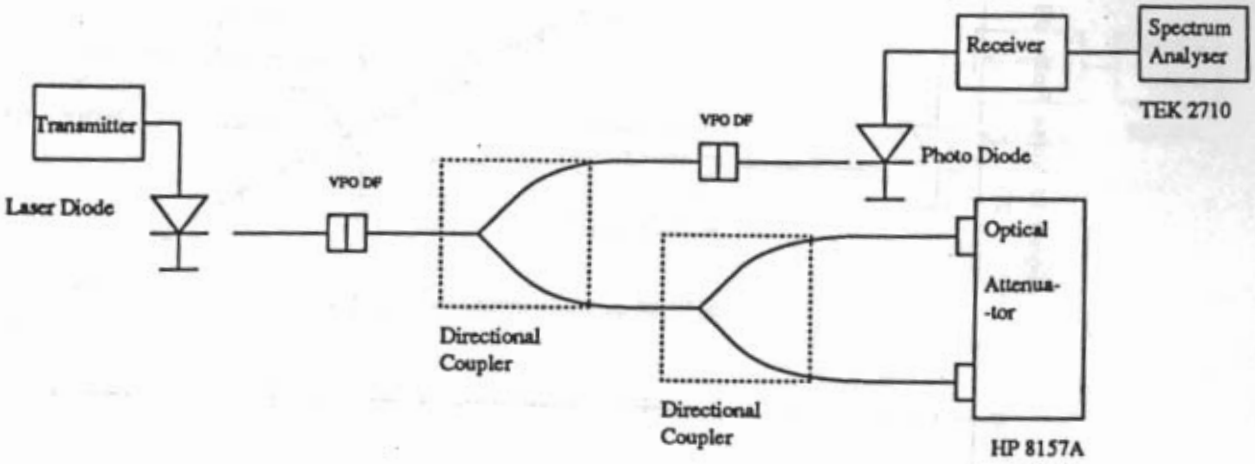

Fig. 4.14 Experimental Set up to measure the effect of optical feedback

- Splitting ratio : 1:1
- Excess loss : < 0.5 dB
- Directivity : > 50 dB

As in the earlier experiment, TEK 2710 is used to measure the noise spectrum of the laser source. Fig.4.14b summarizes the experiment results. At optical reflections weaker than -30 dB, there is no appreciable change in the laser noise performance. This may be due to the fact that the intrinsic noise of the laser is stronger than the reflection induced noise.

4.3.2 Linearity : As discussed in Sec.3.2, linearity can be quantified in several ways. Non linear distortion can be estimated by measuring 2nd order and 3rd order distortion products. Fig.4.15 depicts the experiment set up for the distortion measurement. Two tones f_1 and f_2, separated by a narrow spacing in frequency domain are combined using a power combiner and passed through the link. The output of the link is monitored using the spectrum analyser TEK 2710 and the various IMD products are measured. A bandpass filter is included in the signal path before the laser diode, to filter out spurious products.
The measurement uncertainty is governed by two factors: The amplifiers' non linearity and the instruments non linearity. The accuracy of the measurement is limited by the instruments limit of ±0.5 dB. The results are plotted in Fig. 4.16. The results include the combinations listed in the experiment on SNR measurements.
The first of these combinations showed extremely low distortion levels. The IMD products were below 67 dBc even for the strongest power levels of about 0 dBm. The dynamic range of the Spectrum Analyzer restricted the measurement of IMD products at lower power levels. Low power laser exhibits a pronounced nonlinearity when the optical feedback is about -17 dB. There is a considerable decrease in the distortion levels when the optical reflection is reduced down to -30 dB.
The effect of optical feedback (back reflection) on linearity is also studied by introducing controlled amount of reflection by using a set up similar to the one shown in Fig.4.14a. 3rd IMD products were measured by varying the amount of feedback. The results show that for reflections less than -30 dB, there is no appreciable change in the linearity performance (Fig.4.16b).

4.3.3 Dynamic Range: The dynamic range of the communication system is limited to 15 dB as described in Sec.3.1.5. This is due to the fact that the constraint on the minimum signal that the communication system is allowed to transmit (by the telescope receiver system) is about 100 times the noise power instead of the conventional limit of S/N = 1. The saturation limit of 1 dB compression point and Third Order Intercept point (TOI) are measured using the set up shown in Fig.4.17. The 1 dB compression point was measured with a single tone as well broadband gaussian noise signal. For TOI, a single tone is used . The power meter used for measuring power levels at the input and output stages has a sensitivity limit of -30 dBm. The measurements results are indicated in Fig.4.18.

4.3.4 Phase Stability: To measure phase stability of the communication system, one requires a low drift measurement set up with low phase noise signal sources and a phase meter with a very low noise bandwidth.
The experiment shown in Fig.4.19 consists of a synthesized signal generator HP8644A with low phase noise and a vector voltmeter HP8508A with a resolution of 0.5 deg. of phase. It has a noise bandwidth of only 1 kHz. Phase measurements of the set up are carried out in an air conditioned environment to ensure that temperature related drifts are minimized.
A single frequency of 100 MHz is used for the measurement using a 2.2 km long fiber. The results are recorded on a PC at regular intervals of 15 minutes. The cable

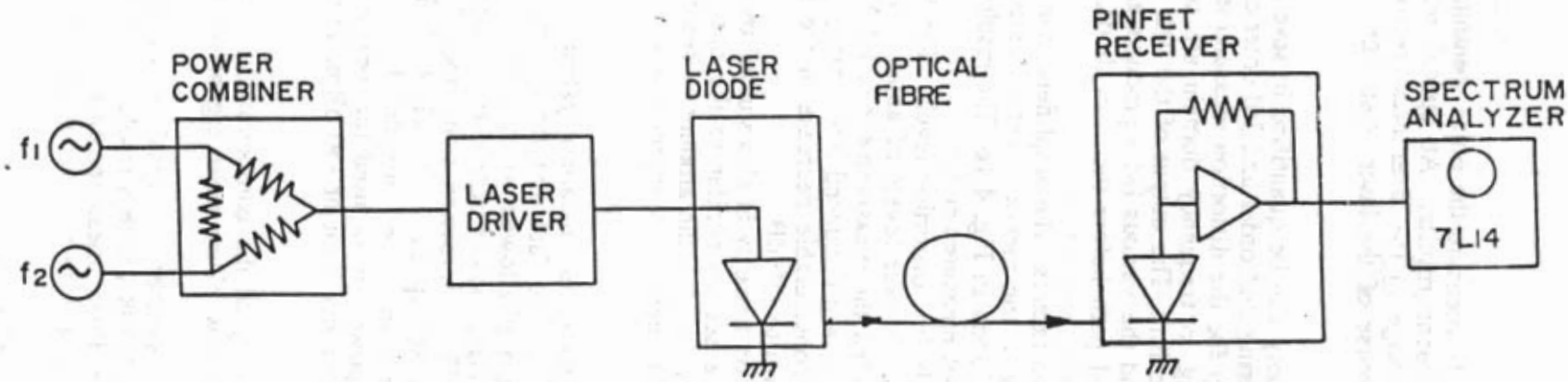

Fig.4.15 TWO-TONE MODULATION TEST SET-UP

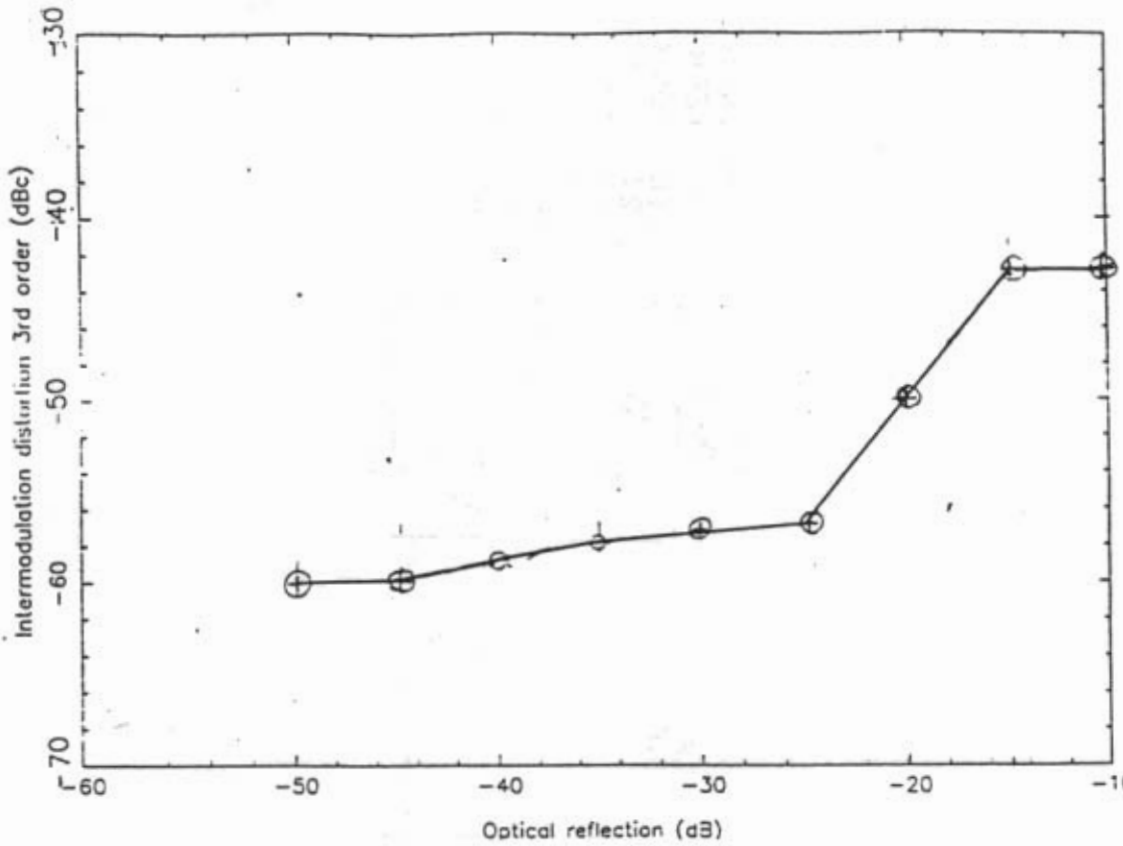

Fig. 4.16 Effect of reflections on linearity performance

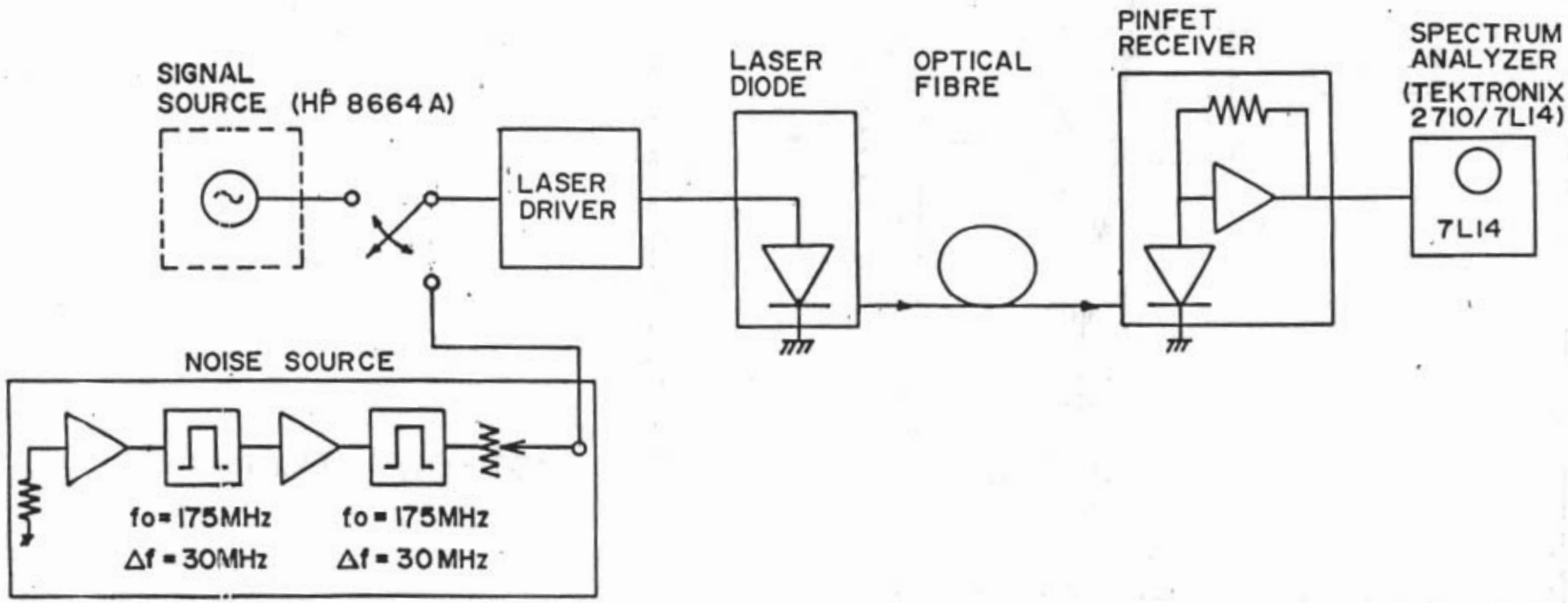

Fig.4.17 EXPERIMENT SET UP FOR LINEARITY MEASUREMENT

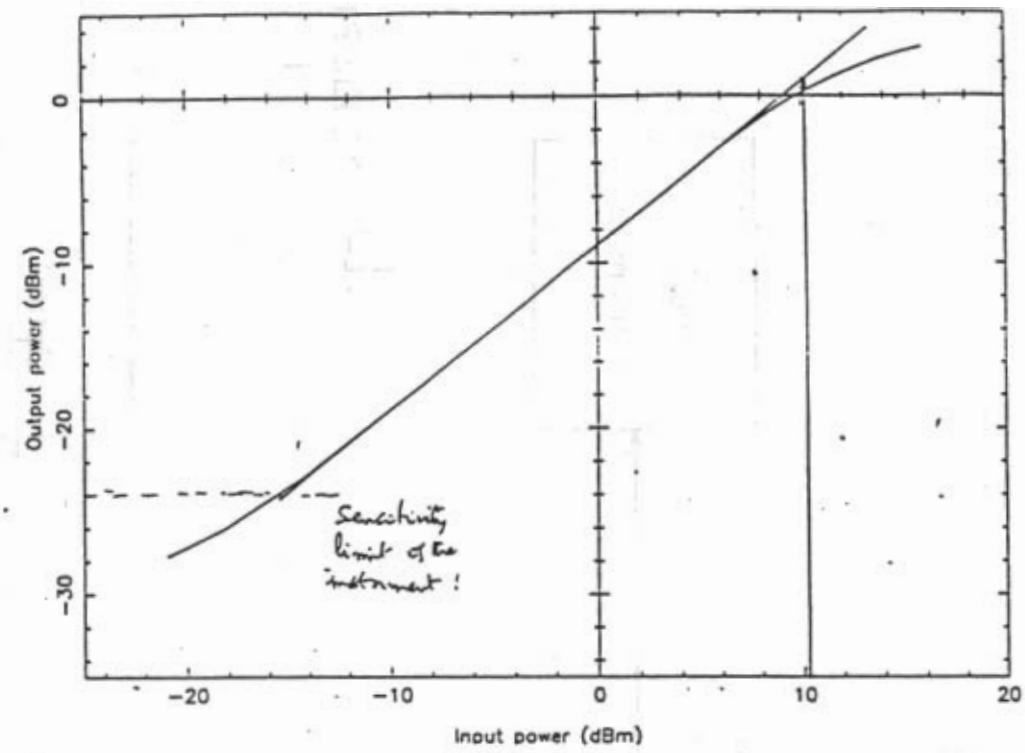

Fig.4.18a 1-dB Compression point of Gaussian noise signal

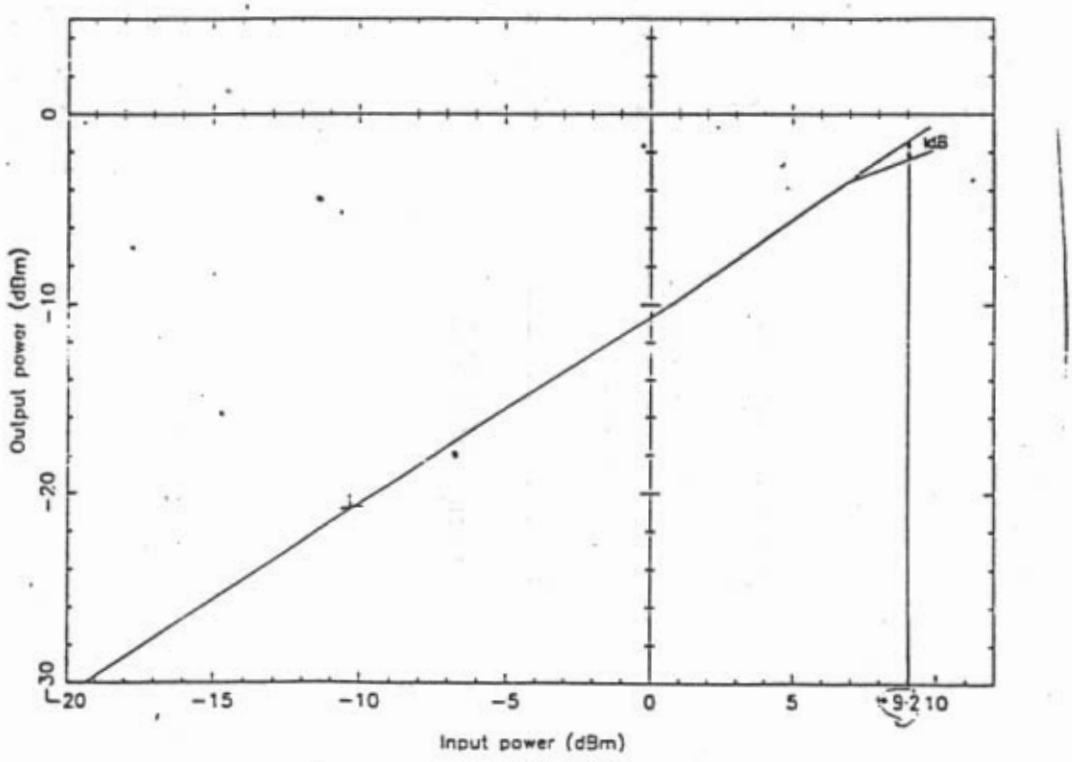

Fig.4.18b 1-dB Compression point of sinusioidal signal

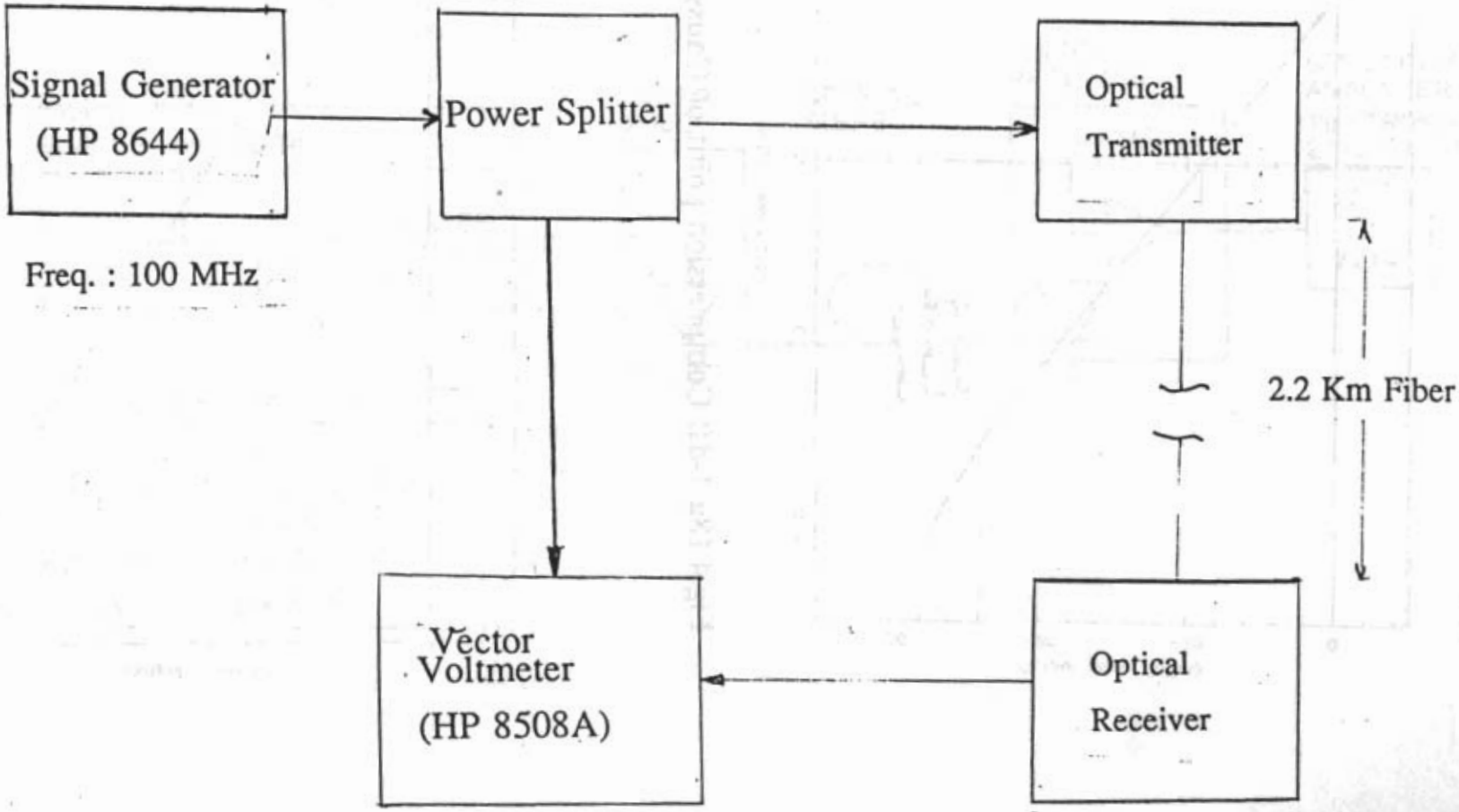

Fig.4.19 Experiment Set up to measure Phase stability

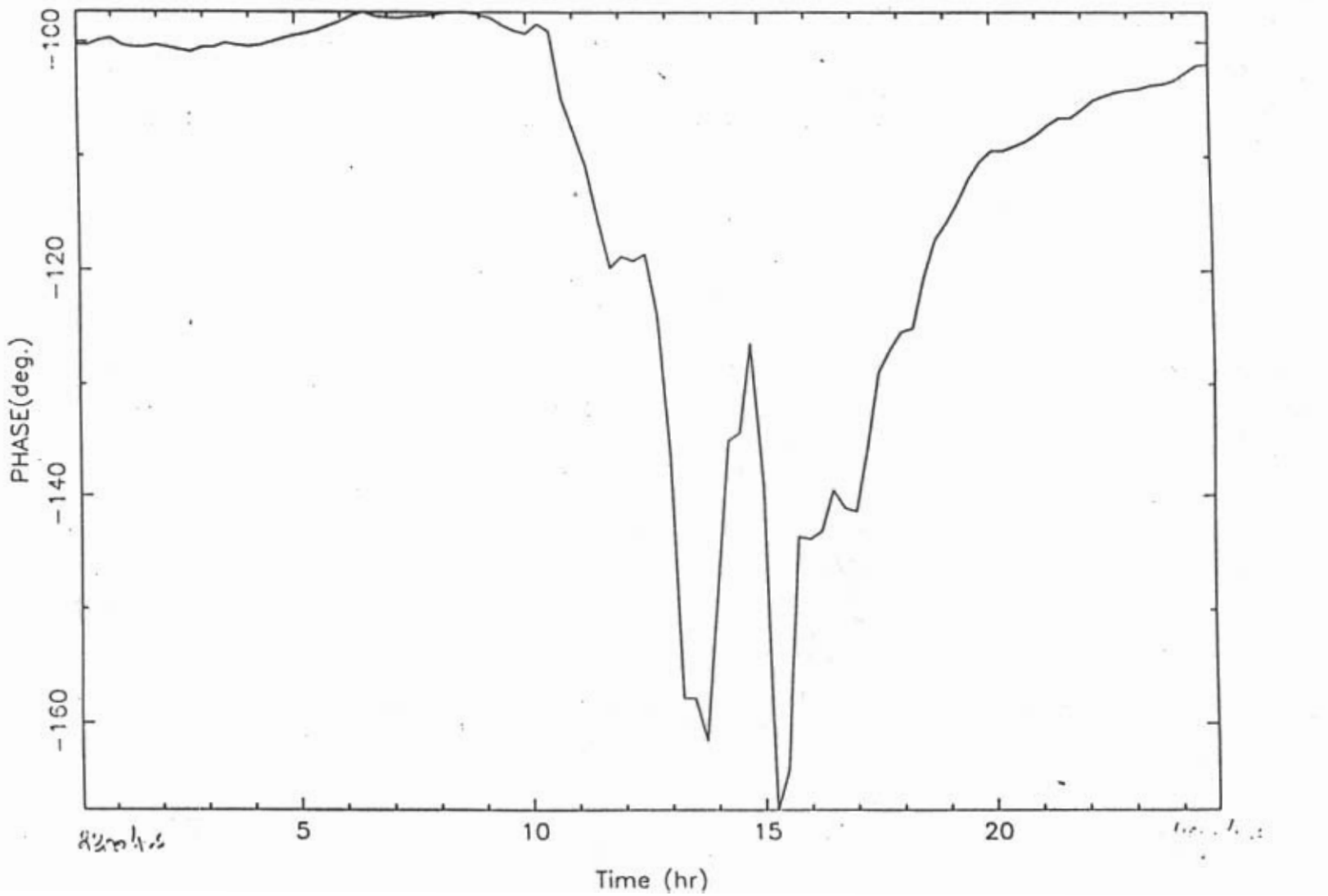
-100
-120
-140
-160
PHASE(deg.)
5
10
15
20
Time (hr)

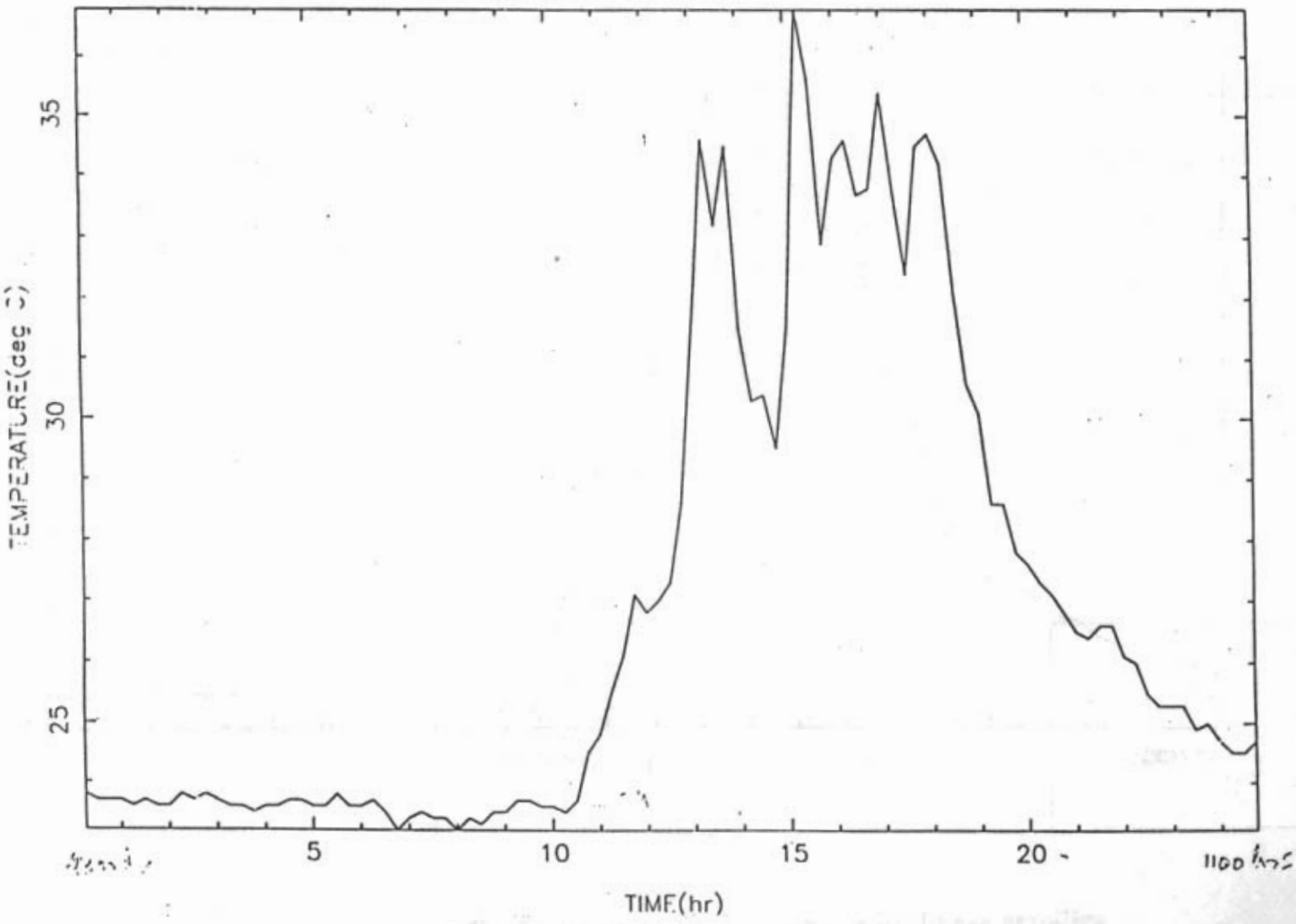

Fig.4.21 Temperature variations

was placed on the terrace of the laboratory building. A temperature probe, LM335 was located beside the cable on the terrace.
Fig.4.20 and 4.21 show the phase and temperature variations as a function of time.
From the data it can be seen that for a maximum temperature variation of 12.5 deg.C, the total change of phase $\Delta\phi$ is 75 degrees.
Substituting these values in eqn.75, Chapter 3, we obtain

$$\alpha_{eff} = 1.1 \times 10^{-5} /^{\circ}C \qquad (37)$$

References

1. M.Asada et al, "*The Temperature Dependence of Threshold Current of GaInAsP/InP DH Lasers*", IEEE Jl. of Quantum Electronics, QE-17, 1981, p.611
2. National Semiconductors Data Book, "*LM336-2.5 Reference Diode*", Linear Devices, Vol.2, pp.7-28 - 7-35, Rev.1, 1989
3. National Semiconductors Data Book, "*LM337, 3 Terminal Adjustable Negative Voltage Regulators*", Linear Devices, Vol.2, pp.1-100 - 1-105. Rev.1, 1989
4. RS Components Catalog, "*Cermet Multiturn 3/8" Square Potentiometer*", pp.526, 1988
5. R.G.Smith & S.D.Personick, "*Receiver Design for Optical Fiber Communication Systems*", New York:Springer Verlag, 1980
6. D.B.Keck et al, "*On the Ultimate lower limit of attenuation in glass optical waveguides*", Applied Physics Letters, 22(7), pp.307-309, 1973

Chapter 5

Conclusions and Suggestions for Further Work

The use of optical fibers in radio astronomy is a new field. Practically not much literature was available on this topic at the inception of the project, although a digital optical fiber communication system had adopted in late 80s for the Australia Telescope. Feasibility study was carried out in 1987, including discussions with some of the experts across the world. A final scheme was arrived at after analyzing various options.

The choice of analog communication system over digital system was made, based upon the simplicity, low cost, low radio frequency interference and ease of maintenance of the system.

Several experiments were conducted to ascertain the feasibility of the analog system. System parameters such as SNR and linearity were measured and found to be satisfactory for radio astronomy applications.

Optical reflections posed a big problem to the system; The laser noise and linearity were found to be adversely affected by optical feedback. A reliable low reflection connector with a back reflection less than -55 dB were identified, to overcome this problem.

Phase coherent local oscillator distribution was not attempted with optical fibers earlier, until preliminary studies were carried out by Sarma [1] in 1988. It was found in his experiments that transmission of phase has the property of reciprocity in optical fibers and that two different fibers sheathed in the same cable can be used for transmission of phase in opposite directions, for the round trip phase measurement method. Measurements were made to quantify phase stability of optical fibers.

The design and development of optical transmitters and receivers was carried out to realize a communication system capable of meeting future requirements. Accordingly, a broadband analog link with a bandwidth of 1 GHz was realized. Automatic power control and temperature control circuits were designed to stabilize the operating conditions of the laser diode.

Low noise MMICs with a high 3 dB frequency of 1 GHz were used in the Optical receivers in conjunction with the photodetector.

Installation procedures for optical fiber cable had to evolve out of the many problems faced during installation. There were many reports, from other parts of the country, where similar cables had been severed by rodents in the field. With low budget constraints, novel schemes have been adopted for burying the non metallic optical fiber cable.

Field splicing was minimized by careful cable lay-out design,. Most of the splicing has been carried out indoors in an airconditioned environment. However, in future maintenance works, it may become necessary to perform field splicing at many places.

Suggestions for Further Work

In the text of the thesis, only analog and digital communication schemes were considered for the communication system. In this work, we adopted amplitude modulated analog system for simplicity. This has the disadvantage of limited dynamic range, although it is barely sufficient for the telescope system. Frequency modulated analog system may provide a better performance in terms of higher dynamic range.

Coherent communication system is a broadband, highly sensitive system that can be used to transmit the RF signals over very long distances. This offers better SNR, wider

bandwidth and better dynamic range. However, the cost of heterodyne/homodyne detection has not yet become commercially viable.

- Optical amplifiers can be used at each receiver end to maintain constant optical power, by electrically controlling the gain of the amplifier. This forms an optical AGC loop. At this stage however, the pump laser and the fiber amplifier do not fit into the low budget of the project.

- The insertion loss of the optical link can be minimized by reactively matching the laser device and the photodetector to the corresponding source and load circuits respectively. This will increase the signal power received at the optical receiver, thus maintaining a better signal to thermal noise ratio than the one achieved with the existing circuit design. optical fiber length for which laser noise limited SNR is maintained.

- The optical receiver's sensitivity can be increased by employing a transimpedance amplifier instead of a low value resistance at the output of the photodetector. This may result in lower frequency, but improves the sensitivity by as much as 20 dB.

- External modulation may be used with the help of Nd:YAG lasers at the transmitter end to increase the SNR and dynamic range. Nd:YAG lasers are reported to have intensity noise approaching thermal noise, and it is possible to achieve quantum limit performance.

References

1. N.V.G.Sarma "*Optical Fiber Links for Reference Frequecny Distribution*"' AT Technical Report AT/23.2/020, 1988